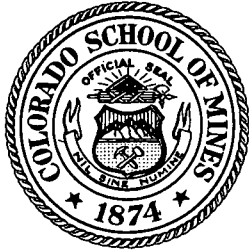


2-P (mix)



APPLICATIONS OF REMOTE SENSOR DATA TO GEOLOGIC  
AND ECONOMIC ANALYSIS OF THE BONANZA TEST SITE, COLORADO

SEMIANNUAL PROGRESS REPORT  
OCTOBER 1, 1971 - MARCH 31, 1972

REMOTE SENSING REPORT 72-4



NASA Grant NGL 06-001-015  
National Aeronautics and Space Administration  
Office of University Affairs  
Washington, D.C. 20546

Reproduced by  
NATIONAL TECHNICAL  
INFORMATION SERVICE  
U S Department of Commerce  
Springfield VA 22151

MAY 1972

121 p.

(NASA-CR-128062) APPLICATIONS OF REMOTE  
SENSOR DATA TO GEOLOGIC AND ECONOMIC  
ANALYSIS ON THE BONANZA TEST SITE, COLORADO  
Semiannual Progress R.G. Reeves (Colorado  
School of Mines) May 1972 121 p CSCL 086 G3/13 16144  
N72-31369  
Unclas

REMOTE SENSING PROJECTS

DEPARTMENT OF GEOLOGY

COLORADO SCHOOL OF MINES ♦ GOLDEN, COLORADO

Semiannual Progress Report  
October 1, 1971---March 31, 1972

Applications of Remote Sensor Data to Geologic  
and Economic Analysis of the Bonanza Test Site, Colorado

Remote Sensing Report 72-4

National Aeronautics and  
Space Administration Grant

NGL 06-001-015

BONANZA REMOTE SENSING PROJECT

Colorado School of Mines  
Department of Geology  
Golden, Colorado

Martin Marietta Corporation  
Denver Division  
Denver, Colorado

**Details of illustrations in  
this document may be better  
studied on microfiche**

May 1972

Applications of Remote Sensor Data to Geologic  
and Economic Analysis of the Bonanza Test Site, Colorado

Semiannual Progress Report

Compiled and Edited by

Robert G. Reeves  
Principal Investigator

Contributors

R. M. Biniki	R. W. Marrs
D. L. Bruns	J. R. Muhm
R. L. Hulstrom	G. L. Raines
L. H. Jefferis	R. G. Reeves
D. H. Knepper, Jr.	S. A. Stadjuhar
K. Lee	K. E. Worman

## TABLE OF CONTENTS

	Page
1.0 Introduction	1
2.0 Research	2
2.1 Data Interpretation	2
2.2 Application of Remote Sensing	2
2.3 Structural Geologic Studies	3
2.4 Rock Discrimination	5
2.5 Quantification of Remote Sensing	7
2.6 Atmospheric Research and Support	9
2.7 Line Scanner Image Processing and Enhancement	11
2.8 Investigation of Thermal Infrared Anomalies	12
2.9 Image Processing	13
3.0 Education	18
4.0 Appendices	
A. Photographic and non-photographic sensor coverage	
B. CSM graduate students' research	
C. MMC scientists' research	
D. Papers presented/written by CSM and MMC personnel	

Application of Remote Sensor Data to Geologic  
and Economic Analysis of the Bonanza Test Site, Colorado

Semiannual Report, Oct. 1 - Mar. 31, 1972

Compiled and Edited by

Robert G. Reeves

## 1.0 Introduction

The Bonanza Project is a joint effort of the Colorado School of Mines (CSM) and the Martin Marietta Corporation (MMC). CSM brings to this effort faculty and graduate students with recognized ability in the geological sciences, while MMC has demonstrated competence in instrumentation and aerospace technology. This combined capability maximizes the extraction of geologic information from remote sensor data. This report summarizes the activities of the CSM faculty and students and the MMC scientists for the period October 1, 1971 to March 31, 1972. During this period, Professors Keenan Lee and R. G. Reeves and graduate students D. L. Bruns, L. H. Jefferis, D. H. Knepper, Jr., and R. W. Marrs of CSM and research scientists R. M. Biniki, R. C. Hulstrom, J. R. Muhm, S. A. Stadjuhar, and K. E. Worman of MMC carried out research under the project.

Most of the remote sensor data analyzed during this period were acquired by NASA aircraft, either for the Bonanza Project directly, or for other investigators. Data have been collected from each of the three current aircraft, the P3A, C130, and RB57.

Photographic and non-photographic sensor coverage is shown in Appendix A. The quality of photography ranges from poor to excellent, being generally good. SLAR imagery was acquired over relatively large areas for regional geologic studies, but the imagery generally has been poor. Fair to excellent thermal infrared imagery, both day and night coverage, was flown over selected smaller areas, mostly for local structural information.

Various types of line data, including infrared spectrometry, multi-frequency microwave radiometry and radar scatterometry, were acquired, most of which yielded little geologic information.

## 2.0 Research

The main emphasis during this period has been in research on 1) assessing the value of remote sensor data for geologic and mineral and water resources investigations through the interpretation of imagery and comparison of the results with actual ground conditions, and 2) determining the effects of the atmosphere on remote sensor data.

### 2.1 Data Interpretation

Photo and associated imagery interpretation techniques have been the main analysis techniques used. This emphasis upon the human interpreter (as opposed to automatic pattern recognition techniques) evolves from three considerations:

- 1) background of researchers. All CSM personnel are geologists, and are experienced in the extraction of geologic information from aerial photographs.

- 2) type and quality of data received.

- 3) anticipated use of remote sensor data. These data should be capable of being used by the average professional geologist in his work, without undue reliance on sophisticated analytical instruments available only in research laboratories.

Despite the emphasis upon photo and imagery interpretation techniques, other interpretation methods are being investigated as well, including optical and digital image enhancement, multi-band color additive projection, video image processing and computer reduction and analysis of infrared spectrometry. These are being carried out by MMC in collaboration with CSM personnel.

### 2.2 Application of Remote Sensing

The rationale for using remote sensing for geology, as for any other discipline, is predicated on what are, by now, familiar arguments. Specifically, the remotely sensed data must provide either:

- 1) new information not obtainable by other means, or
- 2) a reduction in time (cost) necessary to obtain information.

New geologic information derives mainly from the synoptic view afforded by remote sensors or from the measurement of an invisible phenomenon such as heat or conductivity. This "forest for the trees" situation has been used most advantageously in structural geology studies, where discontinuous surface elements are found to define a single geologic structure. Many such examples have been demonstrated most dramatically by space photography.

The reduction in time necessary to obtain geologic information is also a recognized advantage of remote sensing, although it has not been as well demonstrated; the time-saving capability is indicated by the following example.

An area in central Colorado had not been mapped geologically, though the adjacent areas to the north, west and south had been mapped geologically. This is typical of an area comprising about two 7½' topographic quadrangles or about 110 square miles and that would be assigned for a Master's thesis and would entail at least a full summer of field mapping. A photo-geologic map was produced by interpretation of NASA photography, including color, color infrared and low sun-angle photography (LSAP) by a Bonanza Project graduate student in approximately one week. This map is comparable, in detail, to that of the adjacent geologic maps, and it is estimated that only about two weeks would be required in the field to verify interpretations and produce a finished geologic map.

The outstanding application of remote sensing to geologic investigations remains the ability to provide the interpreter with basic geologic information--that is, the surface aspects of lithology and geologic structure. Thus, the Bonanza Project research has been aimed primarily at investigating the capability of remote sensing to 1) discriminate different rock types, and 2) delineate geologic structure.

### 2.3 Structural Geologic Studies

The utility of small-scale aerial and space photography has been demonstrated many times. In particular, such photography often contains abundant information on large regional geologic structures. The synoptic view afforded by photography of the

San Luis Valley and the west flank of the Sangre de Cristo Range allows the interpreter to join together discontinuous lineaments to synthesize one continuous fault zone, the "Sangre de Cristo Fault", separating the range from the valley. Other photos of the area clearly show recent movements along some segments. Color IR photography has a slight advantage over regular color photography because portion of the fault line trace are marked by linear stands of aspen, which are enhanced somewhat by the sensitivity of this film to reflectance from vegetation in the near IR.

Fault control on the base of the Sangre de Cristo mountains is obvious but indications of fairly recent movement along the fault can be seen only in isolated segments. To attempt to find further evidence of recent faulting in this anomalous area, thermal IR scanner imagery was acquired. Recent faulting along the base of the range in this area was not detected on this imagery, but a series of en echelon fault scarps trending away from the mountain front were revealed. Clearly then, recent stress release has occurred all along the Sangres, but in this one area the faulting trended away from the range rather than parallel to it. These faults displace alluvial fans of probably late Wisconsin age, and as such are probably less than 10,000 years old. The demonstration of this style of faulting is significant in that it lends credence to the growing argument that the modern San Luis Valley is tectonically part of the Basin and Range province, rather than the typical Laramide Rocky Mountains. This information is of value in petroleum, mineral, and geothermal exploration.

Low sun-angle photography (LSAP) along the Front Range of Colorado was flown at the optimum time to enhance subtle topographic variations. Geologic structures are enhanced where they are the dominant controls on topography, as for hogbacks. In areas of non-structural control of topography LSAP is useful for geomorphic studies. Black and white IR film (Type 2424) was used with a Wratten 25 filter for this photography, because 1) the 600-900 nm bandpass allows better "penetration" of early morning haze, and 2) the topography is better enhanced by the strong black shadow areas that result from the lack of sensitivity to short wavelength light. Two small studies were conducted to



evaluate more quantitatively the benefit of remote sensing for obtaining geologic structural information. In the first, interpretations of 1) conventional aerial photos were compared with interpretations of 2) color photos and thermal IR imagery. A dramatic increase in structural detail was obtained from (2). Not only was more detail obtained (16 faults vs. two faults), but the information was more accurate, as the original interpretation was later proved erroneous. In this and nearby areas, examination of remote sensor data disclosed 26 linear features interpreted as faults. Subsequent field checking showed 8 of these to be definite faults (all of the major ones), 13 to be geologic discontinuities of some sort (not determinable in the field--either faults or fractures), and 5 to be non-geologic phenomena (fence-lines, trails, etc.). Thsu, roughly 80% of the photo lineaments proved to have geologic significance and 20% were erroneous.

In a somewhat similar study in the Bonanza Mining District, remote sensor data of a complex volcanic area were interpreted for structural information. These data included color and color IR photography and RS14 thermal infrared imagery. The resulting map contained 63 linear features interpreted as faults. Subsequent field mapping proved 44 of these to be faults (again, all of the major faults had been detected), 14 to be non-geologic, and the significance of 5 could not be determined in the field; or about 75% correct and 25% incorrect interpretation.

The conclusions from these two studies are 1) more geologic structural information is available from remote sensing data than from conventional techniques, 2) greater accuracy results from using remote sensing data, 3) all major structural features were detected, 4) of all structural interpretations, about 75% were correct, and 5) interpretation of remote sensing data will not supplant field work, but it enables field work to be done much more efficiently.

#### 2.4 Rock Discrimination

The ability to discriminate between different rock types on remote sensor photography and imagery has so far proved to be one of the most difficult tasks, yet one that is manifestly

fundamental to any geologic application. The advantages of color photography for this task have been amply demonstrated, but color photography may not always be the best tool available in all cases, and other techniques are being investigated as well. One line of research, using multiband photographic techniques, has recently begun by CSM and MMC.

Multiband photography has been used and interpreted in our and others' investigations for some time. During the period covered by this report, research at CSM has been directed toward fundamental rock reflectance studies and machine-assisted data interpretation. Geologists from CSM and atmospheric scientists from MMC have been working together in the field in an attempt to overcome problems of surface irradiance fluctuations due to atmospheric variables, and thus to obtain basic reflectance spectra of rocks on the outcrop. A simple, but effective film/filter combination that records beyond 620 nm and that has the capability to discriminate among three rock types has been identified.

Similar studies are under way to determine the ability of thermal infrared scanners to discriminate between different rock types. Efforts to date have been concentrated on studying the basic rock properties which affect their radiometric temperatures; results so far are encouraging.

Quantitative evaluation of remote sensing capability for rock discrimination is very difficult. Studies so far have not been conclusive but one small study is informative. A test area was selected near the Bonanza Mining District for lithologic interpretation of color and color infrared photography and thermal scanner imagery. Within this test area, 78 fault-bounded areas were interpreted, and one of six lithologic designations was assigned to each of the areas. Subsequent field mapping provided ground control with the result that 62% of the areas had been assigned the proper lithology and 38% were incorrect. These figures are most encouraging, when consideration is given to the complex geology of the areas; all of the rocks in question are Tertiary volcanic rocks, consisting of lava flows, ash flows and lahatic

breccias, and all are rather drab appearing, exhibiting only the most subtle differences in color. Additional studies in this are proposed.

## 2.5 Quantification of Remote Sensing

To date, most of the research carried out by CSM and MMC, like most of the remote sensing research reported in the literature, has been largely deductive. Recently, however, the inductive approach to defining the capability of remote sensing for rock discrimination has been emphasized. In other words, is it even realistic to attempt to discriminate granite, for example, from limestone by using an infrared scanner? Fundamentally then, we are in part returning to step 1 of geologic remote sensing, where our and other researchers' investigations were obviously too limited. Basically, we have examined the following questions:

- (1) What physical and chemical differences exist between different rocks?
- (2) Which of these properties provide sufficient contrast to distinguish the rocks?
- (3) Which of these properties are capable of being remotely sensed? And then logically,
- (4) How can we best use remote sensors to do the job?

Our initial approach has been to examine these questions in terms of specifics, rather than generalities. Consequently, we have defined an area of study (test site, if you will) along the Front Range for this purpose, an area which includes at least 18 different geologic formations. The following procedure evolved:

A. List basic properties: All rock properties were listed. Any basic rock parameter which could be described or measured was included in the list, regardless of any other consideration; 31 parameters were listed.

B. Formation/property matrix: A matrix was formed in which all of the parameters from A could be listed for each of the 18 formations. Each of the spaces in this 18 x 31 matrix were then filled in (where possible) with qualitative descriptors.

C. Select promising parameters: Examination of the matrix focused attention upon those parameters which qualitatively showed promise of having the most contrast between adjacent formations.

D. Quantification: Attempts were made to quantify those parameters selected in C. Emphasis was placed upon methods easy to employ in the field without specialized equipment; for example, color measurements were made using GSA Rock Color Charts, and "albedo" (visible reflectance) was measured with common light meters and standard reflectance cards.

E. Select useful parameters: Based upon the quantitative values determined in D, the parameters found consistently most useful for discrimination were defined.

F. Define contrasts required: An attempt was made to define those contrasts between parameters which are capable of being remotely sensed. The approach here was empirical--that is, rather than simply check manufacturer's instrument specifications (which generally apply to laboratory, or at least optimum, conditions), studies were conducted on typical NASA aircraft-acquired data to estimate what contrasts have actually been detected.

G. Select remote sensor(s): The next logical step when was to cross-correlate the matrices of parameter contrast and sensor capability in order to select the optimum remote sensor(s) which offered the greatest probability of success in discriminating the rocks.

Six different investigators followed the above procedures, each one working independently with different geologic formations within the test site. It should be stressed that these recommendations apply to these specific formations in this specific test site. There is ample bias in this initial study to preclude extrapolation into other areas; nonetheless, the results are informative.

## 2.6 Atmospheric Research and Support

Activities during this period generally were divided into two categories:

(1) atmospheric ground support of NASA Aircraft Missions 168 and 184 and laboratory support involving calibration and checkout of the CSM ISCO spectroradiometer, and

(2) research involving reflectance measurements and atmospheric effects on the nature of incoming solar radiation, which made up the major part of the total effort.

The atmospheric effects research was directed toward the specific problem of developing improved techniques to be used in compensating for atmospheric influences during reflectance measurements and to the general problem of establishing the nature of the temporal and spatial variances of atmospheric effects on the total solar radiation.

### 2.6.1 Atmospheric Science Support Activities

The following support activities were conducted during the past year.

#### 2.6.1.1 Ground Meteorological Measurements

During Mission 168 a portable mechanical weather station was operated near Villa Grove. The station was established to provide continuous meteorological data and to determine if the site was indeed representative of the overall regional micrometeorological conditions. The measurements included rainfall (increments of 0.01 in.), temperature (-30 to +120°F), wind velocity (average wind speed), and wind direction. The region received approximately 0.01 inches of rain near noon of the day preceding the nighttime thermal infrared mission (eleven hours before overflight). Following the rainfall, air temperature increased to 75°F, and winds averaged 20 to 30 mph; therefore, it is concluded that the rainfall probably had little, if any, effect on the thermal characteristics of the ground features that were observed during the subsequent nighttime mission.

The Villa Grove site measurements indicate the location is representative of typical upslope/downslope, mountain/valley,

micrometeorological conditions and thus is recommended as a standard meteorological measurement site for the region. In addition, existing data from the site provides a representative array of meteorological parameters.

#### 2.6.1.2 Solar Radiation Measurements

Measurement of the total (global) solar radiation characteristics were made during Mission 168 at the Villa Grove site. The measurements were made with two Eppley pyranometers, one equipped with a WG-7 filter, transparent from 0.3 to 3 micrometers ( $\mu\text{m}$ ), and one equipped with an RG-8 filter, transparent from 0.7 to 3  $\mu\text{m}$ .

From inspection of the data, one can easily determine when the site was experiencing intermittent cloud shadowing. Cloud "bright spots" (areas of enhanced radiation equivalent to shadows) were observed to occur on both days. Such cloud influences have previously been investigated on the Bonanza program.<sup>1/</sup>

During Missions 168 and 184 ratios of the diffuse-to-total (global) solar radiation were made in order to quantitatively define atmospheric clarity (Appendix C). During Mission 168 this ratio was approximately 11-to-15 percent; during Mission 184 this ratio was approximately 8-to-10 percent. The 8-to-10 percent ratio is considered to be characteristic of extremely "clear" conditions, whereas the 11-to-15 percent ratio is significantly "less clear". Ground photos taken during the mission show noticeable differences in "haze", and a comparison of color aerial photography of the two missions displays dramatic differences in the degree of atmospheric clarity.

#### 2.6.2 Laboratory Support

Laboratory support during the third program year consisted of a complete calibration of the CSM ISCO spectroradiometer, serial number 14760. Calibration correction factors for both the direct incident head and a special six foot fiber optics probe were determined by measuring a known standard, ISCO lamp No. 319. A total of four sets of measurements from 380 to 1550 nanometers were supplied in order to determine the precision of the spectro-

<sup>1/</sup> The "Cloud Bright Spot" Effect on Remote Sensing, R. L. Hulstrom, submitted to Photogrammetric Engineering for publication.

radiometer. In addition to the calibration of the ISCO, numerous electronic checkout tasks were performed.

### 2.6.3 Atmospheric Research Activities

Research concerning the effects of the atmosphere on remote sensing performed during the third program year was directed toward providing an understanding of these effects and development of improved techniques for the measurement and subsequent analyses of data. These include 1) transmission characteristics of the atmosphere, 2) measurement of incoming total and diffuse solar radiation, 3) effects of effects of directional and isotropic radiation on the reflectance spectrum of a target, and 4) development of improved techniques for measuring field reflectance and solar radiation. (Details of this research are given in Appendix C ).

### 2.7 Line Scanner Image Processing and Enhancement

Research was carried out during this period on the quantitative processing and qualitative enhancement of scanner data. This research was limited to two channel data, but the results can be applied to any number of channels. The primary emphasis thus far has been on the development of a laboratory playback (display) system and breadboarding of functional "black boxes" for data workup. Analog signals on  $\frac{1}{2}$  inch, 7-track magnetic tape were used in this effort. Recording mode on all channels is direct, which has some disadvantages over FM recording. The electronic processing of image data in analog form has many advantages over digital techniques. The equipment required is not prohibitively expensive, implementation of enhancement techniques is accomplished with functional modules, and turn-around time is short. In a virtual real-time display, it is possible to conceive an enhancement scheme, build that hardware and test the thesis all within a day or two. Modifications to the concept are implemented and viewed within hours. The use of a storage oscilloscope allows data to be displayed, modified, displayed again until optimized and then recorded on photographic film to provide a permanent record.

The processing of the video data (imagery) is accomplished through the use of an almost infinite variety of linear integrated circuits such as operational amplifiers, voltage followers, comparators, etc. These basic building blocks, along with some external components, permit a wide range of techniques to be explored. The potential of the processing method described here is limited only by imagination. With just a few functions such as variable-gain differential amplifiers, iso-contour generators, and high-, low-, and band-pass filters, many variations in image processing are possible.

## 2.8 Investigation of Thermal Infrared Anomalies

Thermal infrared imagery (8-14 $\mu$ ) obtained during Mission 153 showed a series of anomalous en echelon linear features in a broad alluvial valley south of Beaver Creek, northeast of Canon City. These linears approximately parallel the strike of the underlying Fountain Formation, buried here by as much as 50 feet of detrital material as judge by pits, apparently dug several yeats ago as water wells. The linears were cooler than the adjacent terrain and it was suggested that the cause was an upwelling of ground-water through the thick gravel deposits flooring the valley. The question arose as to whether the anomalies were transient or permanent, or even if they were real, representing warmer and cooler zones and not simple artifacts or extraneous markings on the film imagery. An AGA Thermovision<sup>2/</sup> was used on the site to search for the anomalies. The AGA Thermovision confirmed that the anomalies are real, indicating that the airborne scanner is capable of sensing variable moisture levels, apparently related to bedrock buried under several feet of gravel. There was no obvious excess of soil moisture near the surface, but the vegetation did appear to be somewhat thicker along the linears. Two explanations for the anomalies seem feasible. They could be effects of the paleo-erosional bedrock surface beneath

---

<sup>2/</sup> The AGA is a device for imaging in the 3-5 $\mu$  wavelength region, capable of detecting small thermal anomalies.



the thick valley-fill, or they could indicate a series of strike faults providing a path for ground-water to rise to the surface.

On 21 December 1971, several seismic traverses were run perpendicular to the anomalous linear features. The seismograms recorded during this field trip show good first-arrivals, and energy coupling into the ground is more than adequate. Plots of the time-distance curves showed there was not sufficient distance between the shot-point and the first geophone to yield information about the bedrock depth. The final shot was a reverse profile with the shot-point approximately 1,000 meters from the alluvium-crystalline rock contact. The time-distance plot of this shot indicates the subsurface sediments are faulted.

## 2.9 Image Processing

Research was carried out during this period on the use and application of the video image processing (VIP) system. Several types of airborne imagery were evaluated.

Six types of imagery flown over the Bonanza Test Site on NASA Missions 168 and 184 were subjected to VIP to ascertain the usefulness of the processor and the suitability of the imagery for geologic analysis. New techniques using the video-processor were developed for specific problems, including procedures for lithologic discrimination and linear feature enhancement.

The VIP enables real-time quantization of an image in terms of absolute and (or) relative densities, and pseudo-color display of an image according to programmed density range values. The resulting processed image is enhanced due to the extended density viewing range, increased image contrast, and the ability to discard or suppress irrelevant information, with the primary purpose of performing exaggerative enhancement to make the subtle more obvious or extracting information so the "buried" data in the background become more obvious. The VIP technique expands the gray scale of the photographic H and D curve by substituting colors for the shades of gray, thereby more fully utilizing the response and sensitivity of the human eye. The process also does some pre-conditioning of the photographic image resulting

in reduced eye fatigue, bandwidth compression, and exaggeration of subtle variations in contrast ratios.

The VIP equipment consists of input and controls, signal conditioning (processing), and display and recording components. The overall system design is such that the qualitative and quantitative contribution of each element in the system can be determined.

Image processing was carried out on multiband photography, color photography, color infrared photography, early morning low sun-angle black and white photography, predawn and daytime infrared scanner imagery, and side-looking airborne radar imagery from these missions.

Evaluation of each type of imagery is discussed independently in the following sections and recommendations pertaining to VIP in general and data collection and analysis are in section 2.9.6.

Several specific areas to be investigated were selected by CSM graduate students participating in the Bonanza program. During the video processing, these students worked with the MMC scientists, observed the approach being taken, and commented on procedures. The problems presented were kept simple since it appeared that previous attempts at solving specific problems tended to be too complex for this stage of investigation.

#### 2.9.1 Multiband Photography

In processing Mission 101 and 105 imagery during 1971, a color was assigned to the most obvious or known rock type, its known or visible limits were defined by trial and error methods, and attempts were made to extrapolate this color to other areas. The major deficiencies of this method are that it required previous knowledge of what was being sought and had no set techniques for establishing new data points. To overcome these deficiencies, a new approach was developed. After mounting the multiband frame and displaying it on the video monitor, two points representing lightest and darkest points on the imagery were selected. These correspond to the end-points of the gray scale being seen by the video camera. Using the video analyzer as a line-select oscilloscope, the two movable cross-hairs were centered on each end-point

and sweep voltage for each point read on the digital voltmeter. The video quantizer is then set up to "slice" the total gray scale into equal increments; colors can then be assigned to the slices. The number of slices can range from two very broad bands to 16 relatively narrow ones. The image is displayed on the RGB monitor; each color represents a select portion of the gray scale seen by the analyzer. This system allows the number of slices to be varied, the width of any or all segments to be changed, and points selected within the frame of imagery to be used as calibration points for extrapolation to contiguous areas. This procedure was tested on a single frame of multiband photography from Mission 184. The area was relatively clear of vegetation and the geology had been mapped by both ground and photogeologic methods. The analyzer was set up to slice the gray scale into eight equal segments, a color assigned to each slice, and the image displayed on the RGB monitor. The display was observed in two modes: sharply focused, which presented a wealth of detail, and slightly out-of-focus, which eliminates much of the detail but gave a better display of gross features. A geologic sketch map of the test area was compared to the display. Several geologic units were displayed on the VIP with some degree of accuracy. From this work, a procedure has been developed to use multiband photography to assist in discrimination between different lithologic and soil types. The procedure is repeatable, has definite objective value, and can be used to extend the area of interest over several frames of contiguous photography. Details on the procedure and results are given in Appendix C .

#### 2.9.2 Color and Color Infrared Photography

A single frame of 9x9 inch aerial color film (SO 397) from Mission 168 was subjected to video processing also. Attempts to delineate lithology using the procedures described in section 2.9.1 were not successful, probably due to the low contrast inherent in the color photography. Previous work indicated that subtle linear features, including fault line traces and fractures, could be discriminated and mapped from color aerial photography.

The procedure used differs from that used to discriminate lithology. The video quantizer was set up with very narrow slice of color assigned to a small range of the total gray scale. Then the bias-level control of the quantizer is used to resshade the background and shift the gray scale. By continually changing the bias levels, it is possible to emphasize and enhance linear features in the photograph. It should be noted that this procedure is, by nature, a "knob-twisting" technique and subjective as opposed to that used for discrimination of lithology described in section 2.9.1. Further, the usual caution must be exercised to avoid attributing geologic significance to such straight-line cultural features as roads, power lines, and fence lines.

Attempts to use color infrared photography from Mission 168 in the VIP to discriminate lithology with the procedures used in section 2.9.1, were, generally, no more successful than the attempts with color aerial photography. Success with enhancing linear features was generally similar.

#### 2.9.3 Low Sun-Angle Photography

It was immediately evident that low sun-angle photography, because of large areas of shadow and small density range in the sunlit areas, is not suitable for video enhancement.

#### 2.9.4 Thermal Infrared Imagery (Predawn)

A positive transparency of predawn thermal infrared (8-14  $\mu$ m) imagery from Mission 168 was subjected to VIP.

Using the procedure outlined in section 2.9.1, an attempt was made to discriminate between lithologic units using this imagery. Although there was some indication of discrimination, no clear cut identification was obtained unless a priori knowledge of the units was available.

Attempts to use the thermal imagery to construct a thermal contour map were hampered by lack of sufficient ground and aircraft calibration data. The two IR calibration sources in the scanner did not provide adequate information, either from the imagery or from the analog tape.

Previous work at MMC, unrelated to this contract, has demonstrated that video processing of thermal imagery can be quite successful, but is wholly dependent on adequate ground and aircraft calibration in order to arrive at absolute data points. See Appendix C, Enhancement and Display of Infrared Line Scan Data, for further discussion.

#### 2.9.5 Side-Looking Airborne Radar

Both real- and synthetic-aperture radar from Mission 168 were viewed on the VIP. Due to the nature of the imagery, no lithologic discrimination was attempted.

As radar images are presently used to locate linear features, the scan was processed to enhance these features using procedures previously described. Although many linear features were observed during processing all were visible on the unprocessed imagery. There appeared to be no difference in the quality of the real- versus synthetic aperture imagery as viewed on the processor. Video image processing of airborne radar does not appear to enhance the ability of the interpreter to find and locate linear features.

#### 2.9.6 Summary

Discrimination and identification of lithology was attempted using the six types of imagery available. A new procedure was developed which permits a more quantitative approach and gives repeatability. Low sun-angle photography and side-looking radar were not at all useful for this type of analysis. Color and IR color photography could be used to assist and corroborate lithologic mapping, but this type of imagery tends to emphasize vegetation, masking the rocks and soils. Also, the density range of these films is quite narrow. Predawn thermal IR imagery results were marginal, with indications that some discrimination is possible, but more research is needed. Multiband photography showed great promise, with results repeatable and quite accurate.

The ranking of the imagery for lithologic mapping using the video processor would be as follows in descending order of

usefulness:

- 1) Multiband photography;
- 2) Thermal infrared imagery;
- 3) Color aerial photography;
- 4) Color infrared photography;
- 5) Low sun-angle photography;
- 6) Side-looking airborne radar.

Prior work on discrimination and location of linear features had shown that color, IR color and multiband photography were suitable for this type of problem. This work indicated that side-looking airborne radar and thermal IR imagery also could be used, while low sun-angle photography is generally unsuitable.

The ranking for linear feature mapping using the video processor, would be as follows in descending order of usefulness:

- 1) Side-looking airborne radar;
- 2) Color aerial photography;
- 3) Thermal infrared imagery;
- 4) Multiband photography;
- 5) Color infrared photography;
- 6) Low sun-angle photography.

### 3.0 Education

Faculty working under this grant have developed three graduate courses in geologic remote sensing.

The first course is "Introduction to Remote Sensing", which deals with the theory of active and passive remote sensing systems, using the energy path concept in the ultraviolet through radar portions of the electromagnetic spectrum. Students are introduced to the remote sensing instruments and interpret representative data. Geologic applications are briefly surveyed.

To date, this course has been offered four times, twice as part of the CSM Continuing Education Program, which made the class available to practicing scientists and engineers in the Denver metropolitan area. The combined enrollment has totalled 46 students, including undergraduates, graduate students and professional scientists and engineers.

The second course, "Geologic Applications of Remote Sensing", stresses the application of remote sensing to geologic and mineral resources investigations. The course includes detailed study of remote sensing techniques, with field and laboratory experiments and experience in data reduction, analysis and interpretation. Case studies of demonstrated applications are presented, and potential uses are examined. Students conduct exercises in selection of optimum sensor systems for specific geologic targets and mission planning.

This course is currently being taught for the second time. Combined enrollment totals 15 graduate students.

The third course is a "Seminar in Geologic Remote Sensing", which consists of group discussions and individual student presentations on current literature and research. This seminar has been given twice, with a total enrollment of 13 graduate students.

APPENDIX A  
PHOTOGRAPHIC AND NON-PHOTOGRAPHIC  
SENSOR COVERAGE

9



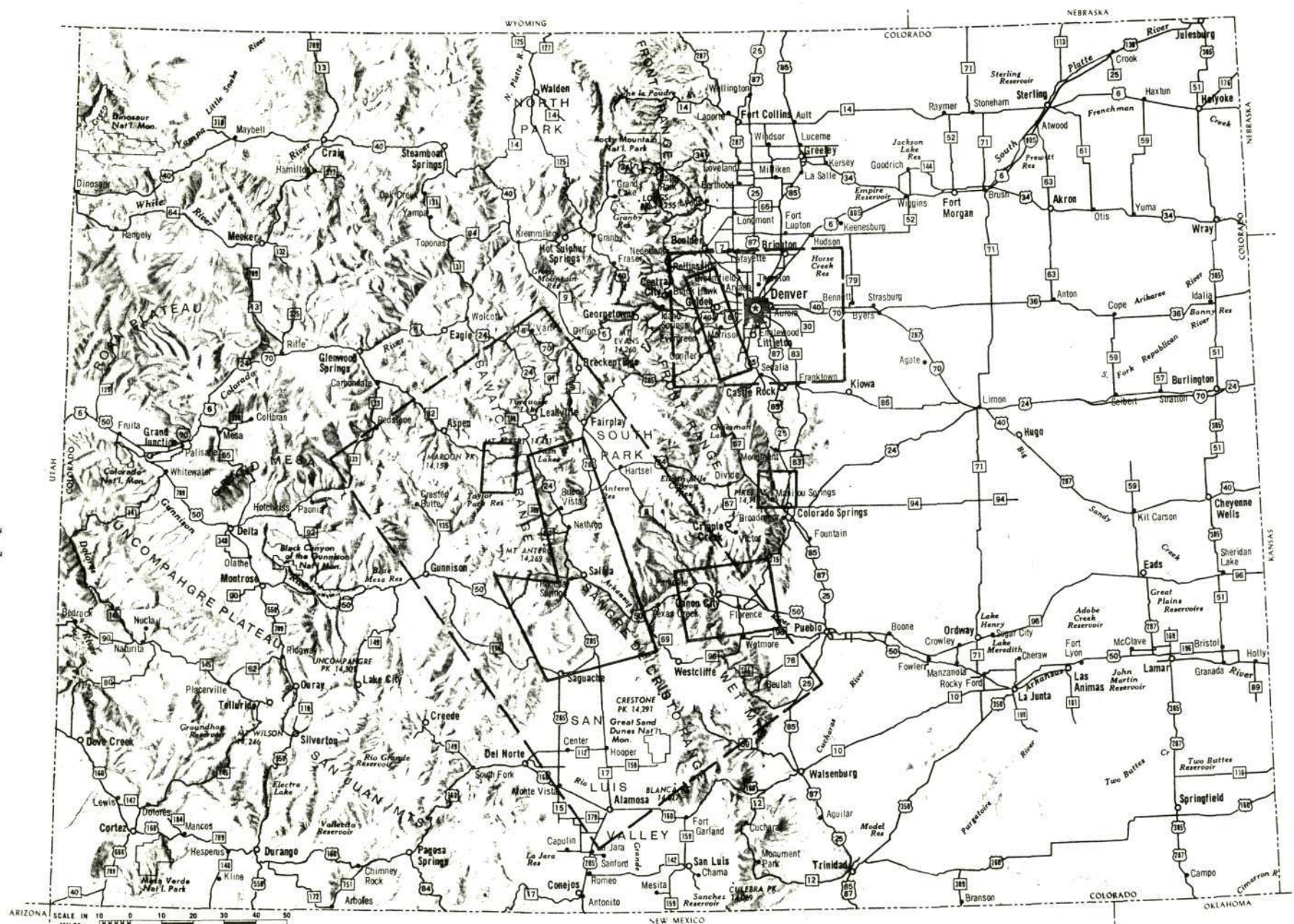


Figure 1. Photographic coverage by NASA aircraft. Areas within dashed line are covered by small-scale ( $>1:100,000$ ) photography, within solid lines the photography is large scale ( $<1:30,000$ ).



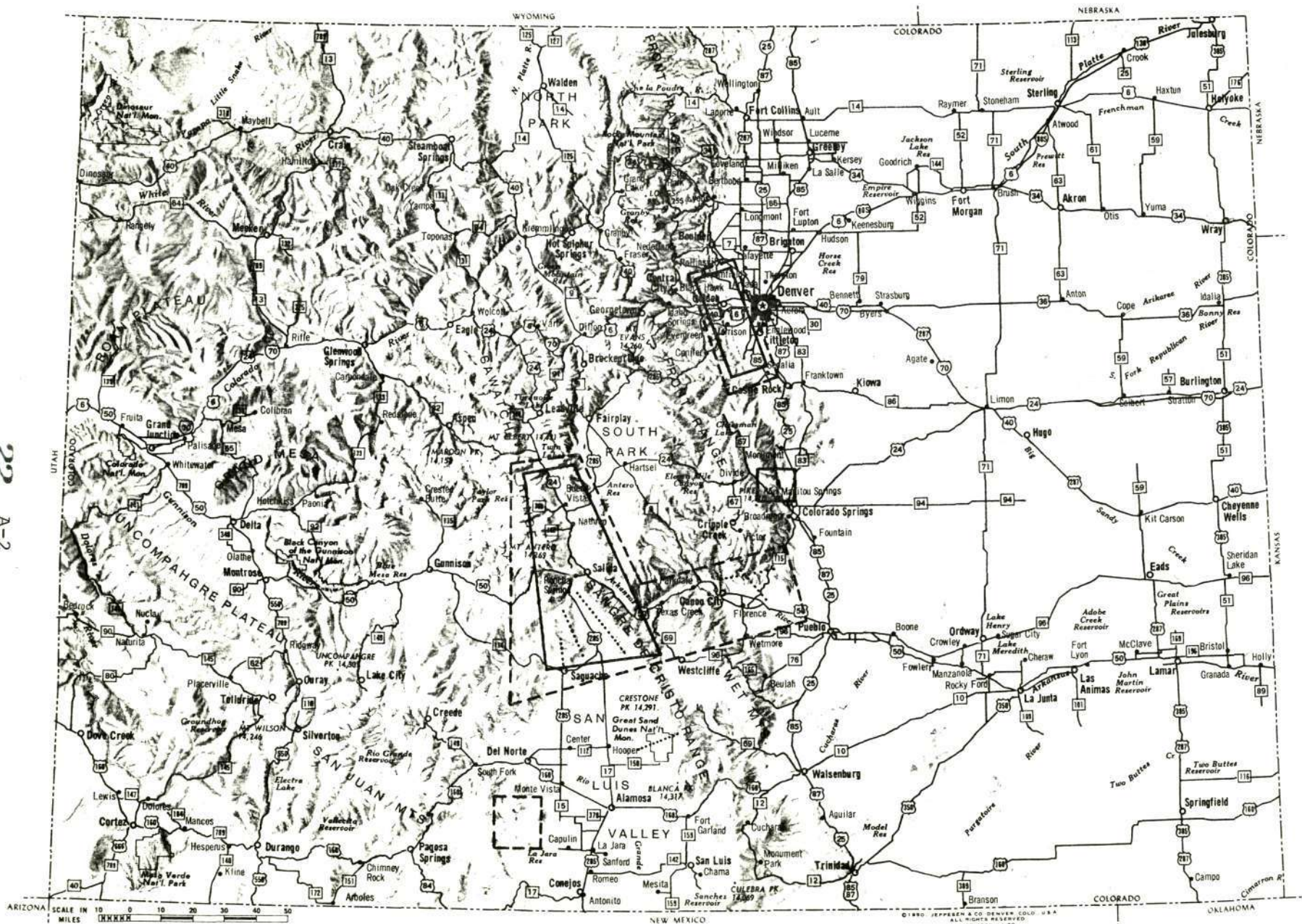


Figure 2. Coverage by non-photographic sensors. Solid lines indicate IR scanner imagery, dashed lines are SLAR coverage, and dotted lines represent line data (microwave radiometry, radar scatterometry and infrared spectrometry).

APPENDIX B  
SUMMARIES OF CSM  
GRADUATE STUDENTS' RESEARCH

## RESEARCH ACTIVITIES OF DENNIS L. BRUNS

1 October 1971 - 31 March 1972

### 1.0 General

This is a summary of the investigation of the application of remote sensing to the problems of geology and mineral exploration in the vicinity of Leadville, Colorado.

### 2.0 Specific Research

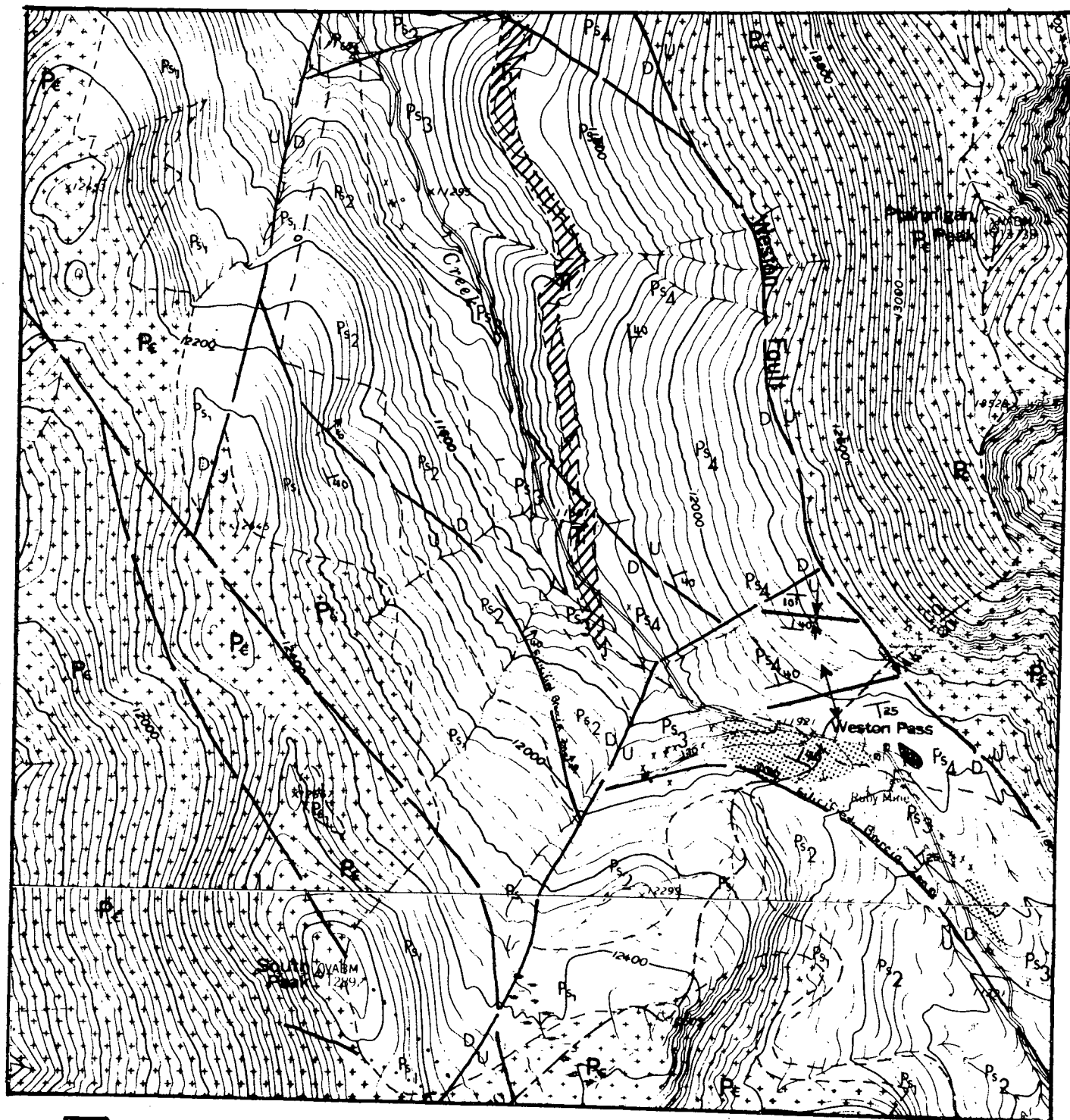
The period was spent in studying available remote sensor data, primarily low altitude color and color infrared (CIR) photography (Mission 184, flown in September, 1971), but also including high altitude color and CIR photography (Mission 101, flown in August, 1969), and side-looking radar imagery (SLAR) (Mission 184). Geologic interpretation of available data generally was limited to the area of the Mosquito Range south of Union Creek and north of Buffalo Peaks during this time period. This work can be subdivided into two parts based on the area studied and the purpose of the study.

#### 2.1 Weston Pass Area

The first area studied in detail was the Weston Pass area. This area, a portion of which is shown in Figure 1, was selected as a "training site" in which the rock units present could be studied because it presumably was well mapped by previous workers, most of the Paleozoic rocks present in the region are also present in this area, and the geology is relatively uncomplicated by later faulting and intrusion. The area shown in Figure 1 includes the Weston Pass mining district which produced small to moderate quantities of lead-silver-zinc ore from about 1900 through 1916. Behre (1932) concluded that the Weston Fault and bedding plane fractures and faults, including the bedding plane fault labeled "silicified breccia zone" on Figure 1, served as a pathway for hydrothermal solutions which deposited the ore in a single favorable stratigraphic horizon in the Leadville Limestone.

Color and CIR photography and SLAR imagery are available for this area. The subdivisions of the rocks of the area, and,






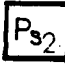
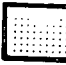

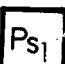
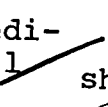

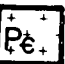
- |  |  |  |          |   |
|--|--|--|----------|---|
|  Tertiary Intrusive           |  Paleozoic Sedimentary Unit 2 |  Alteration Zone    | 1/2 Mile | N |
|  Paleozoic Sedimentary Unit 4 |  Paleozoic Sedimentary Unit 1 |  Fault, showing dip |          |   |
|  Paleozoic Sedimentary Unit 3 |  Precambrian Gneiss           |  |          |   |
| Strike and dip of sedimentary rocks  |  |  |          |   |

Figure 1  
Weston Pass Area

to some extent the utility of these methods of study in mapping and distinguishing the different rock types is shown in Figure 2. SLAR probably would have been more useful if better imagery were available and a different look direction were used.

Stratigraphic Unit (Based on Field Mapping)	Subdivision Recognizable With Various Remote Sensors		
	Color Photography	CIR Photography	SLAR Imagery
Tertiary Intrusives	Ti	Ti	Paleozoic Sedimentary Rocks
Beldon Formation (Shale)	Ps <sub>4</sub>	Ps <sub>2-4</sub>	
Leadville Limestone	Ps <sub>3</sub>		
Dyer Dolomite	Ps <sub>2</sub>		
Parting Quartzite			
Manitou Limestone			
Peerless Formation	Ps <sub>1</sub>	Ps <sub>1</sub>	
Sawatch Quartzite			
Precambrian Gneiss	Pc	Pc	Pc

Figure 2  
Stratigraphic Subdivisions in  
the Weston Pass Area

For mapping faults, CIR photography was most useful although almost all faults mapped on CIR photography also were apparent on color photographs. About half of the faulting shown in Figure 1 had been mapped by previous workers, however, photogeologic interpretation suggested that the faulting was more extensive than shown in any available publications. The silicified breccia zone, representing a bedding plane fault, was generally not apparent except as a zone of displacement in the sedimentary rocks. All other faults shown in Figure 1 were fairly evident in photography. The two small folds north of Weston Pass had not been previously mapped but were easy to identify in color photography and, once

identified, could be seen in CIR photography also. The only fault which could be identified in SLAR imagery was the Weston Fault which appeared as the contact between layered sedimentary and nonlayered metamorphic rocks. This fault was easily identified in photography. In general, the use of color and CIR photography in this area seemed to provide better results than field mapping without the use of photography, and certainly the use of aerial photography in conjunction with field mapping would give the best results.

Three areas of possible hydrothermal alteration were seen in the area of Figure 1. Two of these areas are shown, as at least some alteration was noted in these areas during field reconnaissance. A third possible area was seen, but due to its location was tentatively identified as an old burn area. The interpretation of this area will be field checked during the summer of 1972.

## 2.2 West Slope of the Mosquito Range - Granite Mining District

The second area studied in detail was the west slope of the Mosquito Range south of Union Creek and north of Buffalo Peaks including the old Granite mining district. This represents an area in which virtually no geologic mapping has been done (except for a reconnaissance map recently made by the U. S. Geological Survey in conjunction with a geophysical study, and which has not yet been published). Therefore this area is one in which remote sensing might be expected to add to available geologic mapping and, in the vicinity of the Granite mining district, possibly provide guides for future mineral exploration.

The first activity in the Granite mining district was placer gold mining during the 1860's. Subsequently, lode mining was done for gold and later for lead-silver ore. The district was never a large producer and production generally ended about 1945 (Vanderwilt, 1947). Such published information as is available indicates that the ore deposits mined were gold (probably pyrite), silver, and lead, in Precambrian granite cut by Tertiary dikes (Vanderwilt, 1947).

High and low altitude color and CIR photography and SLAR imagery were interpreted. A set of lineaments, probably representing faults, was mapped (fig. 3). Most of the mines and prospects fall along or near these lineaments. This can be seen in Figure 3 and is even more apparent on aerial photography as the U. S. Geological Survey base map used for Figure 3 only shows one-third to one-half of the mines and prospects actually present in the area. This suggests that the pattern of lineaments mapped represents faulting which served as the structural control for intrusion, alteration, and mineralization in the Granite mining district. The pattern of faulting shown in Figure 3 seems to represent the intersection of northeast- and northwest-trending faults. This is the same pattern that has been reported to the north at Leadville (Behre, 1953) and for the region in general (Badgley, 1960). Field checking done in this area during the summer of 1971 indicated that the faults, which are easily seen in photography, are difficult to detect and map on the ground due to the uniformity of the Precambrian rock in the area.

Several small areas have been tentatively identified as Tertiary intrusives though they may, in fact, be areas of hydrothermal alteration. Several other areas have been tentatively identified as areas of hydrothermal alteration. Such alteration does exist in the two areas shown along Twobit Gulch in the north of the map area as this area was examined during the summer of 1971. It has been noted that the vegetation around several of the larger mines is less dense and less vigorous than elsewhere. This is probably due to the effects of mining; however, several similar areas have been noted elsewhere where little or no mining has been done. These areas will be examined during summer, 1972.

In the area of the Granite mining district, therefore, remote sensing can be expected to provide information now lacking, and difficult to obtain by field mapping alone. The results of work to date, probably outlining the structural control for mineralization in the Granite mining district, and possibly suggesting some specific areas of interest as well, could provide a useful guide for any future mineral exploration in the area. Field checking of most of this area will be done during the summer of 1972.





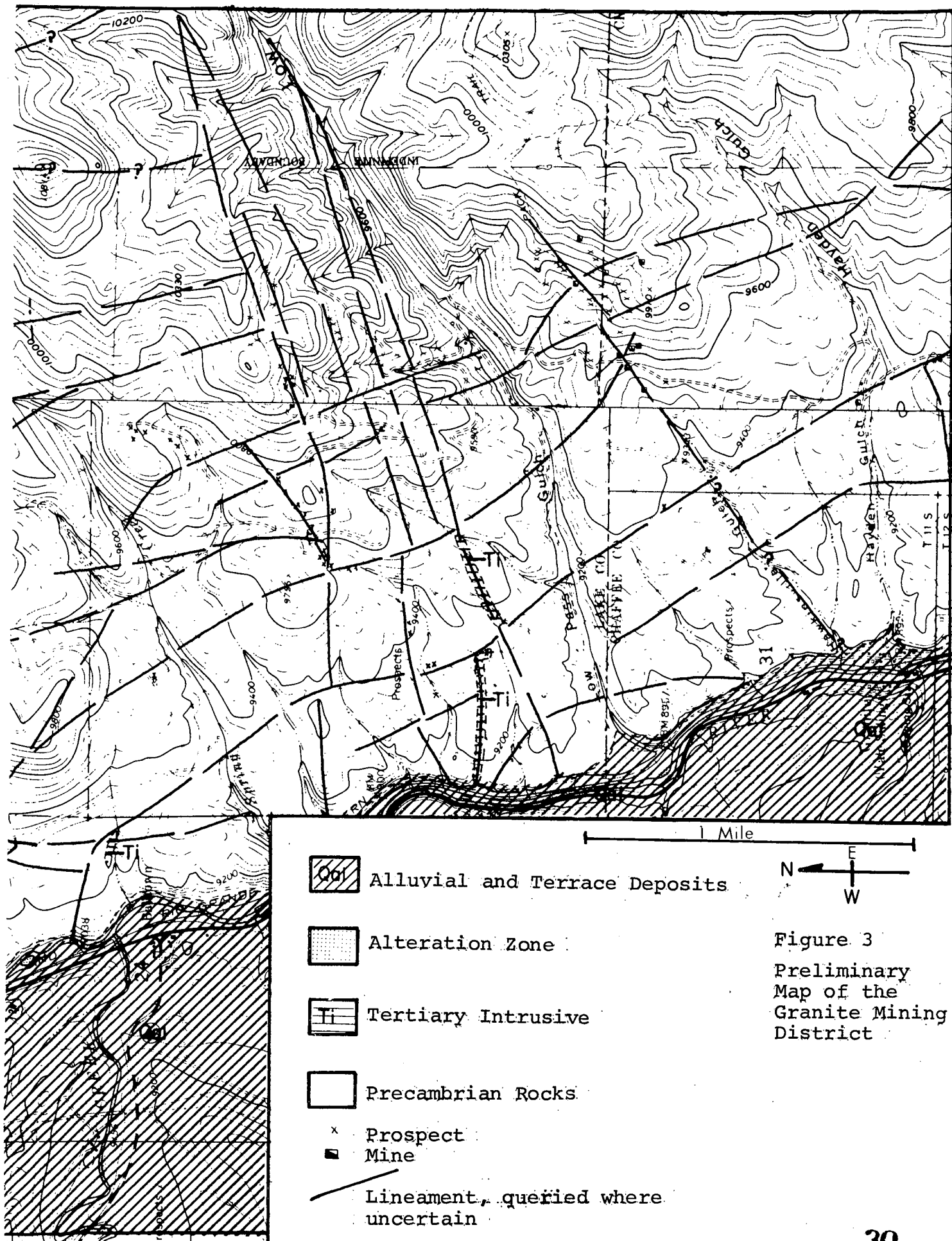


Figure 3  
Preliminary  
Map of the  
Granite Mining  
District

#### REFERENCES CITED

- Badgley, P. C., 1960, Tectonic relationships in central Colorado, in Guide to the geology of Colorado: Geol. Soc. America, Rocky Mtn. Assoc. of Geologists, and Colo. Sci. Soc., p. 165-169.
- Behre, C. H., 1932, The Weston Pass mining district, Lake and Park counties, Colorado: Colo. Sci. Soc. Proc., v. 13, no. 3, p. 53-75.
- Behre, C. H., 1953, Geology and ore deposits of the west slope of the Mosquito Range: U. S. Geol. Survey Prof. Paper 235, 176 p.
- Vanderwilt, J. W., ed., 1947, Mineral resources of Colorado: Colo. Mining Assoc., Denver, Color., p. 46-47.

## RESEARCH ACTIVITIES OF LEE H. JEFFERIS

1 October 1971 - 31 March 1972

### 1.0 General

Studies carried out to date include a thorough examination and mapping of the rocks of the Buena Vista Quadrangle of central Colorado. This research, begun in the summer of 1970 includes two summers in the field and the intervening periods working on the published material on the geology of the study area and on studies of remote sensor data collection techniques and technology. This research has generated a geologic map for the previously unmapped area along with maps which show the interpreted geology from various remote sensors on the NASA aircraft. In addition to the Buena Vista Quadrangle which was mapped before obtaining the remote sensor data, the NW 7½ quadrangle of the Cameron Mountain Quadrangle, adjacent to the Buena Vista area was mapped from the remote sensor data to provide a test of the data in unknown areas.

### 2.0 Specific Research

The examination and evaluation of the NASA remote sensor data, primarily from NASA Missions 101, 168 and 184, were carried out by interpretation using a stereoscope (where applicable) on a light table. This work was completed prior to the field season of 1972 when the final field checks are to be carried out on the data interpretations. Table I shows the data which were examined and used to make geologic and lithologic maps of the study area. Table II gives the film/filter combinations which were selected for the multiband photography on Mission 168 and the reasons for their selection.

Results of the interpretation of the remote sensor data indicates that the color photography provided the most useful information for the study, while other types of photography were also found to be quite useful for the mapping of the area. In general it was found that both the thermal infrared (IR) and side-looking radar imagery (SLAR) contained less information useful for geologic study and were most useful when worked in con-

TABLE I.

Remote sensor data used in the study of the Buena Vista and Cameron Mountain areas

Data	Mission	Approx. Scale	Coverage	Remarks
Color Photography	101	1:110,000	complete	some cloud problems
	168	1:20,000	complete	good photography
	184	1:20,000	North $\frac{1}{4}$	better than 168
Color IR photography	101	1:110,000	complete	cloud problems
	168	1:20,000	complete	good photography
	184	1:20,000	North $\frac{1}{4}$	best of color IR
Multiband photography	168		2 lines	OK
Low Sun Angle photo.	168	1:30,000	2 lines	sun too high for topography
Thermal IR imagery	168		2 lines	
	184		4 lines	good imagery
SLAR imagery	168	1:250,000	2 lines	poor quality

\*  
TABLE II.

Film/filter combinations for Mission 168 Photography

Band No.	Film / Filter	Transmission Range	Objectives
1	2402/W32 + W2c	390 - 500 nm. and 610 - 750 nm. (- green)	subdue vegetation and enhance rock contrasts
2	2402 / W8	475 - 750 nm (- blue)	reduce shadows and haze enhance rock discrimination
3	SO 246/ W25	590 - 1000 nm (red + IR )	Rock discrimination
4	SO 246 / W 87	750 - 1000 nm (IR)	Enhance vegetation contrast

\* After Bonanza Project Report 72-1, p. 6.

junction with photography. The results for the various sensors studied are given below.

## 2.1 Color and Color Infrared Photography

These two are discussed together because the results of interpretation were very similar. I prefer color photography because it gives the most faithful representation of the rock colors and because I could map the rock contacts with good accuracy on it. The same contacts were available on color IR photography and on Forest Service panchromatic photos, if the interpreter knew what to look for, but they were initially most obvious on the color photography.

On both the color and color IR photography contacts for rock units were easily mapped, and a complex set of fracture patterns were mappable in the areas of Precambrian rocks. These both must be checked in the field to verify the accuracy of the interpretations.

The effect of scale on the photography was also studied and it was found that much lithologic and structural information was available on both scales (large - 1:15 to 25,000 and small - 1:100,000). For detailed studies of lithologic contrasts I preferred to use the 1:20,000 photography, although very good information was available from the 1:110,000 photography when using the Old Delf Scanning Stereoscope at 4X magnification. Obviously, one must select the proper scale for the type of research being carried out, and the results of this work indicate that the small scale is excellent for regional work on both structural and lithologic features while the large scale is superior for locating contacts and doing a fracture analysis in local areas.

## 2.2 Multiband Photography

The problems with the Mission 168 photography were discussed in the Bonanza Report 72-1. Analysis in this study indicates that bands 1 and 2 gave the best information while bands 3 and 4 were difficult to use and provide information of lower quality.

The analysis of the multiband was carried out in an area of Precambrian rocks where a quartz monzonite intrusive cross-cuts dark biotite-rich rocks. The photos were studied using a

stereoscope which gave the added advantage of showing where trees were giving a dark tone to the terrain rather than the dark color of the rocks.

### 2.3 Low Sun-Angle Photography

This black and white photography which provided good coverage in many areas of the Bonanza Project was flown too late in the day for the topography of the Buena Vista quadrangle to provide the data on fracture patterns which would be comparable to the SLAR imagery obtained from NASA. However, the photography was of superior quality and could easily be used as high sun photography for more conventional photogeologic study.

### 2.4 Thermal Infrared Imagery

Thermal infrared imagery was obtained over most of the area of investigation, the only gap being along one line in the 184 Mission. Analysis of the imagery indicated that many of the contacts mapped in the field could be found on the imagery, though not all the mapped units were identifiable on the imagery. The most useful applications found from the study would be the mapping of the contact between the valley fill in the Arkansas Valley and the Precambrian rocks, and the construction of an outcrop map which would be easily done when the scale of the imagery is close to that of the base map. The major problem encountered in using thermal IR imagery was the transferring of data from imagery to base map, as many of the identifiable features on the map are difficult to locate on the imagery. If possible, the best way to aid in this transferal is to use some large scale photography to aid in the identification of stream patterns and outcrop patterns.

### 2.5 SLAR Imagery

The NASA DPD-2 imagery used for the study was of poor quality and provided very limited information for the research. In one image which was flown the length of the study area a number of very long lineaments were mapped. None of these linear features were observed on any of the photography studied, and



if the linears are in fact expressing structural features of the area and not chance topographic alignments, then the SLAR image is capable of providing good additional data on the structural geology of the area.

## 2.6 Conclusions

The result of the study of the various sensing systems indicated that photography is the best over-all remote sensor for geologic studies. Although I preferred the color photography to color IR, I feel that both types of photography provide essentially the same information and that the choice is based more on the preference of the interpreter than on the superiority of one type of photo.

At this time it appears that multiband photography, low sun-angle photography, thermal infrared imagery, and SLAR imagery are very specialized techniques which could be used in conjunction with more conventional photography and (or) used in the solving of specific problems where they can give specialized information.

## RESEARCH ACTIVITIES OF DANIEL H. KNEPPER, JR.

1 October 1971 - 31 March 1972

### 1.0 General

To date, the primary thrust of this research has been toward the preparation of a geologic map of an area of approximately 1,100 square miles in central Colorado, centered along the Rio Grande Depression. The Rio Grande Depression, or Rift Zone, is a major tectonic element of Late Tertiary age, extending from southern New Mexico northward for some 600 miles into central Colorado. The structurally and topographically low San Luis and Arkansas Valleys follow the internal portion of the depression. The bordering mountain ranges on the west and east are composed of Precambrian igneous and metamorphic rocks, complexly deformed Paleozoic sedimentary rocks, and Tertiary igneous plutons. Oligocene volcanic rocks of the Bonanza volcanic field form the mountains in the southwestern part of the area (fig. 1). The internal portion of the depression is filled with semi-consolidated valley-fill sediments of the Miocene-Pliocene Dry Union Formation.

Geologic mapping of the study area has been accomplished by 1) compilation of previous geologic mapping in the area, 2) detailed and reconnaissance field mapping (this study), and 3) interpretation of various remote sensor data with subsequent field checks. The major activities have been 1) the interpretation of remote sensor data and attempts to evaluate video image processing (VIP) for regional geologic mapping and 2) completion of the geologic mapping and compilation of a geologic map on a 1:62,500 topographic base.

### 2.0 Specific Research

#### 2.1 Sensor Data Interpretation

Low-altitude color and color infrared (IR) photography (Missions 168 and 184) and low sun-angle photography (Mission 168) were utilized in geologically mapping the remaining unmapped portions of the study area after three months of field work. The color photography was found superior to color IR for general rock-

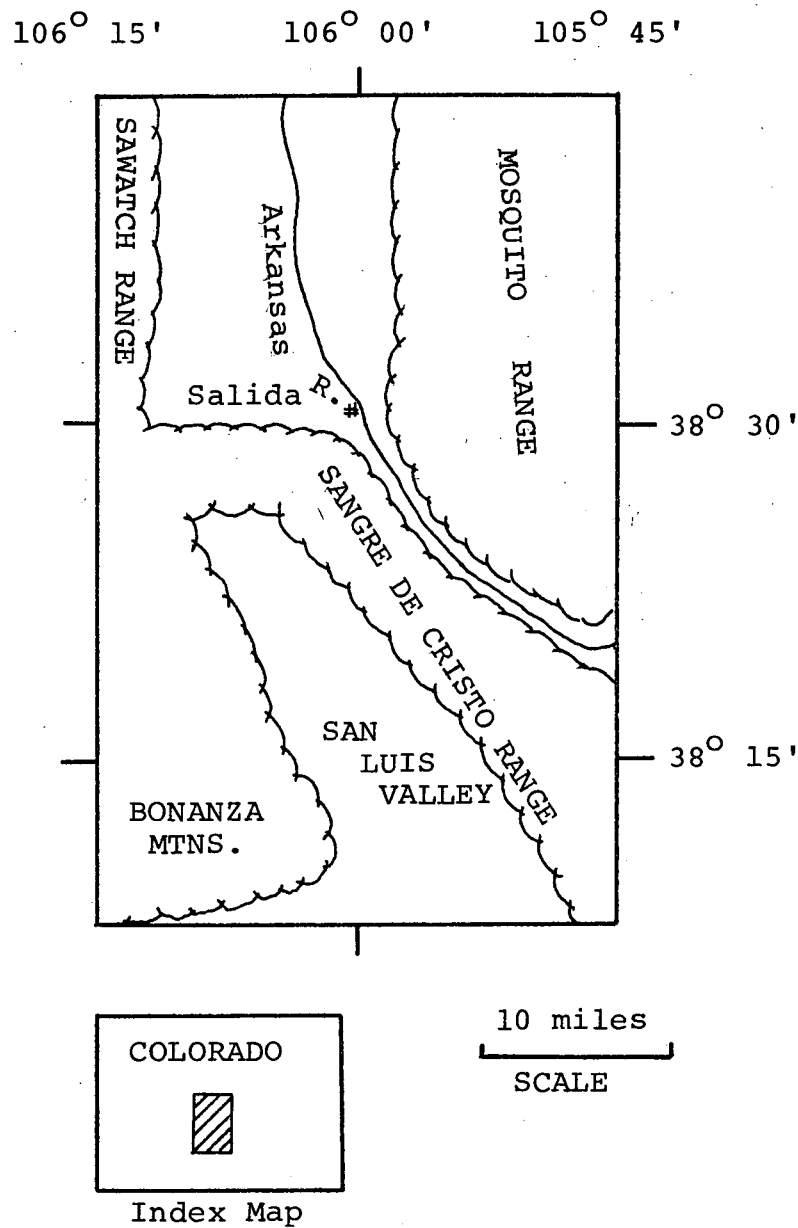


Figure 1. Location of Regional Geologic Mapping Project along the Rio Grande Depression.

type discrimination. However, color IR photography was best for 1) discriminating between the several types of Precambrian rocks and 2) photographically measuring dips in the Pennsylvanian-Permian red beds. The Precambrian rocks are dominantly shades of red or pink with gray and black rocks being abundant. The red bed sequence is composed of rocks of red or pink colors with thick interstratified beds of gray and gray-green sandstone. The color IR photography apparently has the ability to better discriminate between subtle shades of red or pink (i.e., greater contrast between subtle color changes in the red). The overall similarity of color between these two highly contrasting rock types accounts for the same types of sensor data being useful within each sequence.

Low sun-angle photography (LSAP) was found extremely useful for mapping Quaternary pediment and stream terrace surfaces within the Arkansas Valley. The surfaces are defined by their heights above modern stream base and above each other. The shadowing produced by low sun angles helps to accurately delineate these surfaces and makes them easier to find on the LSAP than on photography as normally taken at high sun angles. The sun angle was low enough to enhance topographic differences on the order of 10 feet, but high enough to allow much detail to be detected, except in the most mountainous terrains, where massive shadowing was produced.

## 2.2 Video Image Processing

Video image processing (VIP) was applied to selected imagery to test and evaluate its usefulness in regional geologic mapping. The processing was done by Mr. R. Biniki (MMC) with some assistance from the author. Color Polaroid photographs of 1) the original image on the TV display (B/W), 2) the processed image, both focused and de-focused, and 3) the density level slices were supplied to the author for analysis.

Thermal IR imagery was studied in an attempt to 1) discriminate between adjacent volcanic and sedimentary rocks and 2) detect faults in the vicinity of Poncha Hot Springs. Rock discrimination

generally was unsuccessful at all slicing levels utilized. Several known faults were detected and several thermal linear of as yet unknown origin were found.

Color IR transparencies were processed in an attempt to

- 1) discriminate between limestone and quartz monzonite and
- 2) detect faults and fractures in the quartz monzonite.

Rock discrimination generally was unsuccessful. Detection of linear features was very successful and a fracture map prepared from the processed image compared favorably with a similar map produced by stereoscopic viewing of the original transparency. The major interpretational differences resulted from the inclusion of linear features of non-geologic significance (not fractures or faults) on the processed image fracture map. In addition, the time and expense involved with VIP was not proportional to an increase in geologic information as compared to conventional interpretation methods and was, therefore, judged unnecessary for this study.

Multiband photography was processed in the same area as the above color IR transparencies. The results again did not indicate a significant increase in geologic information over more conventional interpretation methods.

## RESEARCH ACTIVITIES OF RONALD W. MARRS

1 October 1971 - 31 March 1972

### 1.0 General

The evaluation of remote sensing techniques for geologic mapping in the Bonanza volcanic center, which was begun in June, 1970, is now nearing completion. During the period covered by this report, evaluations of multiband photography, low sun-angle photography, thermal infrared imagery, and side-looking airborne radar were completed, and are summarized herein. A detailed discussion of the entire investigation conducted in the southwest Bonanza volcanic field is presently being prepared<sup>1/</sup>.

### 2.0 Specific Research

#### 2.1 Multiband Photography

Multiband photography of the Bonanza volcanic center was flown to ascertain if lithologic contrasts could be enhanced by 1) selectively photographing in those bands where contrasts between various lithologic units is greatest, based on ground spectral reflectance measurements; 2) filtering out or subduing the photographic bands where the expression of non-geologic features (vegetation, haze, etc.) is strongest; and 3) combining or subdividing various photographic bands by video image processing and density slicing techniques to produce enhanced contrasts. The Bonanza area multiband photography did not fully produce the desired results. The combination of subtle reflectance differences between the volcanic lithologies, and "noise" produced by soils, vegetation, and variable surface properties of single rock units thwarted all attempts to discriminate the volcanic lithologies. Very little new information was gained from multiband photography that was not readily detectable on color and color infrared photography.

The above results indicate that multiband photography is not yet a tool for routine geologic investigations. Continued

---

<sup>1/</sup> Marrs, R. W., (in progress), Application of remote sensing techniques to the geology of the Bonanza volcanic field: Colorado School of Mines Ph.D. thesis.

research should be aimed at determining the utility of multi-band photography for solving specific geologic problems. Test areas should be chosen where the geology is relatively simple and "noise factors" are at a minimum.

## 2.2 Low Sun-Angle Photography

One line of low sun-angle photography (LSAP) was flown over the Bonanza volcanic terrain in order to test the capability of LSAP for enhancing topographically-expressed structures. The scale of the LSAP (1:24,000) proved too large; the major structures were obscured by unnecessary detail. A scale of 1:100,000 or smaller might be more suitable for this application.

Certain low-relief features were enhanced on the Bonanza area LSAP. Low ridges corresponding to sedimentary bedding form a distinct shadow pattern which permits the sedimentary outcrops to be easily distinguished from the even-textured volcanic rocks. Low-relief structures such as mounds and micro-drainages occurring on sediments and gravel terraces are well-shown on the LSAP. Such detail provides very valuable information for discrimination and identification of these low-relief surfaces.

## 2.3 Side-Looking Airborne Radar

Concentric and radial faults of the Bonanza caldera provide an excellent opportunity to test the effect of look direction on side-looking airborne radar (SLAR). Four lines of radar were flown over the Bonanza volcanic center on Mission 168. Each provided radar imagery with a different look direction (NW, NE, SE, and SW). In addition, two lines of Mission 184 radar provided imagery of the Bonanza caldera with east and west look directions. Evaluation of all this radar resulted in several significant conclusions.

1. High-altitude radar provides good enhancement of regional topographic features, but little or no tonal or textural information useful in discrimination of lithologies.

2. The "best" look direction for enhancement of regional topography is down-slope from a flight line running parallel or nearly parallel to the features to be enhanced.

3. Except in very special cases, where the "down-slope consideration" warrants it, there is little justification for flying opposite-looking radar lines.

4. One or two properly-chosen flight lines contain nearly as much information for geologic mapping as four lines looking in four directions. In the Bonanza area, where the topography is largely non-directional and there are definite down-slope considerations, the combination of NE- and SE-looking radar revealed 94 percent of the information found on the suite of four Mission 168 radar lines. This percentage should be even higher in areas where a dominant slope-direction is present.

An accurate appraisal of the relative utility of LSAP vs. SLAR was impossible due to difference in scale. However, attempts to use both in the Bonanza area suggest that LSAP is generally superior because it provides better resolution in addition to the topographic enhancement common to both. On the other hand, the SLAR would be the more useful tool if weather or look direction were a critical constraint.

#### 2.4 Thermal Infrared Imagery

An initial evaluation of daytime thermal infrared (IR) imagery was completed in 1970, and the results of this test were reported in the Mission 105 Summary Report<sup>2/</sup>. More recently, evaluations of the daytime and pre-dawn thermal IR imagery flown on Missions 168 and 184 have been completed. These evaluations confirm the conclusions reached in earlier work. The daytime imagery is dominated by thermal contrasts related to topography, but thermal contrast can also be seen which is related to faults. The topographic effects are somewhat subdued on the pre-dawn thermal IR imagery but are still present in areas of high relief. However, in areas of lower relief, many of the major thermal contrasts are related to soil moisture and vegetation. Some of these patterns are in turn, related to faulting and (or) bedrock-

<sup>2/</sup> Lee, Keenan and others, 1971, NASA Mission 105, Flight 5, Summary Report, p. 38-41.



soil relationships. Pre-dawn thermal imagery appears to provide the most important geologic data, and is most effective in areas of low relief. Unfortunately, the pre-dawn thermal imagery, even in the low-relief areas, revealed no thermal contrasts that could be uniquely related to lithology.

## 2.5 Conclusions

The program for the evaluation of remote sensor data for geologic mapping in the Bonanza area has demonstrated that color, color infrared and low sun-angle photography, side-looking airborne radar imagery, and thermal infrared imagery provide considerable information about topography, soil moisture, vegetation, and surface hue, tone, and texture which can be related to the geology. Geologic structures can be located and identified; surficial deposits and sedimentary rocks can be mapped; the various volcanic units of the Bonanza area cannot be distinguished by the remote sensing techniques tested.

APPENDIX C  
MMC SCIENTISTS' RESEARCH

## APPENDIX C

### MARTIN MARIETTA CORPORATION Denver Division

#### Report Contributor:

R. M. Biniki  
R. C. Hulstrom  
J. R. Muhm  
S. A. Stadjuhar  
K. E. Worman

1.	Introduction	1-1
2.	Atmospheric Science Research and Support	2-1
2.1	Atmospheric Science Support Activities	2-1
2.1.1	Ground Meteorological Measurements	2-1
2.1.2	Solar Radiation Measurements	2-3
2.2	Laboratory Support	2-9
2.3	Atmospheric Research Activities	2-9
2.3.1	Transmission Characteristics	2-9
2.3.2	Measurement of Total and Diffuse Radiation	2-10
2.3.3	Effects on the Reflectance Spectrum of a Target	2-16
2.4	Development of Improved Techniques for Measuring Field Reflectance and Solar Radiation	2-19
3.	Line Scanner Image Processing and Enhancement	3-1
3.1	Data and Equipment	3-1
3.2	Processing Techniques	3-1
3.3	Data Quality	3-8
4.	Infrared Spectrometer Data Reduction	4-1
5.	Investigation of Thermal Infrared Anomalies	5-1
6.	Image Processing	6-1
6.1	Background and Theory	6-1
6.2	Equipment	6-1
6.4	Data Collection	6-2
6.4	Technical Procedures and Discussion	6-3
6.4.1	Multispectral Photography	6-4

6.4.2	Color Photography	6-11
6.4.3	Color Infrared Photography	6-11
6.4.4	Low Sun Angle Photography	6-11
6.4.5	Thermal Infrared Imagery (Predawn)	6-11
6.4.6	Side-Looking Airborne Radar	6-11
6.5	Summary	6-12
6.6	Conclusions	6-14
6.7	Recommendations	6-14
6.7.1	Data Collection	6-14
6.7.2	Processing	6-14
7.	Field Support Activities	6-15

## Figures

1-1	Bonanza Test Site (NASA Site 185) . . . . .	1-2
2-1	Location of Mx 168 Meteorological Station and Nature of Circulation Pattern . . . . .	2-2
2-2	Meteorological Measurement Station Used During Mx 168 at Villa Grove . . . . .	2-3
2-3	Meteorological Ground Support Measurements . . . . .	2-4 thru 2-6
2-4	Global Solar Radiation, 0.3 to $3\mu$ , at Villa Grove During Mx 168 - June 14, 1971 . . . . .	2-7
2-5	Global Solar Radiation, Mx 168, 0.3 to $3\mu$ , June 15, 1971, (Villa Grove). . . . .	2-8
2-6	Global Solar Radiation, Mx 168, 0.7 to $3\mu$ , June 15, 1971, (Villa Grove). . . . .	2-8
2-7	Spectral Measurements of Global Solar Radiation . . . . .	2-11
2-8	Global Diffuse Solar Radiation. . . . .	2-12
2-9	Optical Extinction Coefficient Model - Elterman, 1968. . . . .	2-14
2-10	Spectral Measurements of the Ratio of Diffuse to Total Radiation as Functions of Solar Zenith Angle. . . . .	2-15
2-11	Mounting Bracket for ISCO Fiber Optics Bundle, Used for Measuring Global and Reflected Radiation . . . . .	2-17
2-12	Instrumentation and Setup for Measuring Field Reflectance and Global Radiation. . . . .	2-18
2-13	Reflected Measurements and Effects of the Nature of Incoming Radiation. . . . .	2-19
2-14	Comparison of Reflectance Determinations Using Actual and Computer Measurements. (Time lapse equals 6 min.). . . . .	2-22
2-15	Comparison of Reflectance Determinations Using Actual and Computer Measurements. (Time lapse equals 22 min.). . . . .	2-23
2-16	Comparison of Reflectance Determinations Using Actual and Computer Measurements. (Time lapse equals 29 min.). . . . .	2-24

## Figures

2-17	Comparison of Reflectance Determinations Using Actual and Computer Measurements. (Time lapse equals 59 min.). . . . .	2-25
2-18	Comparison of Reflectance Determinations Using Actual and Computed Measurements. (Time lapse equals 71 min.). . . . .	2-26
2-19	Comparison of YSI and Measurements . . . . .	2-27
2-20	Computer (CDC 6400) Analysis Tabulation of Field Data. . . . .	2-29
3-1	Laboratory Setup of Image Display Equipment . . . . .	3-2
3-2	Line Scan Image Processing Setup. . . . .	3-3
3-3	"Black Box" Video Mixer with Variable Gain. . . . .	3-5
3-4	Iso-Density Contour Generators . . . . .	3-6
5-1	AGA Thermovision Overlooking Valley . . . . .	5-2
5-2	AGA Thermovision Image Showing Anomalous Linear Feature (1), and Ground Observer with Butane Torch (2). . . . .	5-2
5-3	Seismic Profiling Across Anomalous Area. . . . .	5-3
5-4	Typical Seismogram Showing First Arrivals. . . . .	5-4
5-5	Time-Distance Plot, Reverse Profile. . . . .	5-6
5-6	Section View Through Valley. . . . .	5-7
6-1	Multispectral Photo (620-1000nm) of Test Area Showing Control Points A and B . . . . .	6-5
6-2	Video-Processed Photo of Test Area Using Eight-Slice Density Scale . . . . .	6-6
6-3	Video-Processed Photo of Test Area Defocused Eight-Slice Density Scale. . . . .	6-6
6-4	Geologic Sketch Map of Test Area . . . . .	6-7
6-5	Test Area in New Setup With Sketch Map Superimposed . . . . .	6-8
6-6	Video-Processed Photo of Contiguous Area . . . . .	6-9
6-7	Video-Processed Photo of Area Contiguous to Test Area . . . . .	6-9
6-8	Video-Processed Photo of Area Contiguous to Test Area . . . . .	6-10

Tables

6-1	Colors Assigned to Densities for Figures 6-2 and 6-3 . . . . .	6-7
6-2	Colors Assigned to Densities for Figures 6-5, 6-6, 6-7, and 6-8 . . . . .	6-8

## 1. INTRODUCTION

This report summarizes and discusses Martin Marietta's research activities in support of the third year of the Bonanza Program. Primary emphasis this year involved the development of a straightforward procedure for field measurement and computer reduction of atmospheric parameters which have been shown to affect remote sensor data. To a lesser extent, we continued our experimentation with video enhancement of imagery, and with attempts to electronically enhance and display IR scanner data.

Data acquisition was not nearly the problem this year as had been the case in previous years. Two missions, one in June and one in September, were flown and each yielded considerable data. Nevertheless, two tasks programmed for this year could not be performed because data were not available. One was the continued experimentation with computer recognition of rock outcrops using infrared spectrometer data; the other was to have been our first attempt at handling and interpreting multichannel scanner data. We still have no firm idea when multichannel scanner data will be available to us.

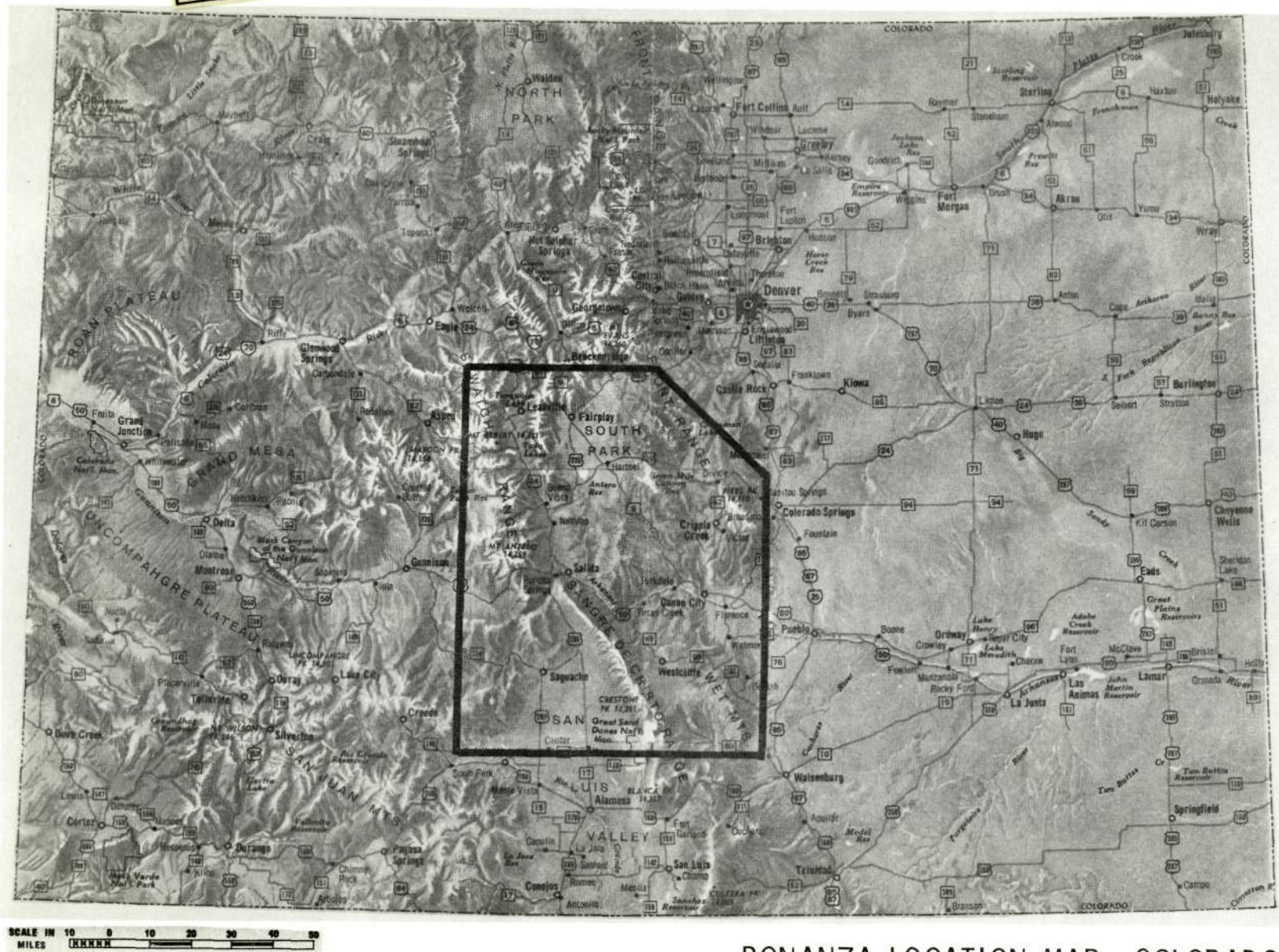
It is evident at this point that a changing emphasis is being applied to the program tasks as originally planned. Atmospheric effects, hardly mentioned at program inception, have now taken on major significance. Conversely, experimentation involving enhancement of photography has now been confined to use of the video processing system. We think these total efforts are more realistic and more efficient from the point of utilizing Martin Marietta's unique resources. Figure 1-1 shows the location of the Bonanza test site (NASA Site 185).



Reproduced from  
best available copy.



1-2



## BONANZA LOCATION MAP, COLORADO

Figure 1-1 Bonanza Test Site (NASA Site 185)

## 2. ATMOSPHERIC SCIENCE RESEARCH AND SUPPORT

Activities during the third program year were generally divided into two categories. One consisted of atmospheric ground support of NASA aircraft Missions 168 and 184, and laboratory support involving calibration and checkout of the CSM ISCO spectroradiometer. The second category concerned research involving reflectance measurements and atmospheric effects on the nature of incoming solar radiation. The latter activity made up the major part of the total effort.

The atmospheric effects research was directed toward the specific problem of developing improved techniques to be used in compensating for atmospheric influences during reflectance measurements and to the general problem of establishing the nature of the temporal and spatial variances of atmospheric effects on the total solar radiation.

### 2.1 Atmospheric Science Support Activities

The following support activities were conducted during the past year.

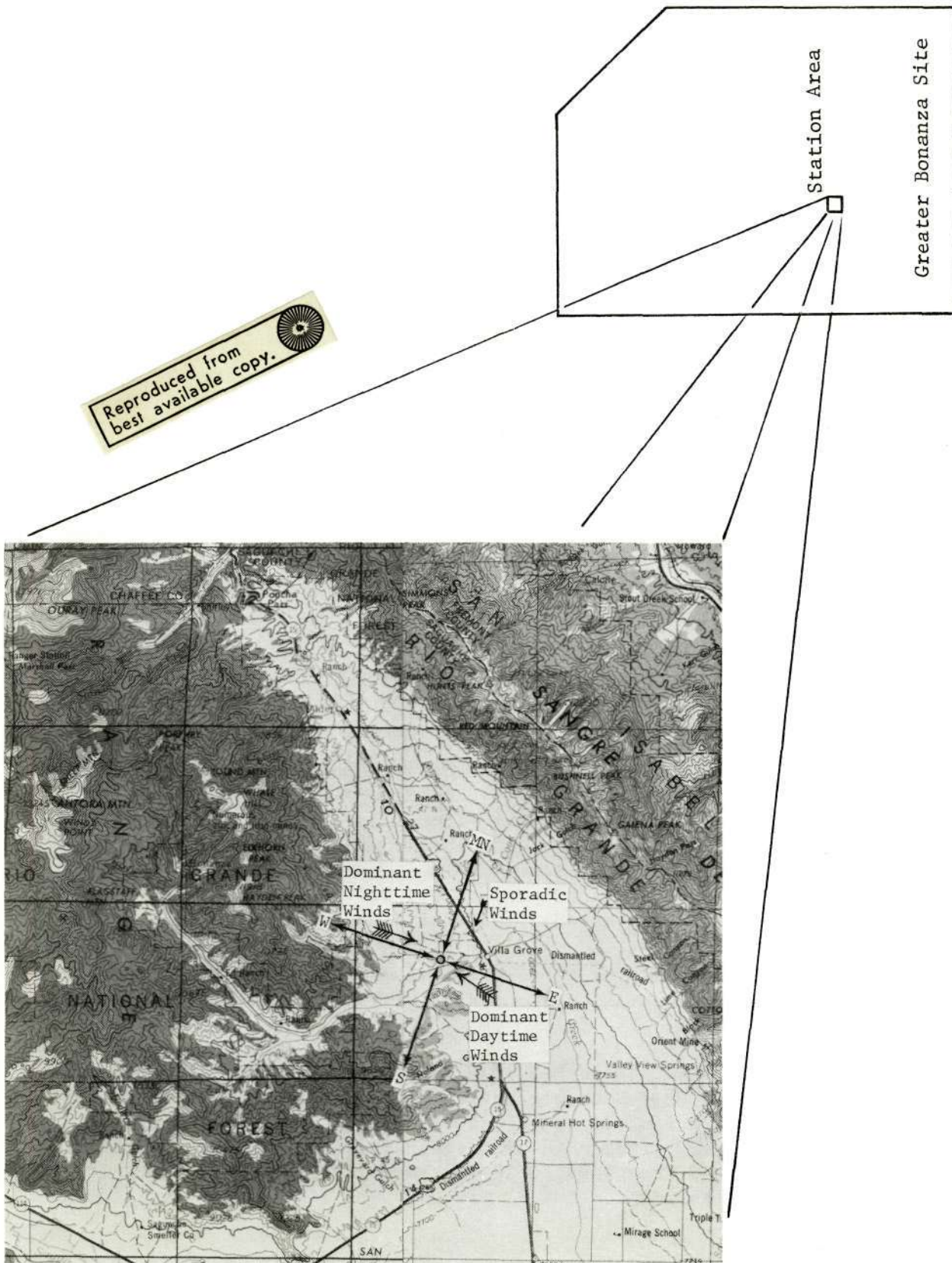
2.1.1 Ground Meteorological Measurements - During Mission 168 a meteorological measurement station was operated near Villa Grove (Figure 2-1).

The station was established to provide continuous meteorological data and to determine if the candidate site was indeed representative of the overall regional micrometeorological situation. The facility consisted of a mechanical weather station equipped with a rain gage shown in Figure 2-2. The measurements included rainfall (increments of 0.01 in.), temperature (-30 to + 120°F), wind run (average wind speed), and wind direction.

Figure 2-3 shows the meteorological ground support measurements for the entire mission from 0830 (MST) on June 14 to 0800 on June 17, 1971.

As is shown on Figure 2-3, the region received approximately 0.01 in. of rain near noon of the day preceding the nighttime thermal infrared mission (11 hours before overflight). Following the rainfall, an increase in air temperature to 75°F was experienced, along with winds of 20 to 30 mph average speed; therefore, it is concluded that the rainfall probably had little, if any, effect

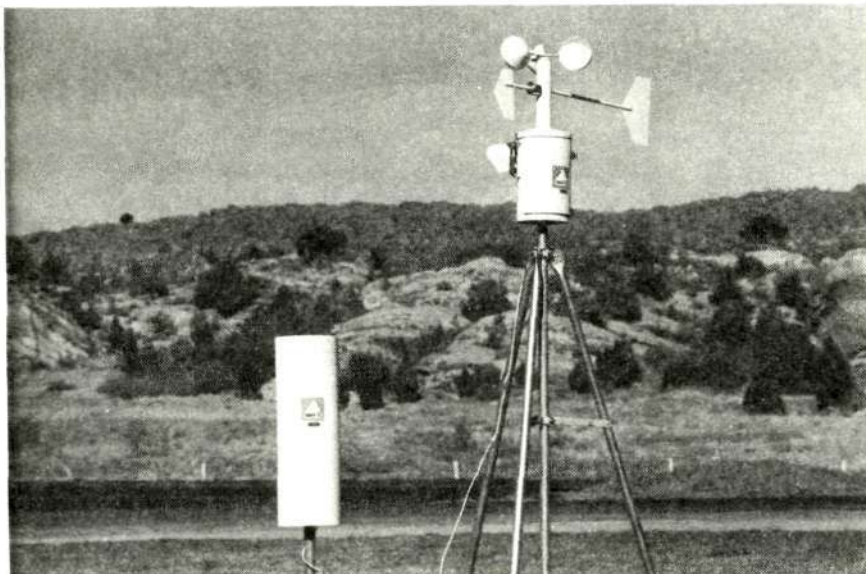




Reproduced from  
best available copy.

Figure 2-1 Location of Mx 168 Meteorological Station and Nature of Circulation Pattern

on the thermal characteristics of the ground features that were observed during the subsequent nighttime mission.



*Figure 2-2 Meteorological Measurement Station Used During Mx 168 at Villa Grove*

The Villa Grove site measurements indicate the location is extremely representative of typical upslope/downslope, mountain/valley, micrometeorological conditions. This is indicated by the dominant wind directions shown in Figure 2-1.

Based on the exploratory meteorological measurements made during Mission 168, the Villa Grove site is recommended as a standard meteorological measurement site for the region. In addition, existing data from the site provides a representative array of meteorological parameters.

2.1.2 Solar Radiation Measurements - Measurements of the total (global) solar radiation characteristics were made during Mission 168 at the Villa Grove site. The measurement equipment involved two Eppley pyranometers, one equipped with a WG-7 filter, transparent from 0.3 to  $3\mu$ , and one equipped with an RG-8 filter, transparent from 0.7 to  $3\mu$ . The measurements shown in Figure 2-4 are for June 14, 1971 and the ones shown in Figures 2-5 and 2-6, are for June 15, 1971.

From inspection of the data, one can easily determine when the site was experiencing intermittent cloud shadowing. Cloud "bright spots" (areas of enhanced radiation equivalent to shadows) were observed to occur on both days. Such cloud influences have previously been investigated on the Bonanza program.





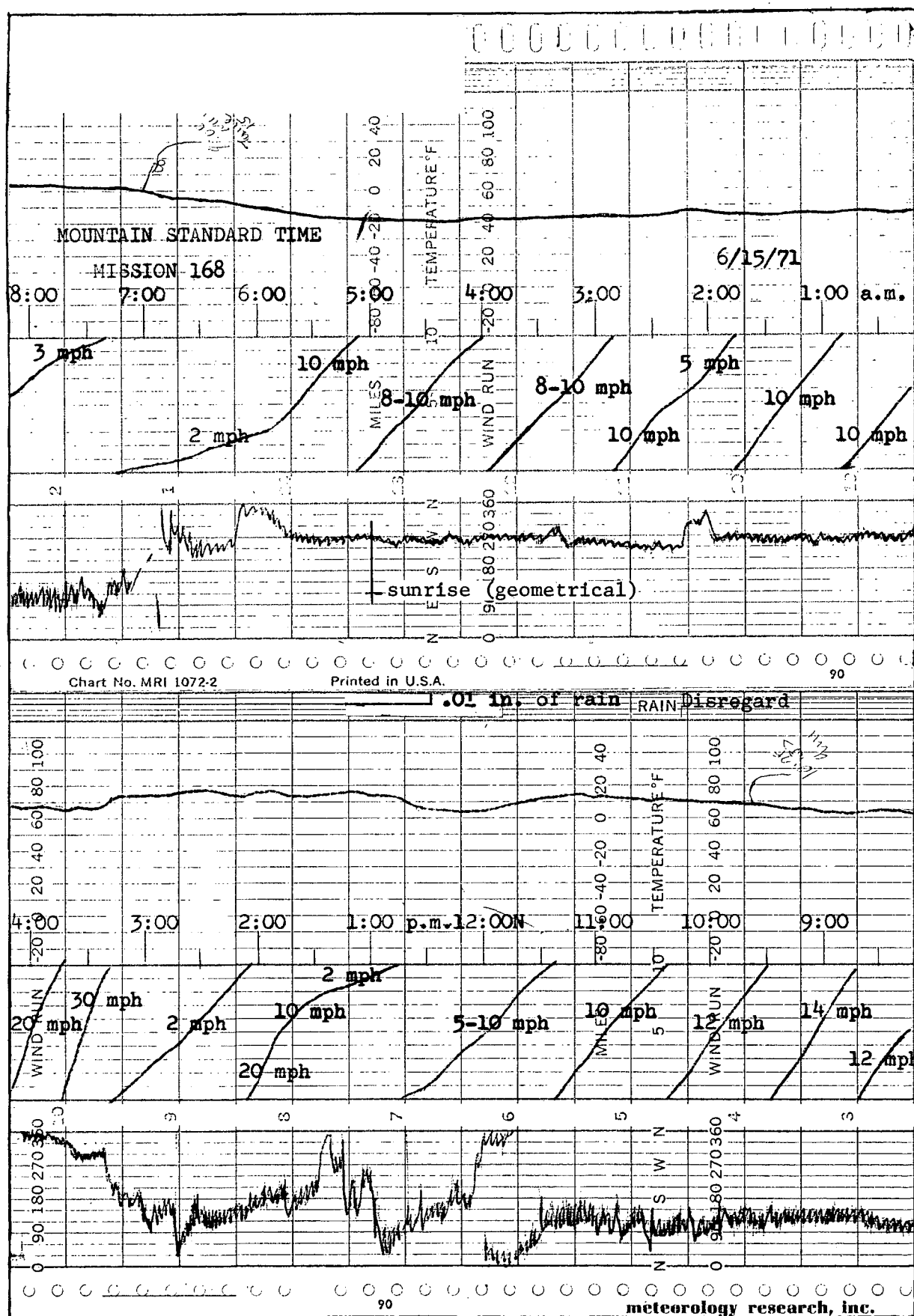


Figure 2-3 Meteorological Ground Support Measurements - Continued

2-5



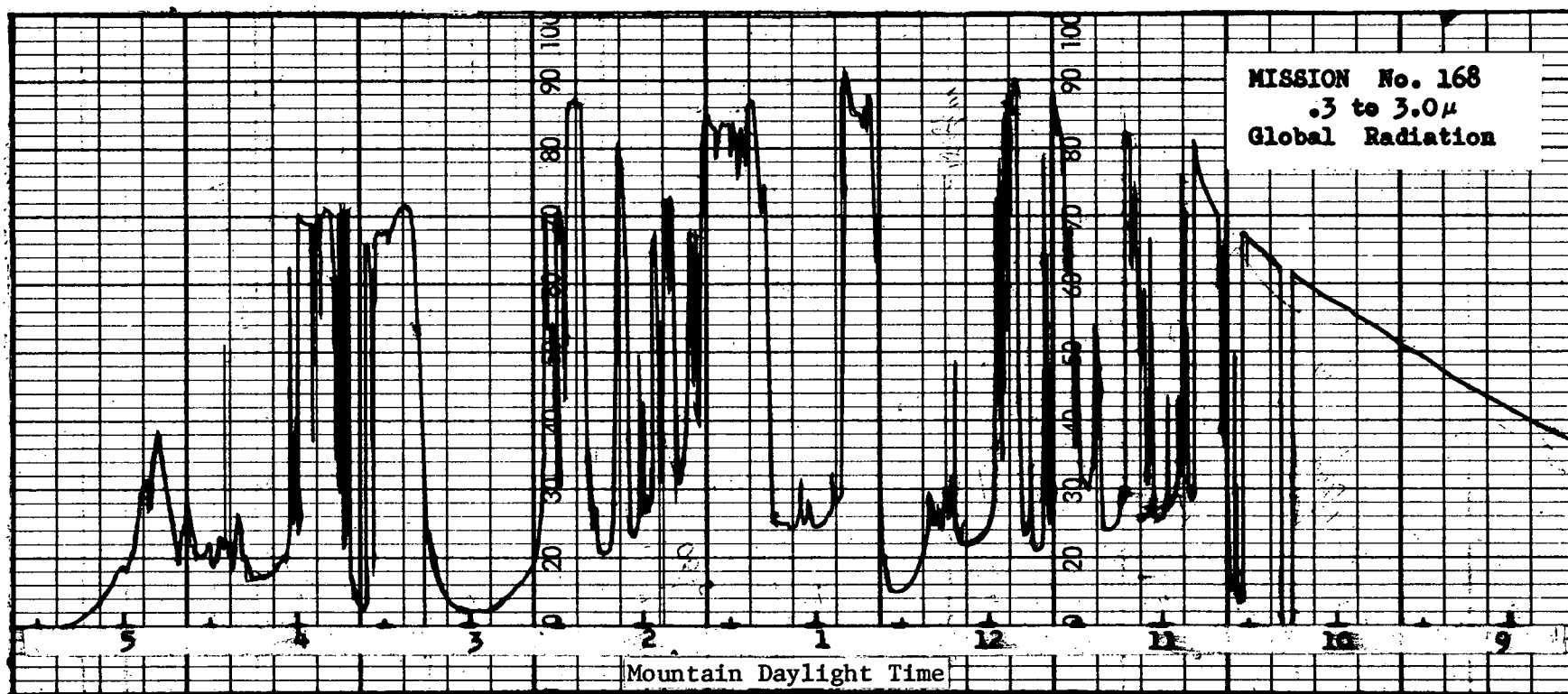


Figure 2-4 Global Solar Radiation, 0.3 to 3 $\mu$ , at Villa Grove  
 During Mx 168 - June 14, 1971



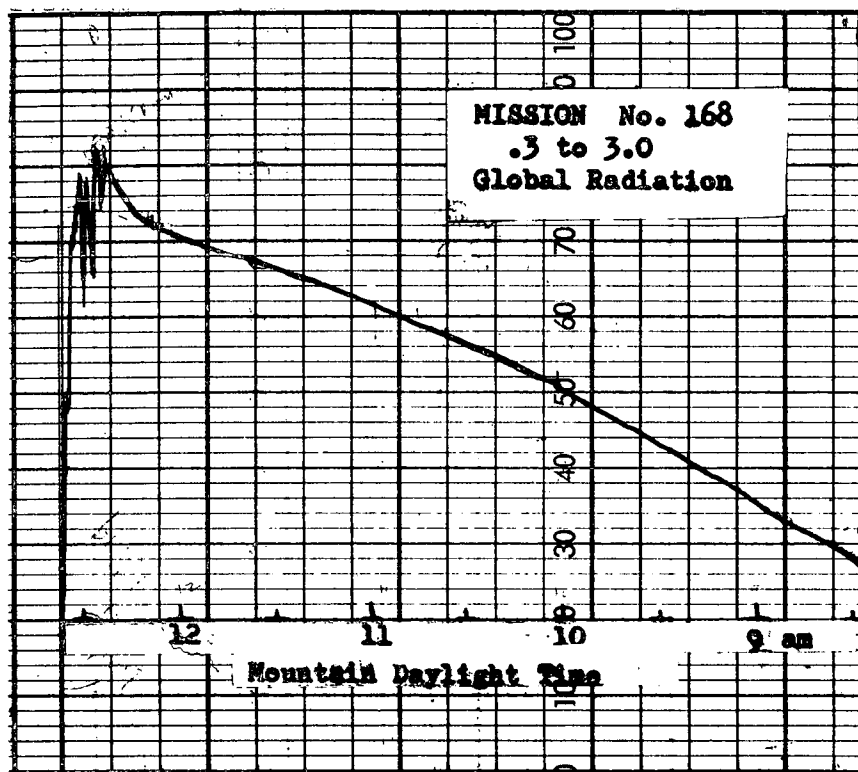


Figure 2-5 Global Solar Radiation, Mx 168, 0.3 to 3 $\mu$ , June 15, 1971, (Villa Grove)

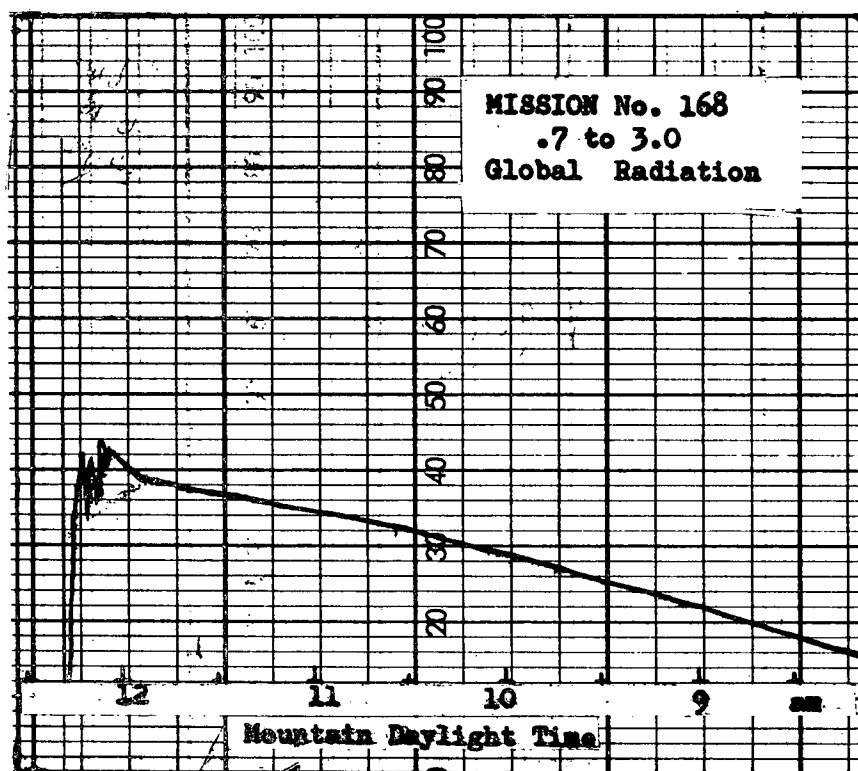


Figure 2-6 Global Solar Radiation, Mx 168, 0.7 to 3 $\mu$ , June 15, 1971, (Villa Grove)

During Missions 168 and 184 ratios of the diffuse-to-total (global) solar radiation were made in order to quantitatively define atmospheric clarity. During Mission 168 this ratio was approximately 11-to-15%; during Mission 184 this ratio was approximately 8-to-10%. The 8-to-10% ratio is considered to be characteristic of extremely "clear" conditions, whereas the 11-to-15% ratio is significantly "less clear." Ground photos taken during the missions show noticeably different "hazy" appearances, and a comparison of color aerial photography of the two missions displays dramatic differences in the degree of atmospheric clarity.

## 2.2 Laboratory Support

Laboratory support during the third program year consisted of a complete calibration of the CSM ISCO Spectroradiometer, serial number 14760. Calibration correction factors for both the direct incident head and a special six foot fiber optics probe were determined by measuring a known standard, ISCO lamp No. 319. A total of four sets of measurements from 380 to 1550 nanometers were supplied in order to determine the precision of the spectroradiometer. In addition to the calibration of the ISCO, numerous electronic checkout tasks were performed.

## 2.3 Atmospheric Research Activities

Research concerning the effects of the atmosphere on remote sensing performed during the third program year was directed toward providing an understanding of these effects and development of improved techniques for the measurement and subsequent analyses of data.

2.3.1 Transmission Characteristics - Spectral measurements of total\* and diffuse solar radiation were made using the ISCO spectroradiometer. Measurements in the wavelength region from 400 to 750 nanometers (nm) were made in 25 nm-increments and measurements in the region from 750 to 1350 nm were made in 50 nm-increments. Although the ISCO instrument is capable of a 15 nm half-band width in the 400 to 750 nm region and a 30 nm half-band width in the 750 to 1350 nm region, the 25 and 50 nm increments are the more commonly used. Therefore, in order to assure direct application of the atmospheric research to other on-going activities, the increments of 25 and 50 nm were used in the following analyses.

---

\*Total - global solar radiation - solar radiation on a horizontal surface from a field of view of 180°.

2.3.2 Measurements of Total and Diffuse Solar Radiation - A series of nine sets of measurements of total and diffuse solar radiation were made. The nine measurement sets correspond to relative air masses of 1.40, 1.40, 1.42, 1.46, 1.48, 1.55, 1.67, 1.73, and 1.82. Relative air mass is defined as the  $\sec \theta_0$ , where  $\theta_0$  is the solar zenith angle. The term,  $\sec \theta_0$ , simply describes the relative increase in geometrical path length through which the direct sunlight passes before reaching the ground. This parameter is used for comparison between given times of day, month, etc. The set of nine total solar radiation measurements is shown in Figure 2-7. Quite apparent are the effects of ozone (500-500 nm) and water vapor (940 and 1140 nm) absorption. The ISCO, using the 25 and 50 nm increments, sufficiently defines these particular atmospheric effects. The well known strong oxygen absorption band at 770 nm is not defined by such incremental measurements, although it can invariably be seen on the ISCO strip chart records. In fact, for analysis of atmospheric effects and reflectance measurements, the oxygen (770 nm) absorption band can be used for calibration of the ISCO wavelength scan from 750 to 1550 nm, instead of the customary procedure (wavelength-reader line-up) recommended by ISCO.

The large variations in total solar radiation shown occurring at 575 nm (Fig. 2-7) are thought not to be real; instead, they are probably the result of nonuniformity in reading the wavelength scan (400 to 750 nm).

The sets of total solar radiation measurements can best be compared to each other by comparing their respective air masses. A detailed analysis of these measurements in terms of specific atmospheric parameters is not within the scope of this report; instead, they will be used in the following analyses to relate such measurements to remote sensing activities.

The corresponding set of nine measurements of the diffuse sky radiation are shown in Figure 2-8. Because the atmosphere was extremely clear, the diffuse sky radiation is sharply peaked in the blue region (450 nm). The diffuse measurements exhibit a similar comparison to air mass as do the total solar radiation measurements. The diffuse measurements shown in Figure 2-8 readily point out that the characteristic irradiance of shaded targets is very different than in sunlit areas (Figure 2-7). As a consequence, their reflected "signature" is significantly altered.

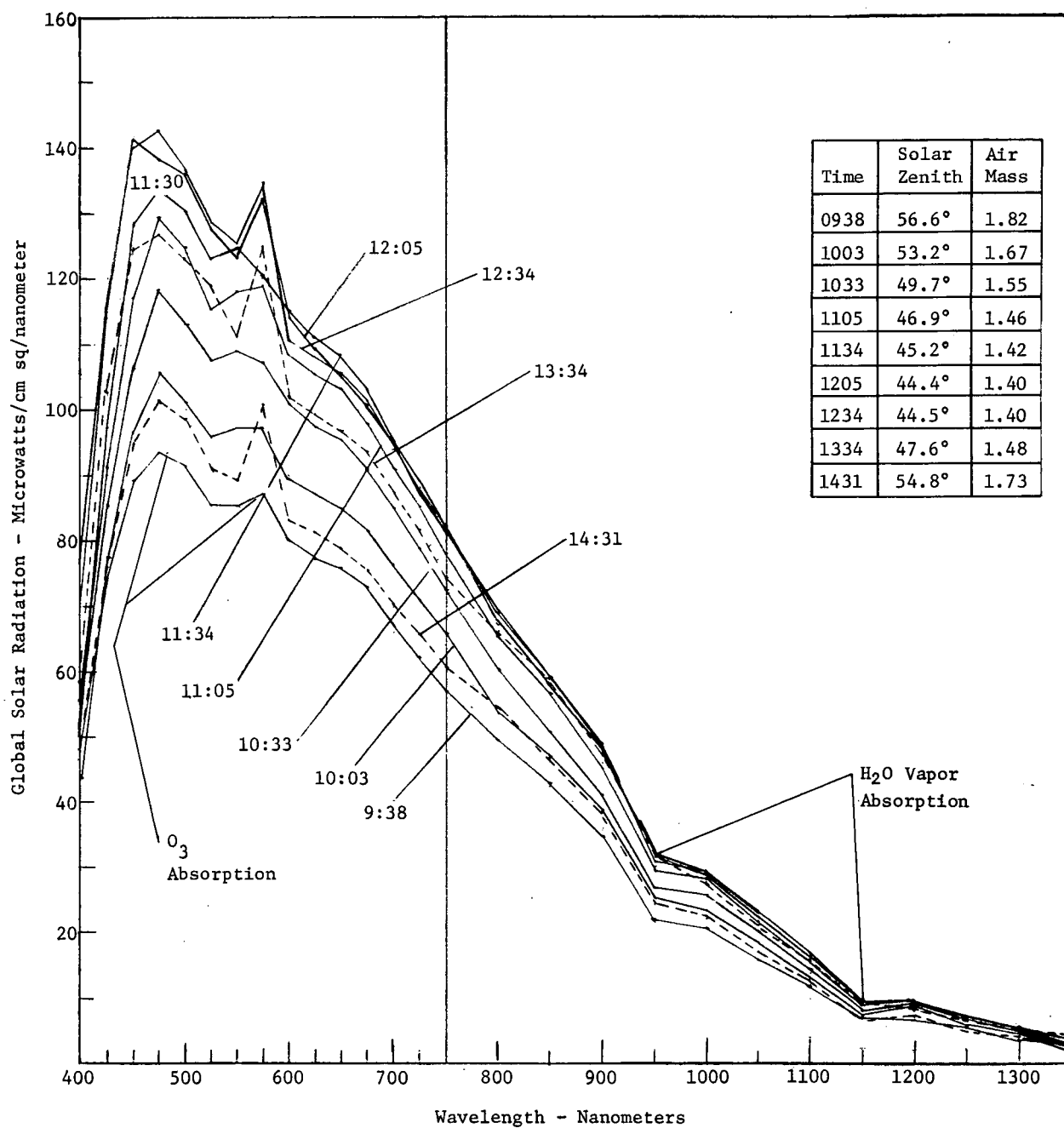


Figure 2-7 Spectral Measurements of Global Solar Radiation

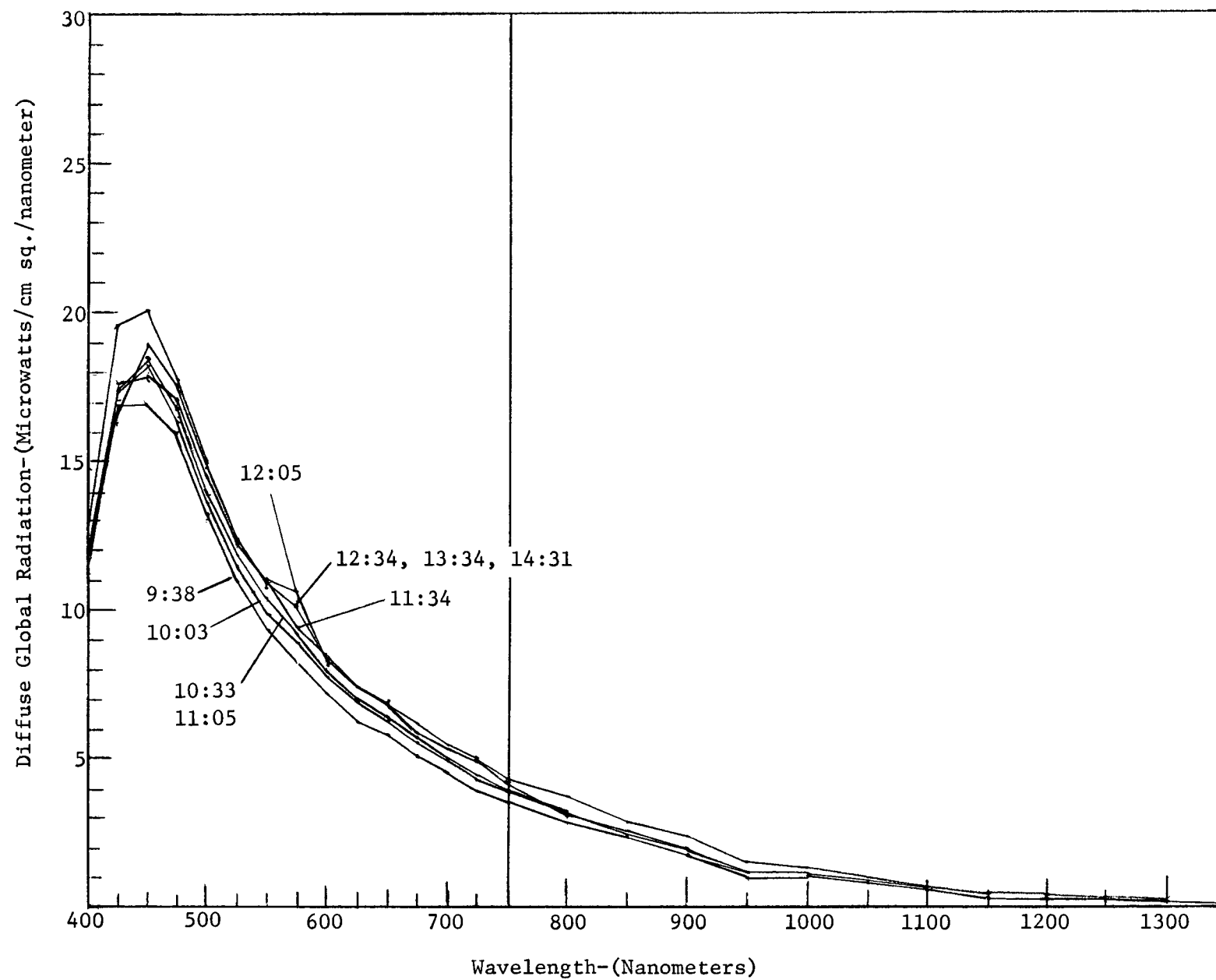


Figure 2-8 Global Diffuse Solar Radiation.

Although an awareness of atmospheric attenuation of the spectral character of solar radiation falling on a target is important, the ratio of diffuse-to-total (D/T) radiation is a more useful parameter for assessing atmospheric effects on remote sensing. This is because the amount of diffuse radiation is indicative of the amount of molecules and aerosols in the path of the direct solar beam.

In addition, the amount of light scattered is a function of wavelength ( $\lambda$ ). For molecules, the well known Raleigh scattering law of a  $1/\lambda^4$  dependence describes the "blue sky" appearance, while aerosol scattering (Mie scattering) is much less dependent on wavelength, approximately  $1/\lambda^{13}$ . The combined effects of atmospheric molecules, aerosols, and path length can be expressed by the product of the optical extinction coefficient,  $\tau\lambda$ , and the path length,  $\sec \theta_o$ . The relative influences of molecular and aerosol scattering processes can be determined by inspecting Figure 2-9, after L. Elterman, 1968.\* As can be seen, molecular scattering is dominant throughout the short wavelength region to approximately 525 nm, at which point the aerosol scattering continues as the dominant process into the infrared.

The amount of solar radiation scattered both downward and upward within the atmosphere follows a similar relationship to that discussed using Figure 2-9; i.e., molecules account for both strong downward and upward scattering in the short wavelengths whereas aerosols account for this scattering in the longer wavelengths. The amount of downward and upward scattering during a remote sensing mission is of importance from the standpoint of atmospheric backscattering of light into the aircraft or satellite sensor, and from the standpoint of "filling in" of shadows on the surface; both cause contrast reduction and errors in the remote sensor data.

Research during the past year attempted to quantitatively define the atmospheric scattering processes by field measurements, and determine significant temporal variances. Spectral measurements of the D/T ratio were made in order to determine the degree of scattering as a function of spectral region and solar zenith angle,  $\sec \theta_o$ . These measurements are shown in Figure 2-10. Ten spectral regions were investigated; 425, 450, 475, 500, 550, 650, 800, 950, 1250 and the broadband, 300 to 2800 nm; the wavelength dependence of the D/T ratio is depicted extremely well by

---

\*Elterman, L., 1968. *UV, Visible, and IR Attenuation for Altitudes to 50 km.* AFCRL 68-015, 3 April 1968, ERP No. 285.

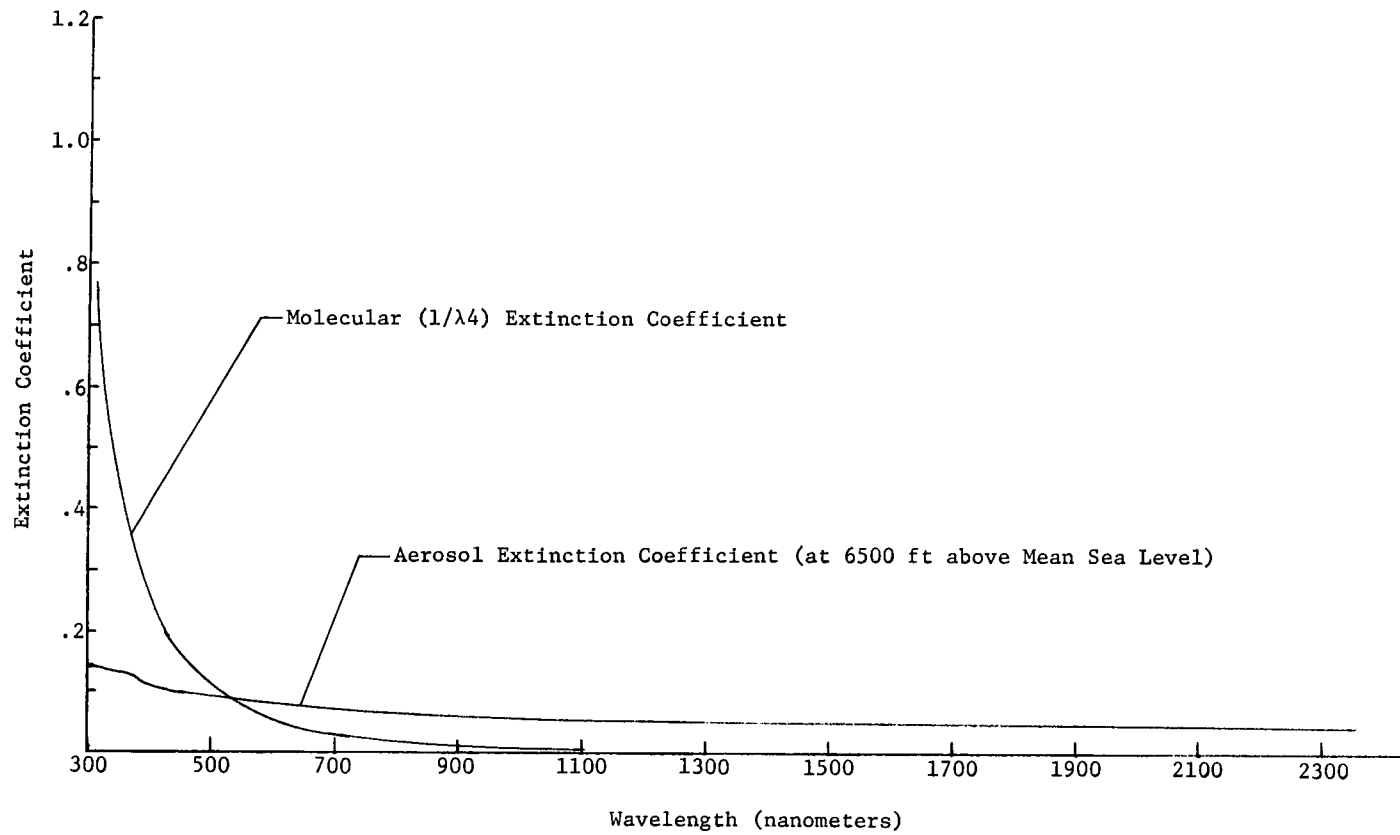


Figure 2-9 Optical Extinction Coefficient Model -  
Elterman, 1968.

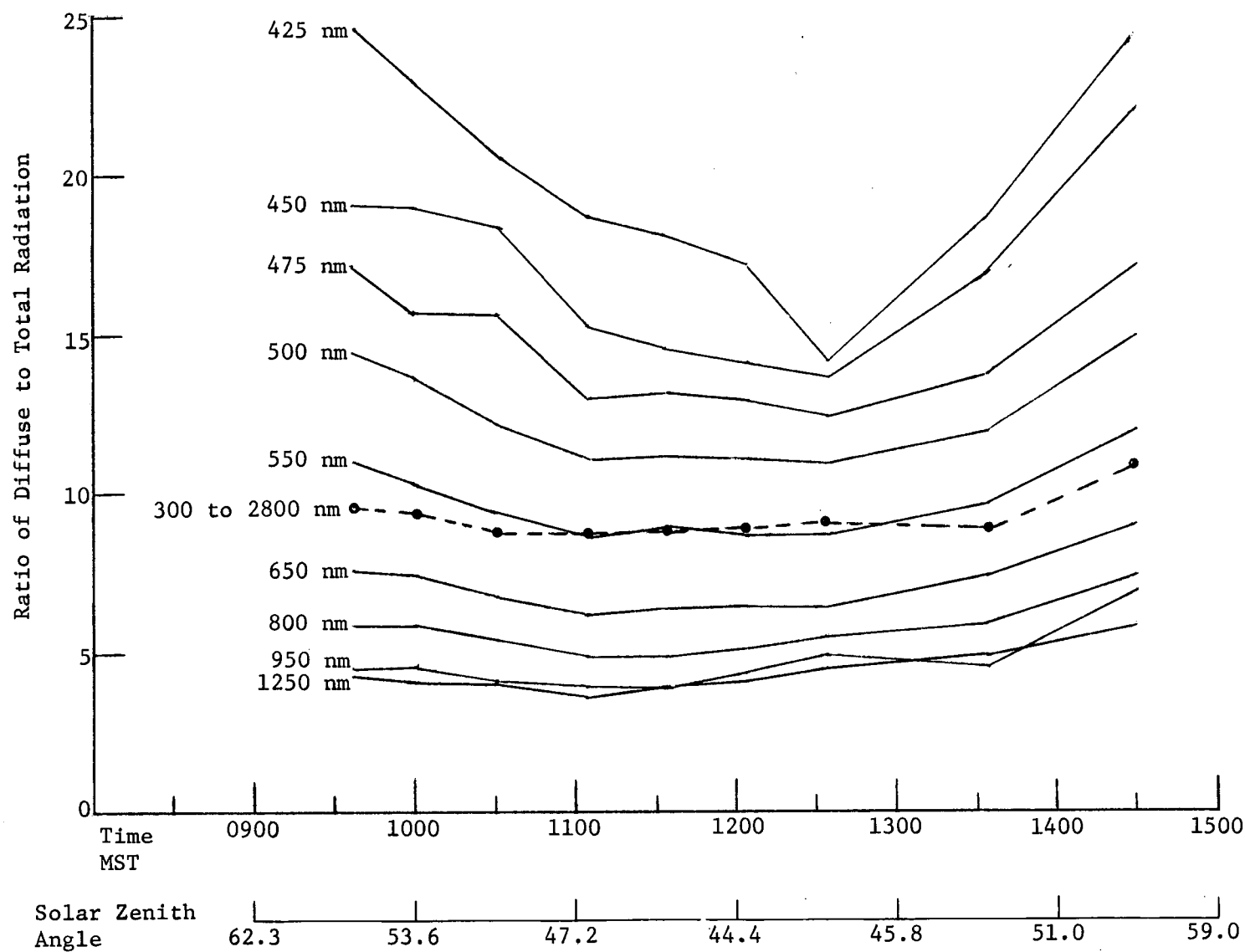


Figure 2-10 Spectral Measurements of the Ratio of Diffuse to Total Radiation as Functions of Solar Zenith Angle.



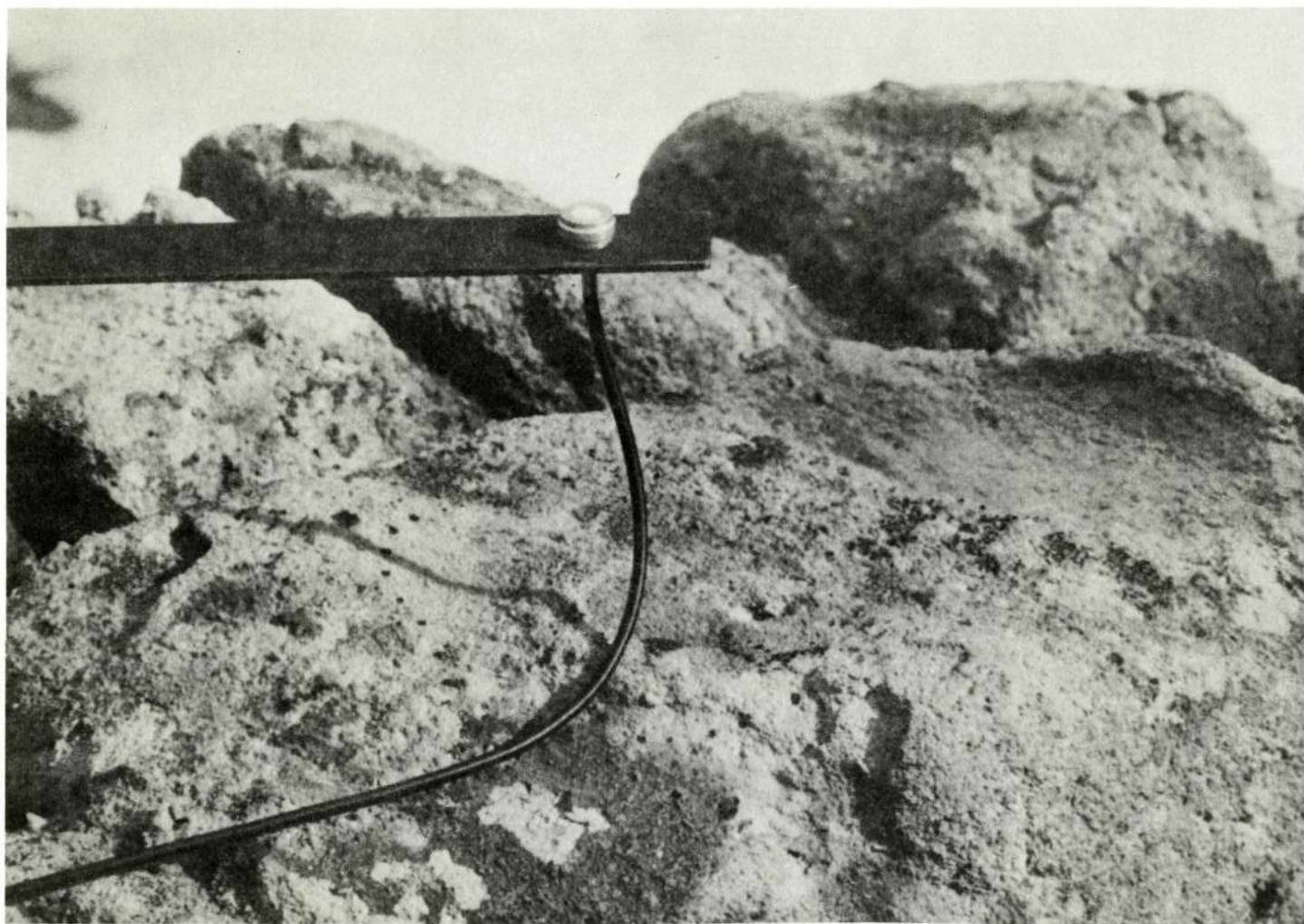
the measurements. The shorter wavelengths (425-500 nm) exhibit high ratios and a strong dependence on solar zenith angle, whereas the longer wavelengths (650-1250 and the broadband 300 to 2800 nm) exhibit low ratios and slight dependence. The path-length independence,  $\sec \theta_0$ , causes all curves to exhibit a minimum near noon; the major character of the curves is determined by the magnitude of the optical extinction coefficient. Hence, the 425-nm curve exhibits large changes in D/T radiation from 0930 to 1230, whereas the 1250 nm curve exhibits very small changes.

The results shown in Figure 2-10 have particular significance to remote sensing. For example, if a multispectral photography/scanner mission was flown which used bands ranging from 425 to 1250 nm, the following observations can be made;

- 1) The optimum time to fly the mission is approximately noon to 1230 if the objective is to collect data in wavelength bands 425 to 650 nm. Atmospheric scattering would be minimum and contrast maximum. The longer wavelengths are not nearly as constrained in terms of time.
- 2) The degrading effects of atmospheric scattering and reduced contrast which are dependent on time of day (solar zenith angle) are most critical in the 425-475 nm wavelength band.

The 300 to 2800 nm D/T ratio has previously been studied in terms of its relationship to atmospheric clarity; it was found that ratios of 6-to-10% represent extremely "clear" conditions. The set of data shown in Figure 2-10 is then indicative of minimal atmospheric scattering. Also, past measurements of the 300 to 2800 nm D/T ratio have shown that for seemingly "clear" days this ratio can be as high as 15%. Therefore, one would expect that the spectral ratios would all correspondingly increase. This being the case, it is expected that the wavelength region where scattering is least significant would vary from one day to the next.

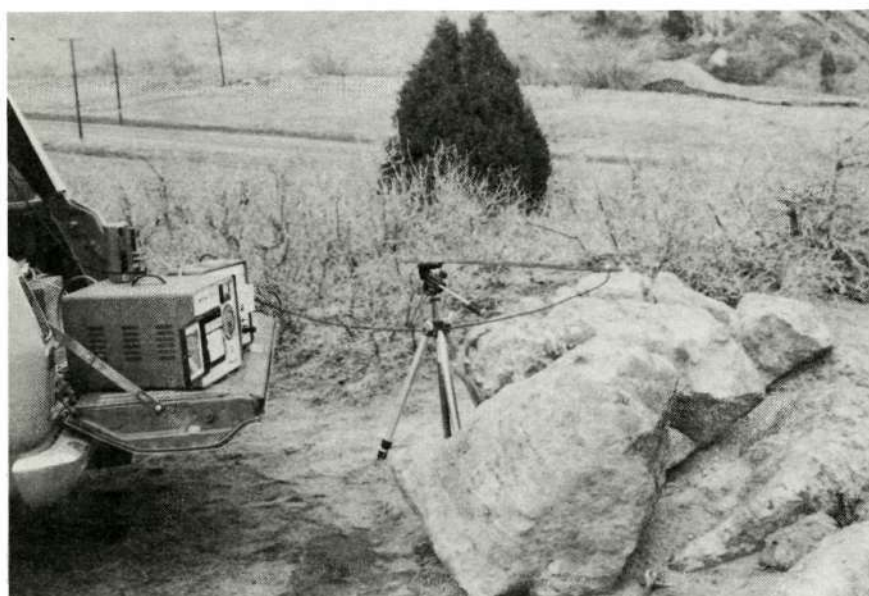
2.3.3 Effects On the Reflectance Spectrum of a Target - Another aspect of atmospheric effects of solar radiation is the relative influence of directional (the direct solar beam) radiation and isotropic radiation (diffuse, sky radiation) on the reflectance spectrum of a target. The combination results in illumination conditions upon a target that are neither 100% directional nor 100% diffuse. As shown in the previous section, the degree of diffuse and directional conditions is extremely dependent on wavelength. During the past year, the effect of these various degrees of directional versus diffuse illumination was investigated to determine the differences between target reflectance under diffuse



*Figure 2-11 Mounting Bracket for ISCO Fiber Optics Bundle, Used for Measuring Global and Reflected Radiation*

illumination as opposed to target reflectance under normal "clear" day conditions.

To determine these effects, reflectance measurements of two different sites were made under "clear" day conditions and measurements of the same sites were made under completely overcast conditions (100% diffuse conditions). Figure 2-11 shows a special mount used to house the ISCO probe in order to always position it at exactly the same position with respect to the target.



*Figure 2-12 Instrumentation and Setup for Measuring Field Reflectance and Global Radiation*

Figure 2-12 shows the entire field setup used.

The procedure used for determining the target reflectance was simply to measure the total incoming solar radiation ( $180^\circ$  global), then immediately point the probe at the target to measure the reflected radiation. Precautions were taken to assure that any stray light reflected from nearby objects was insignificant. Target percentage-reflectance is calculated by dividing the reflected radiation by the total incoming radiation. Since the sensor field of view is  $180^\circ$  in both cases, the derived target reflectance is defined as its hemispherical reflectance signature.

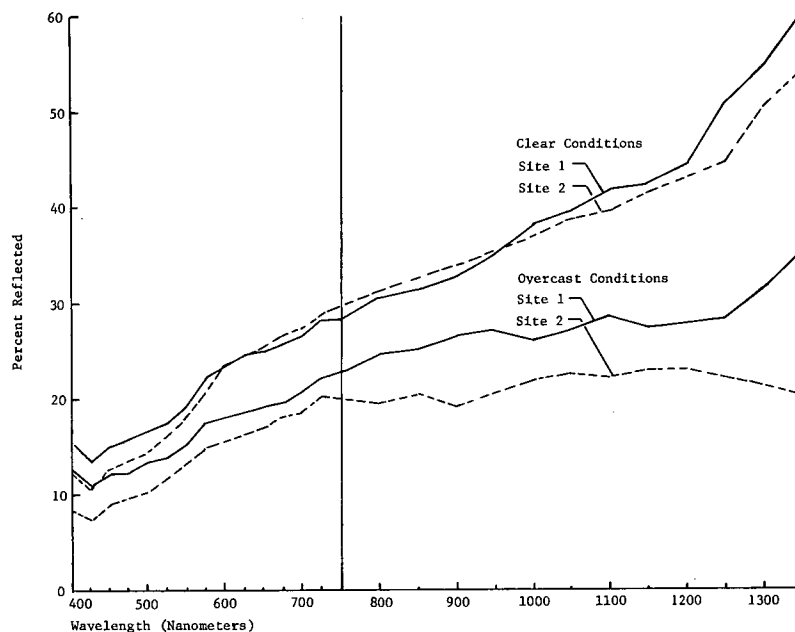


Figure 2-13 Reflectance Measurements and Effects of the Nature of Incoming Radiation

Figure 2-13 shows the results of the measurements. Site 1 is an outcrop of Lyons Sandstone and Site 2 is an outcrop of amphibolite. All curves represent the average of three separate (different days and times of day) spectra.

It is apparent that in both cases the "clear-day" reflectance is greater in magnitude than the diffuse, overcast reflectance. However, their relative spectral character does not significantly change despite the different illumination conditions.

#### 2.4 Development of Improved Techniques for Measuring Field Reflectance and Solar Radiation

A common technique for measuring target reflectance in the field is to:

- 1) Measure the incoming total solar radiation (T);
- 2) Measure the reflected radiation from the target (R);
- 3) Record a second measurement of the incoming radiation ( $T_2$ ) which is averaged ( $T_{avg}$ ) with T.

The target reflectance ( $\rho_\lambda$ ) is then calculated by the equation,

$$\rho_{\lambda} = R_{\lambda}/T_{\text{avg}}(\lambda) \quad [1]$$

where

$$T_{\text{avg}}(\lambda) = \frac{T_1(\lambda) + T_2(\lambda)}{2} \quad [2]$$

During the past year, the following aspects of the techniques described were investigated:

- 1) Does the average of the total measurements represent the actual total that existed simultaneously with the reflected measurement;
- 2) Can the measurement of the second total be eliminated if a complementary, second instrument is used in conjunction with the ISCO; this would result in a 33% reduction in data processing.
- 3) Can the spectral characteristics of the total solar radiation be extrapolated in both time and space by using a simple pyranometer in conjunction with the ISCO spectroradiometer; this would provide a much more complete knowledge of the solar radiation environment existing over an entire test site.

A series of measurements was performed where the common reflectance measurements were compared with continuous pyranometer measurements. A YSI pyranometer was used because it is sensitive to the broadband region from 400 to 1100 nm which is similar to the ISCO scan. The total solar radiation for either the broadband pyranometer or the spectral ISCO measurements is given as:

$$T = D + S \quad [3]$$

Where T is the total radiation, D is the direct solar radiation, and S is the scattered solar radiation. The direct solar radiation can further be given as

$$D = I_0 \cos \theta_0 e^{-\tau_{\lambda} \sec \theta_0} \quad [4]$$

Where,  $I_0$  is the solar constant (at top of the atmosphere),  $\theta_0$  is the solar zenith angle and  $\tau_{\lambda}$  is the solar coefficient as discussed in the previous sections. Hence the broadband ( $\Delta\lambda$ ) measurements can be related to the spectral ( $\lambda$ ) measurements by the following:

$$T(\lambda) = I_0(\lambda) \cos \theta_0 e^{-\tau \lambda \sec \theta_0} + S(\lambda) \quad [5]$$

$$T(\Delta\lambda) = I_0(\Delta\lambda) \cos \theta_0 e^{-\tau(\Delta\lambda) \sec \theta_0} + S(\Delta\lambda) \quad [6]$$

It can be seen by comparing equations 5 and 6 that both the broadband and spectral total solar radiation are similarly dependent upon the solar zenith angle,  $\theta_0$ , which is in turn determined by changes in time of day and year. Because of this similarity in terms of time variance, it was decided to determine if a simple ratio relationship could be used to relate the changes in the spectral total radiation to changes in the broadband total radiation; this ratio is given as:

$$\frac{T(\lambda)_1}{T(\Delta\lambda)_1} = \frac{T(\lambda)_2}{T(\Delta\lambda)_2} \quad [7]$$

Where the subscripts 1 and 2 refer to different times of measurement. The second unknown spectral total can then be related to the first known spectral total; the first known broadband total and the second known broadband total by

$$T(\lambda)_2 = T(\lambda)_1 + T(\Delta\lambda)_2 / T(\lambda)_1 \quad [8]$$

The target reflectances are then calculated by equation 2 and by

$$\rho_\lambda = R(\lambda) / T(R)\lambda \quad [9]$$

Where  $T(R)\lambda$  (calculated) was determined by equation 8 using previous measurements which differed in time by the following sequence: Figure 2-14, 6 minutes; Figure 2-15, 22 minutes; Figure 2-16, 29 minutes; Figure 2-17, 59 minutes; and Figure 2-18, 71 minutes. These figures depict the error in the determination of the target reflectance as a result of using extrapolated spectral total radiation instead of the actual  $T_{avg}$  spectral total measurement. It is evident that the extrapolated spectral total is adequate for the 6-minute interval. This indicates that the customary second spectral total measurement could be eliminated without significant errors in the percentage reflectance determination. As the time interval becomes larger the reflectance error increases. This is because the time rate of change in broadband total is not equivalent to the time rate of change for the spectral total. Figure 2-19 depicts this more specifically. In Figure

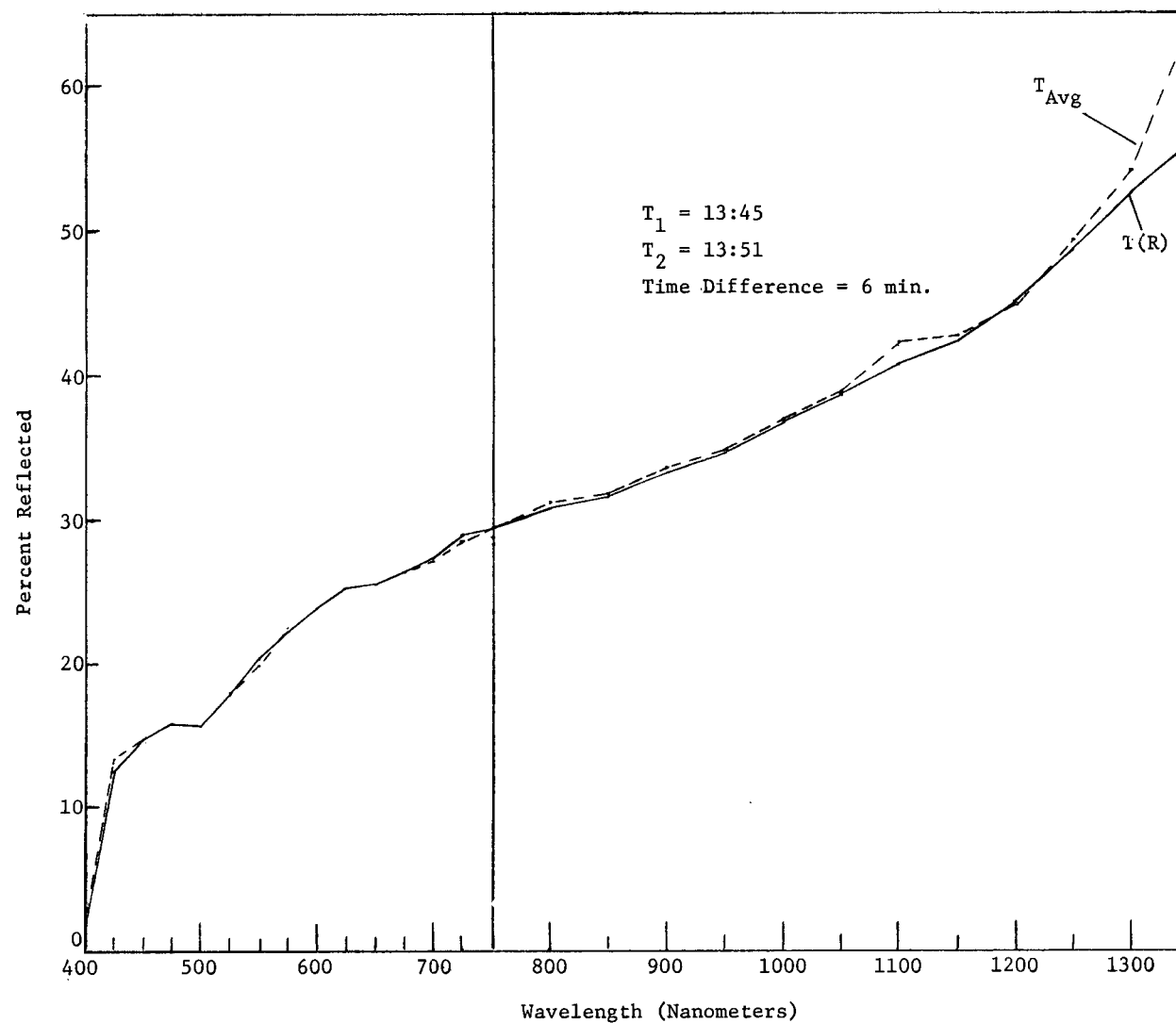


Figure 2-14 Comparison of Reflectance Determinations  
Using Actual and Computed Measurements.  
(Time lapse = 6 min.)

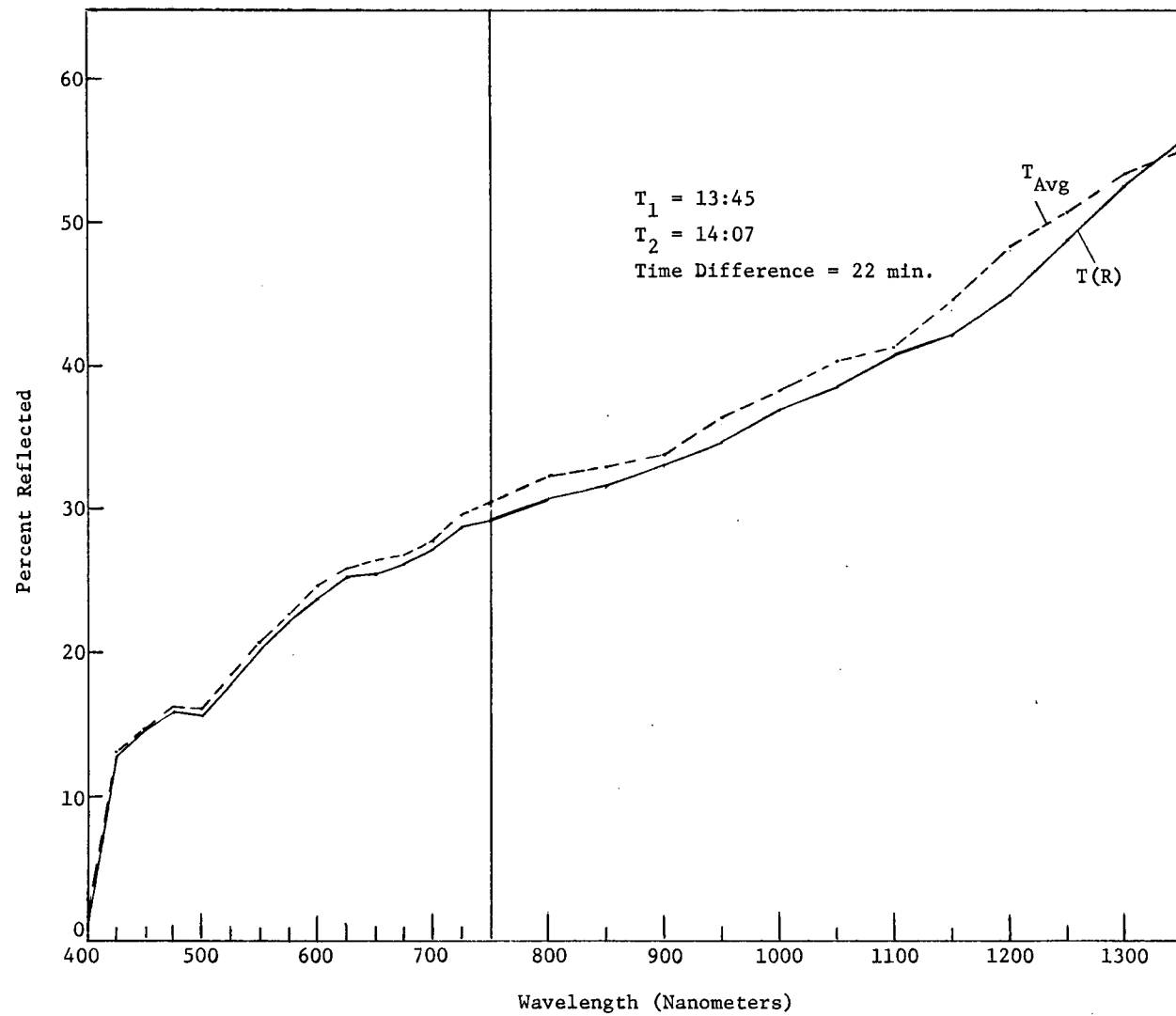


Figure 2-15 Comparison of Reflectance Determinations  
 Using Actual and Computed Measurements.  
 (Time lapse = 22 min.)



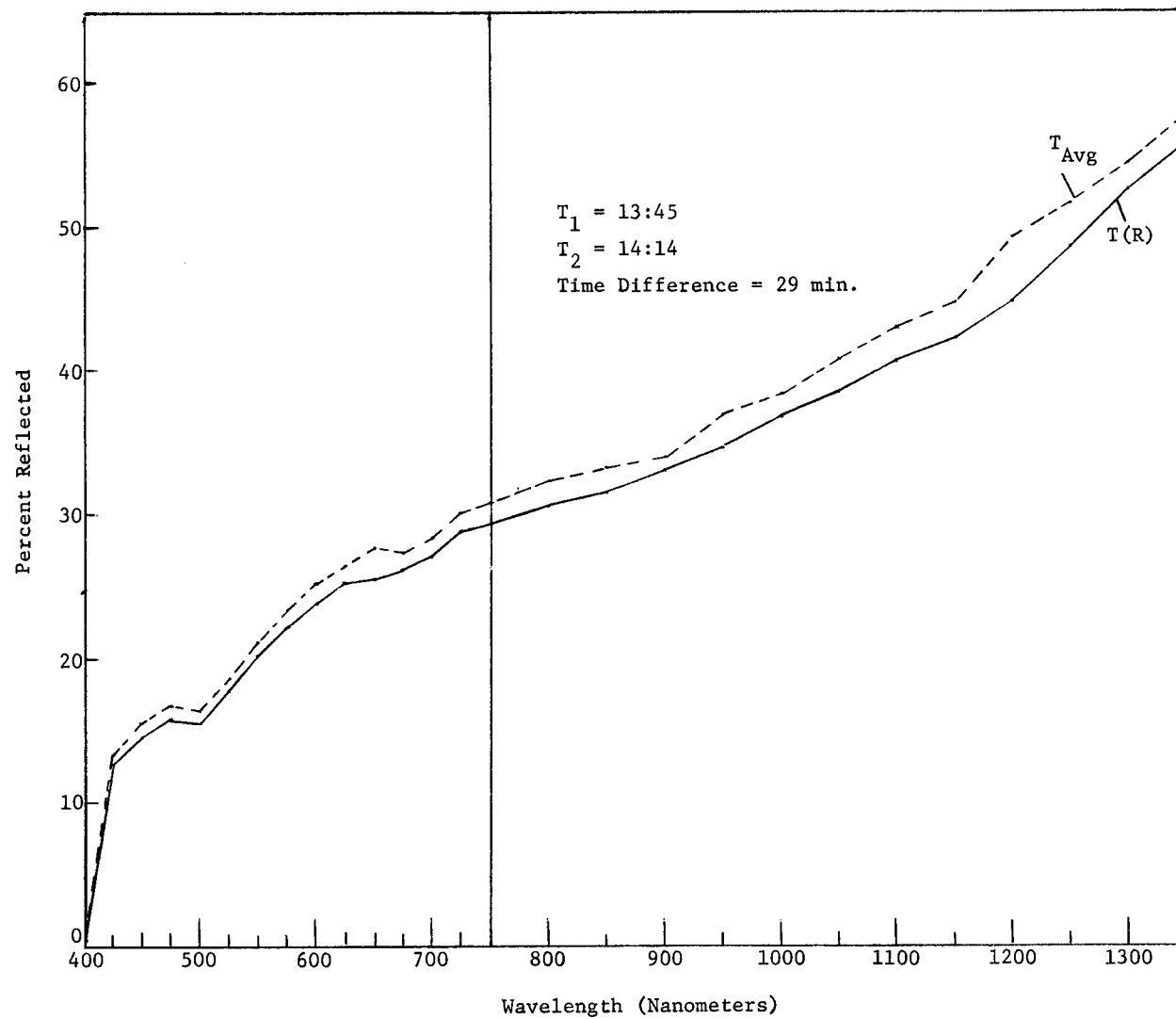


Figure 2-16 Comparison of Reflectance Determinations  
 Using Actual Computed Measurements.  
 (Time lapse = 29 min.)

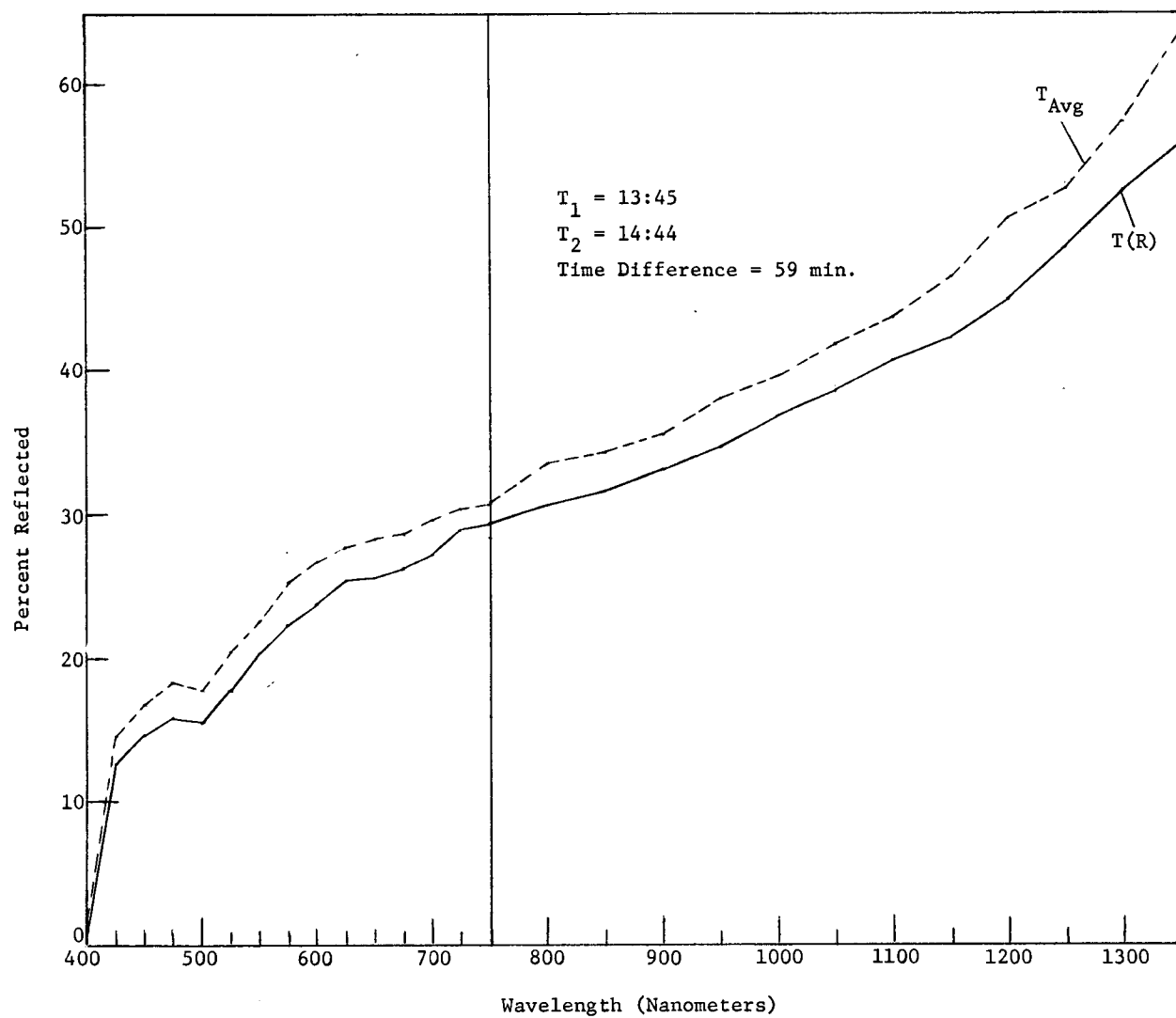


Figure 2-17 Comparison of Reflectance Determinations  
 Using Actual and Computed Measurements.  
 (Time lapse = 59 min.)

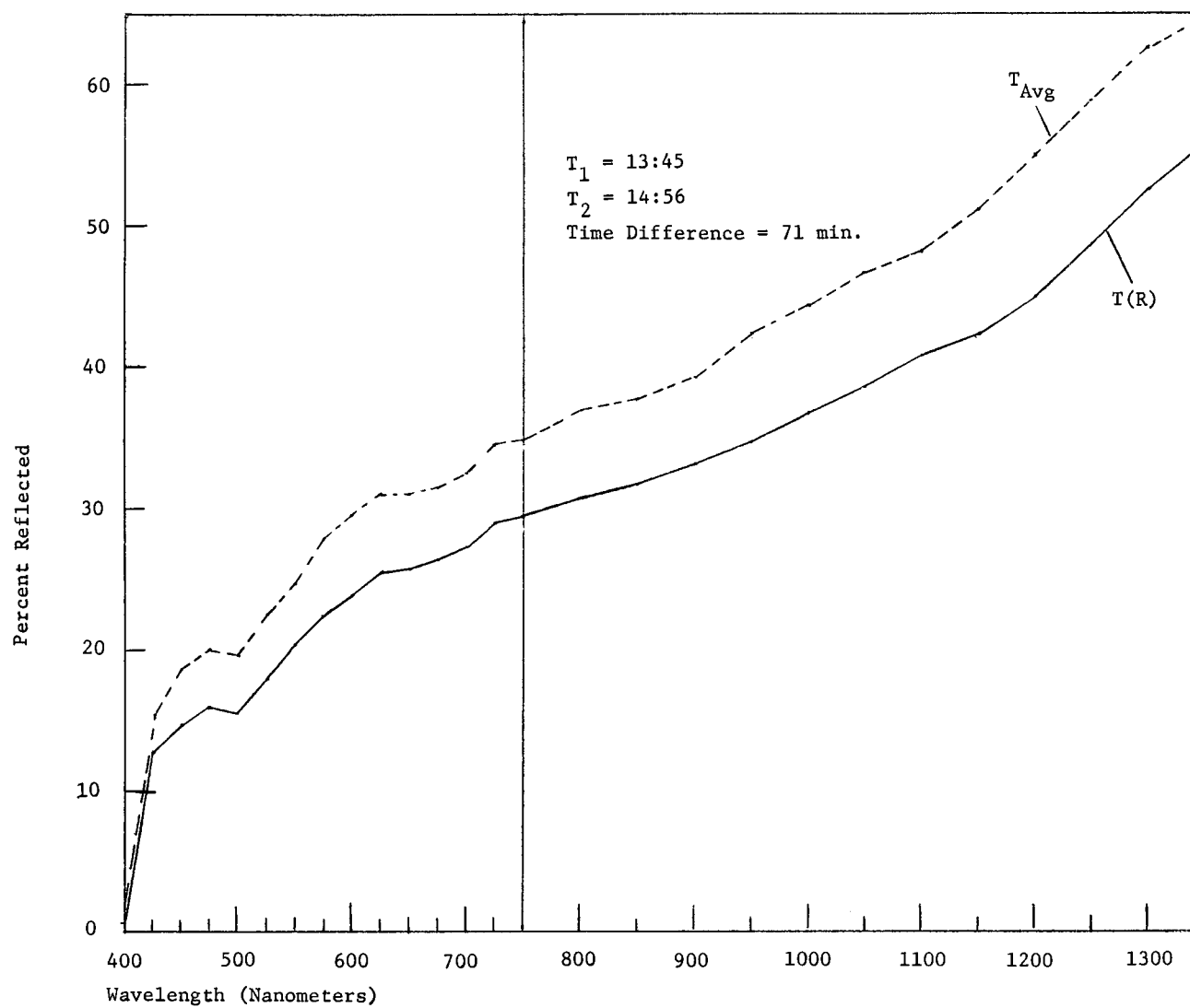


Figure 2-18 Comparison of Reflectance Determinations  
Using Actual and Computed Measurements.  
(Time lapse = 71 min.)

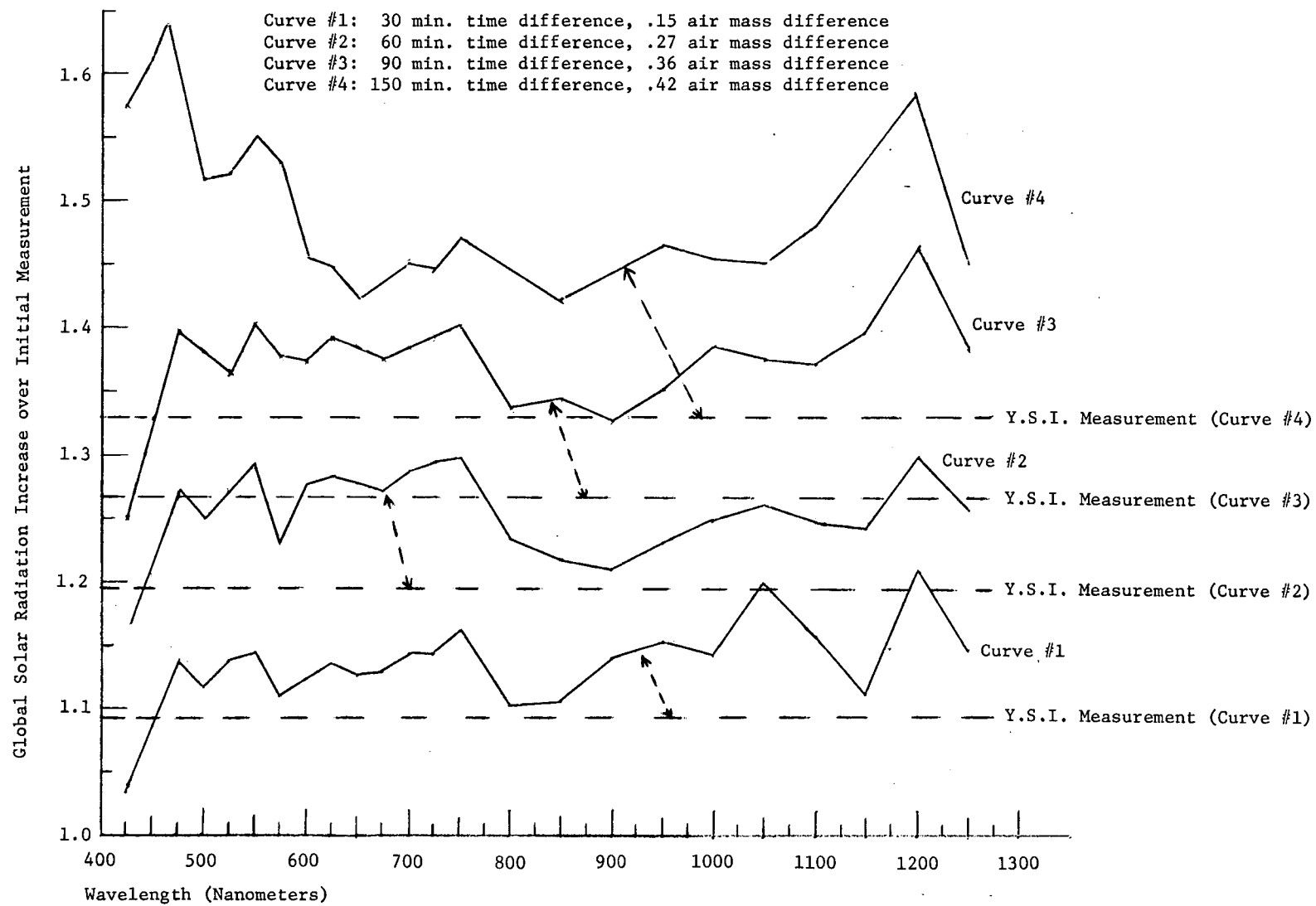


Figure 2-19 Comparison of YSI and Measurements

2-19, the ratio  $T(\lambda)/T(\lambda)_2$  is plotted versus wavelength, and for comparison, the broadband ratio  $T(\Delta\lambda)_1/T(\Delta\lambda)_2$  is given for each corresponding spectral curve. The time differences shown in Figure 2-19 are not intended to be the same as shown in Figures 2-14 to 2-18. It should be pointed out that the rate of change of time is in actuality a rate of change in the relative air mass ( $\sec \theta^\circ$  path length) assuming that the optical extinction coefficient remains constant. For this reason the corresponding air mass changes are given.

A detailed computer tabulation of measurements and calculations similar to those discussed above are shown in Figure 2-20. The columns from left to right are:

- 1) Wavelength;
- 2) Instrument correction factor;
- 3) Raw instrument data (strip chart record);
- 4) The initial spectral total measurement;
- 5) The initial broadband total measurement (YSI);
- 6) The raw reflected radiation;
- 7) The absolute reflected radiation;
- 8) The YSI measurement simultaneous with the previous reflectance measurement;
- 9) The calculated instantaneous spectral total;
- 10) The percentage reflectance of the target;
- 11) The percentage difference between the instantaneous spectral total and the raw, second spectral total;
- 12) The absolute second spectral total;
- 13) The corresponding broadband total measurement;
- 14) The calculated second spectral total;
- 15) The percentage difference between the actual and calculated spectral totals;
- 16) The average of the measured spectral totals;
- 17) The target percentage reflectance using the average of the measured totals.

ISCO DATA PROBE 6FT MMC SITE NO.1 MMC DATE 1-31-72  
 SKY CONDITION CLEAR S.E.ANGLE

TYPE OF DATA TOTAL - REFLECTED - TOTAL YSI CONTINUOUS

RUN NO. 1 2 11  
 TIME (HR. MIN) 13.45 13.47 14.56

THE HIRSHIN 15.45 15.47 15.50																	
WAVE- LENGTH (NM)	COR- RECTION FACTOR	TOTAL (1)			REFLECTED			TOTAL	T1-TR		TOTAL (2)			TOTAL	T2-T2C	AVG.	PCNT
		RAW	ABS	YSI	RAW	ABS	YSI	(R)	R	PCNT DIFF	RAW	ABS	YSI	CALC	DIFF	TOTAL	R-AVG
VIS																	
400	39.180	.540	21.157	.808	.003	.118	.801	20.974	.56	.87	.360	14.105	.545	14.271	1.17	17.631	.67
425	13.220	3.660	48.385	.808	.460	6.081	.801	47.966	12.68	.87	2.310	30.538	.545	32.636	6.64	39.462	15.41
450	10.380	6.360	66.017	.808	.930	9.653	.801	65.445	14.75	.87	3.630	37.679	.545	44.529	16.66	51.848	18.62
475	8.629	9.300	80.250	.808	1.470	12.685	.801	79.554	15.94	.87	5.460	47.114	.545	54.129	13.86	63.682	19.92
500	7.113	10.440	74.260	.808	1.620	11.523	.801	73.616	15.65	.87	6.120	43.532	.545	50.089	14.01	58.896	19.57
525	6.291	11.910	74.926	.808	2.120	13.337	.801	74.277	17.96	.87	7.080	44.540	.540	50.074	11.70	59.733	22.33
550	6.867	11.490	78.902	.808	2.300	15.794	.801	78.218	20.19	.87	7.140	49.030	.540	52.731	7.27	63.966	24.69
575	5.087	11.850	60.281	.808	2.600	13.226	.801	59.759	22.13	.87	6.810	34.642	.540	40.287	15.07	47.462	27.87
600	4.831	14.700	71.016	.808	3.480	16.812	.801	70.400	23.88	.87	8.940	43.189	.540	47.461	9.42	57.102	29.44
625	4.899	13.710	67.165	.807	3.440	16.853	.801	66.666	25.28	.75	8.510	41.690	.540	44.943	7.51	54.428	30.96
650	5.035	13.380	67.368	.807	3.380	17.018	.801	66.867	25.45	.75	8.430	42.445	.540	45.079	6.02	54.907	30.99
675	5.033	12.630	63.567	.807	3.280	16.508	.801	63.094	26.16	.75	8.160	41.069	.540	42.535	3.51	52.318	31.55
700	4.940	12.090	59.725	.809	3.250	16.055	.801	59.134	27.15	.99	7.960	39.322	.540	39.866	1.37	49.523	32.42
725	5.049	11.340	57.256	.809	3.250	16.409	.801	56.689	28.95	.99	7.620	38.473	.540	38.218	.67	47.865	34.28
750	5.364	10.260	55.035	.806	2.980	15.985	.800	54.625	29.26	.75	6.930	37.173	.540	36.872	.81	46.104	34.67
IR																	
750	11.670	4.830	56.366	.810	1.350	15.755	.801	55.740	28.26	1.12	3.010	35.127	.545	37.925	7.66	45.746	34.44
800	8.194	5.450	44.657	.810	1.659	13.594	.801	44.161	30.78	1.12	3.570	29.253	.545	30.047	2.68	36.955	36.78
850	8.433	4.630	39.045	.810	1.446	12.194	.801	38.611	31.58	1.12	3.050	25.721	.545	26.271	2.12	32.383	37.66
900	8.427	3.500	29.495	.813	1.140	9.607	.801	29.059	33.06	1.49	2.320	19.551	.545	19.772	1.13	24.523	39.18
950	7.872	2.860	22.514	.813	.975	7.675	.801	22.182	34.60	1.49	1.750	13.776	.545	15.092	9.12	18.145	42.30
1000	7.299	2.880	21.021	.813	1.041	7.598	.801	20.711	36.69	1.49	1.830	13.357	.545	14.092	5.35	17.189	44.20
1050	5.768	2.950	17.016	.813	1.119	6.454	.801	16.764	38.50	1.49	1.850	10.671	.545	11.407	6.66	13.843	46.62
1100	4.200	2.320	9.744	.813	.930	3.906	.801	9.600	40.69	1.49	1.550	6.510	.545	6.532	.34	8.127	48.06
1150	4.891	1.270	6.212	.813	.528	2.582	.801	6.120	42.20	1.49	.800	3.913	.550	4.202	7.13	5.062	51.01
1200	5.045	1.720	8.677	.813	.762	3.844	.801	8.549	44.97	1.49	1.050	5.297	.550	5.870	10.26	6.987	55.02
1250	2.668	2.080	5.549	.813	.996	2.657	.801	5.468	48.60	1.49	1.300	3.468	.550	3.754	7.91	4.509	58.93
1300	2.002	1.870	3.744	.813	.972	1.946	.805	3.707	52.50	.99	1.240	2.482	.550	2.533	2.00	3.113	62.51
1350	2.955	.300	.886	.815	.165	.488	.805	.876	55.68	1.23	.210	.621	.550	.598	3.66	.754	64.71

Figure 2-20 Computer (CDC6400) Analysis Tabulation of Field Data

The complete data analysis program is available at Martin Marietta.

In summary, the above investigation has shown that for short periods of time the spectral total solar radiation can be calculated from previous measurements of both spectral and broadband total radiation. This eliminates the necessity for taking a second spectral total measurement following the target reflectance spectrum, thereby resulting in a 33% decrease in data handling, processing, and analysis. Such calculations of spectral total radiation involving long periods of time result in significant errors of target reflectance, depending on wavelength and exact time interval (air mass change).

### 3. LINE SCANNER IMAGE PROCESSING AND ENHANCEMENT

This section describes the effort to date directed to the quantitative processing and qualitative enhancement of scanner data. Although this discussion is limited to the utilization of two-channel data, the techniques described here could be applied to any number of channels. The primary emphasis of work thus far has been the development of a laboratory playback (display) system and breadboarding of functional "black boxes" for data workup.

#### 3.1 Data and Equipment

The data utilized in this effort are in the form of analog signals on  $\frac{1}{2}$  inch, 7-track magnetic tape. Recording mode on all channels is direct. Direct recording rather than FM has some disadvantages that will be discussed at the end of this section. The data contained on the magnetic tape is formatted as follows: Tracks one and two contain 3-5 $\mu$  and 8-14 $\mu$  video signals, respectively; track three contains sync pulses; track four has IRIG time; track five is a 50-kHz reference signal and track six is the output of a nadir-looking PRT-5 IR radiometer. Voice on track seven provides a means of locating specific lines and areas of interest.

Figure 3-1 is a photograph of the equipment and Figure 3-2 is a line drawing of same. The electronic equipment shown consists of an Ampex SP300 tape recorder and Tektronics model 5103N oscilloscope. The "black box" signal-processing unit is basically an operational amplifier(s) in various gain and filter configurations.

The operation of the system is extremely simple and requires only three connections to operate. The oscilloscope must be made to produce an X- and Y-sweep. Timing of the X-sweep is adjusted to equal one scan, and the Y-sweep rate is determined by the size of the cathode ray tube (CRT) spot, velocity/height (V/H) of the original data, etc. In practice, slight image distortion is tolerable since the objective of the display is to observe the effect of signal processing. The processed image is displayed on a storage oscilloscope and, when optimized, may be photographed using a Polaroid oscilloscope camera.

#### 3.2 Processing Techniques

The electronic processing of image data in analog form has many advantages over digital techniques. The equipment required is not prohibitively expensive, implementation of enhancement techniques is accomplished with functional modules, and turn-around time is



Reproduced from  
best available copy.

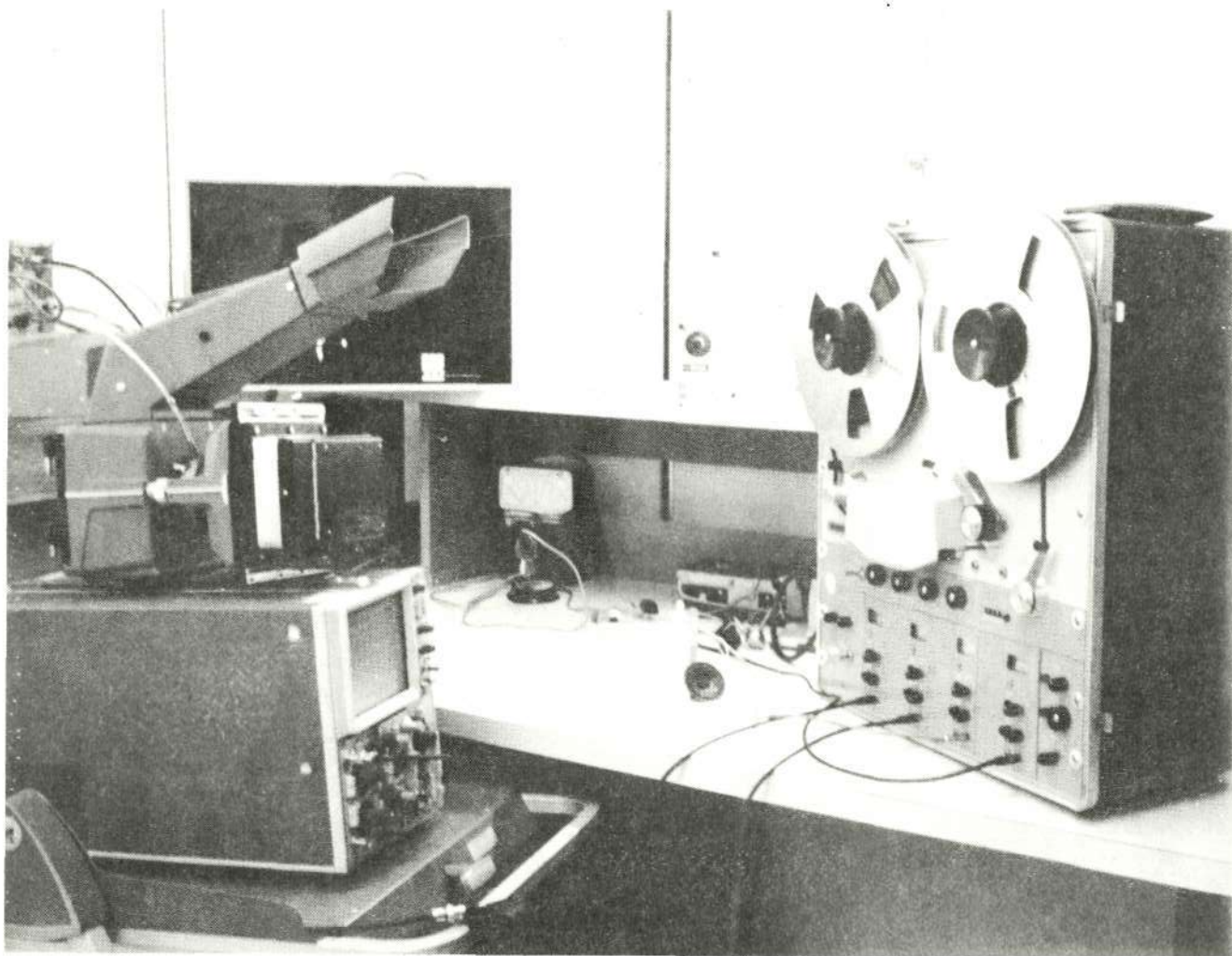


Figure 3-1 Laboratory Setup of Image Display Equipment

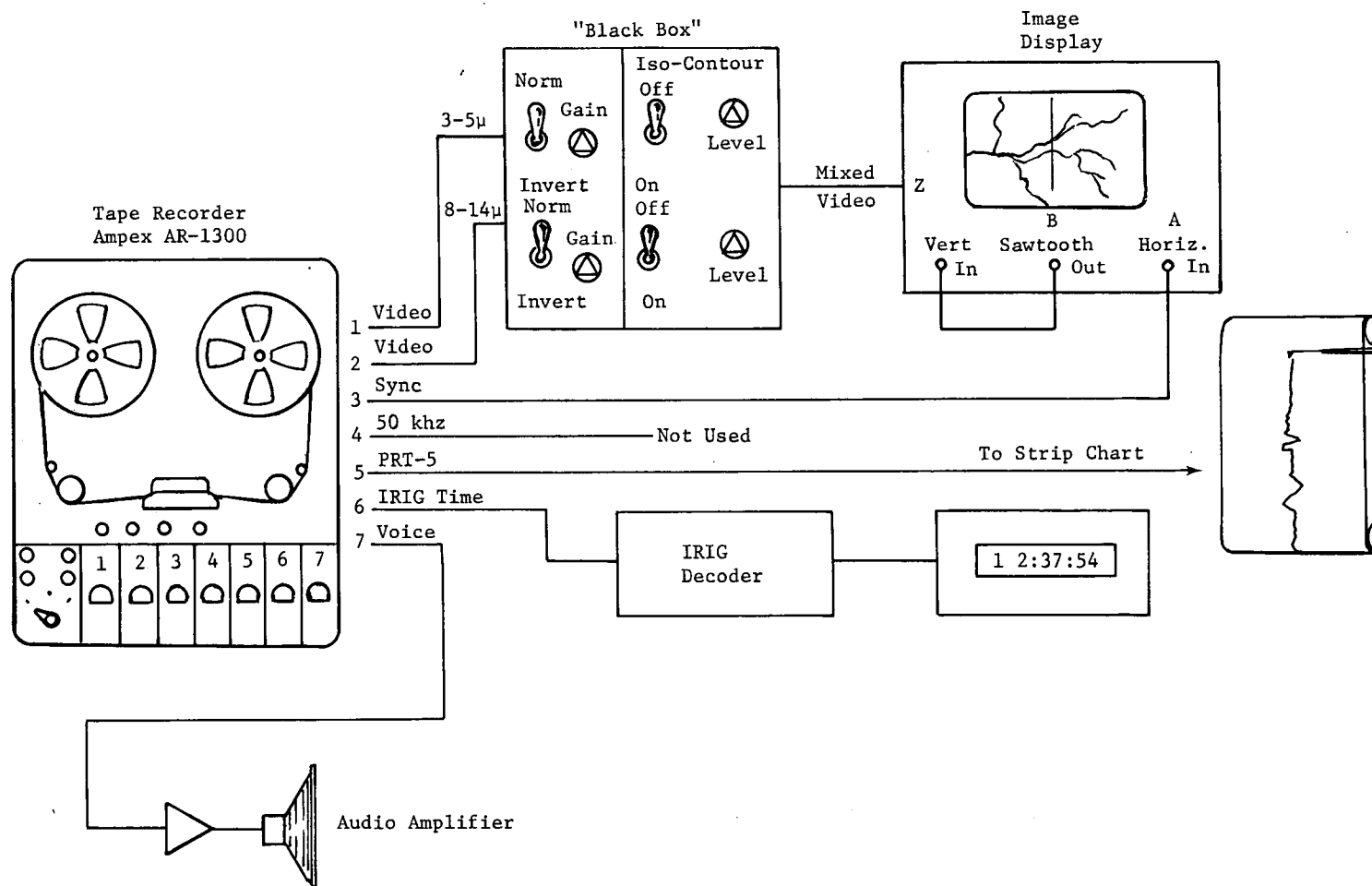


Figure 3-2 Line Scan Image Processing Setup

short. In a virtual real-time display such as the one described here it is possible to conceive an enhancement scheme, build the hardware and test the thesis all within a day or two. Modifications to the concept are implemented and viewed within hours. The use of a storage oscilloscope allows data to be displayed, modified, displayed again until optimized and then recorded on photographic film to provide a permanent record.

The processing of the video data (imagery) is accomplished through the use of an almost infinite variety of linear integrated circuits such as operational amplifiers, voltage followers, comparators, etc. These basic building blocks, along with some external components, permit a wide range of techniques to be explored.

Figure 3-3 shows a very simple circuit which permits two video channels to be added together; one channel subtracted from the other; both channels subtracted from a fixed level; and the two signals mixed at varying levels.

Figure 3-4 shows another circuit in which a pulse is generated each time the signal level passes through a preset threshold. These pulses, when mixed with the original video signal, yield iso-density contours which highlight areas of equal intensity, or in the case of thermal imagery, equal temperature zones or isotherms.

At the time of this writing, only a few of the following concepts have been implemented, but all will be investigated in the coming months. A few more basic functional modules will be required such as tunable filters for high-pass, low-pass and band-pass processing. Using just the functions described thus far, the number of permutations is large. For example, one spectral band could be high-pass filtered and another low-pass filtered and these two then superimposed. The resulting image would show small features (high-pass) over large features (low-pass) whereby vegetation cover would be suppressed in one band while linear features or similarly structured indicators are emphasized. Another technique is to low-pass-filter one channel of thermal infrared imagery, plot iso-density levels of the other, and superimpose the results. Vegetative masking that might otherwise obscure some subtle details is thus removed.

The potential of the processing method described here is limited only by imagination. With just a few functions such as variable-gain differential amplifiers, iso-contour generators, and high-, low-, and band-pass filters, many variations in image processing are possible.

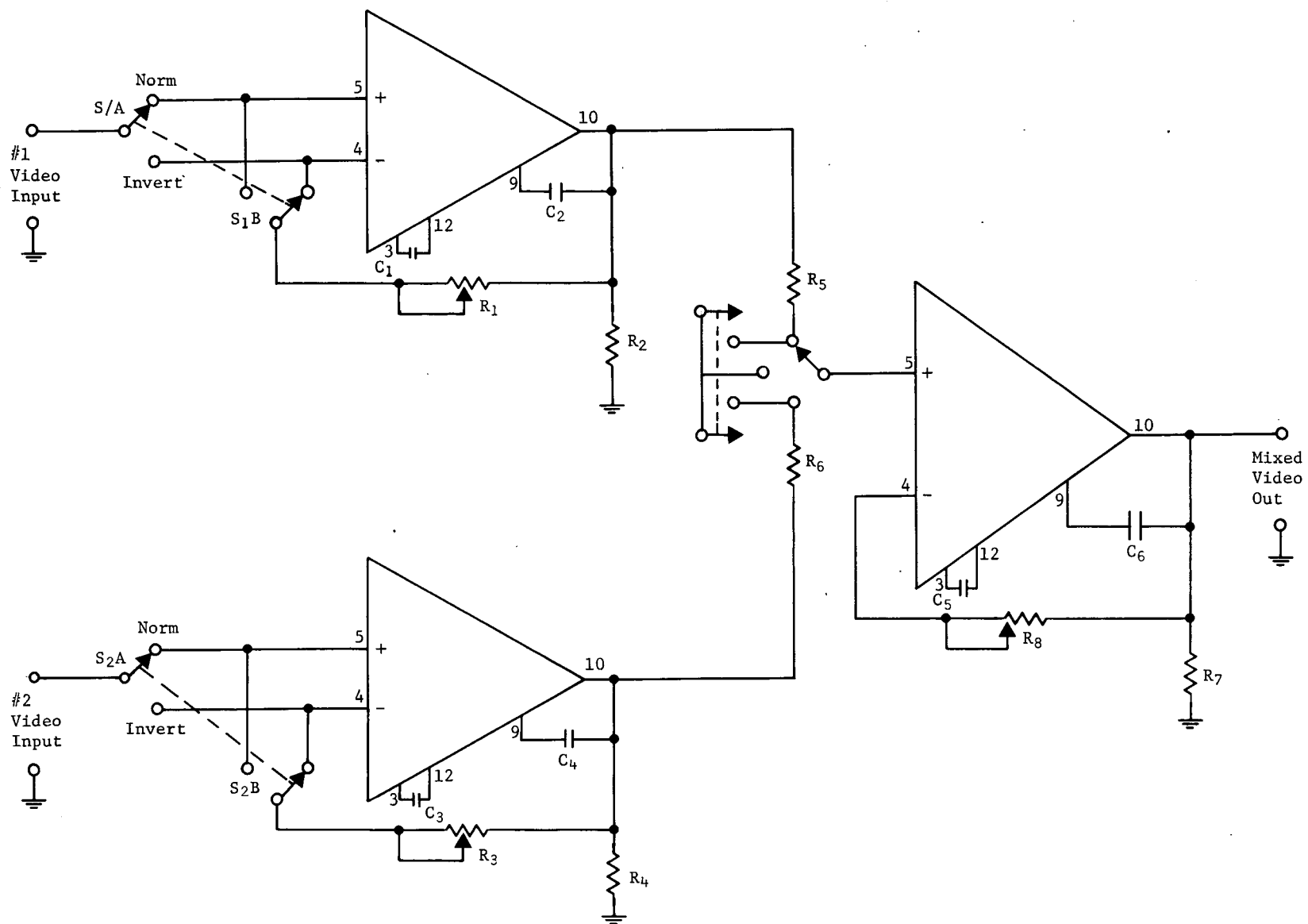


Figure 3-3 "Black Box" Video Mixer with Variable Gain

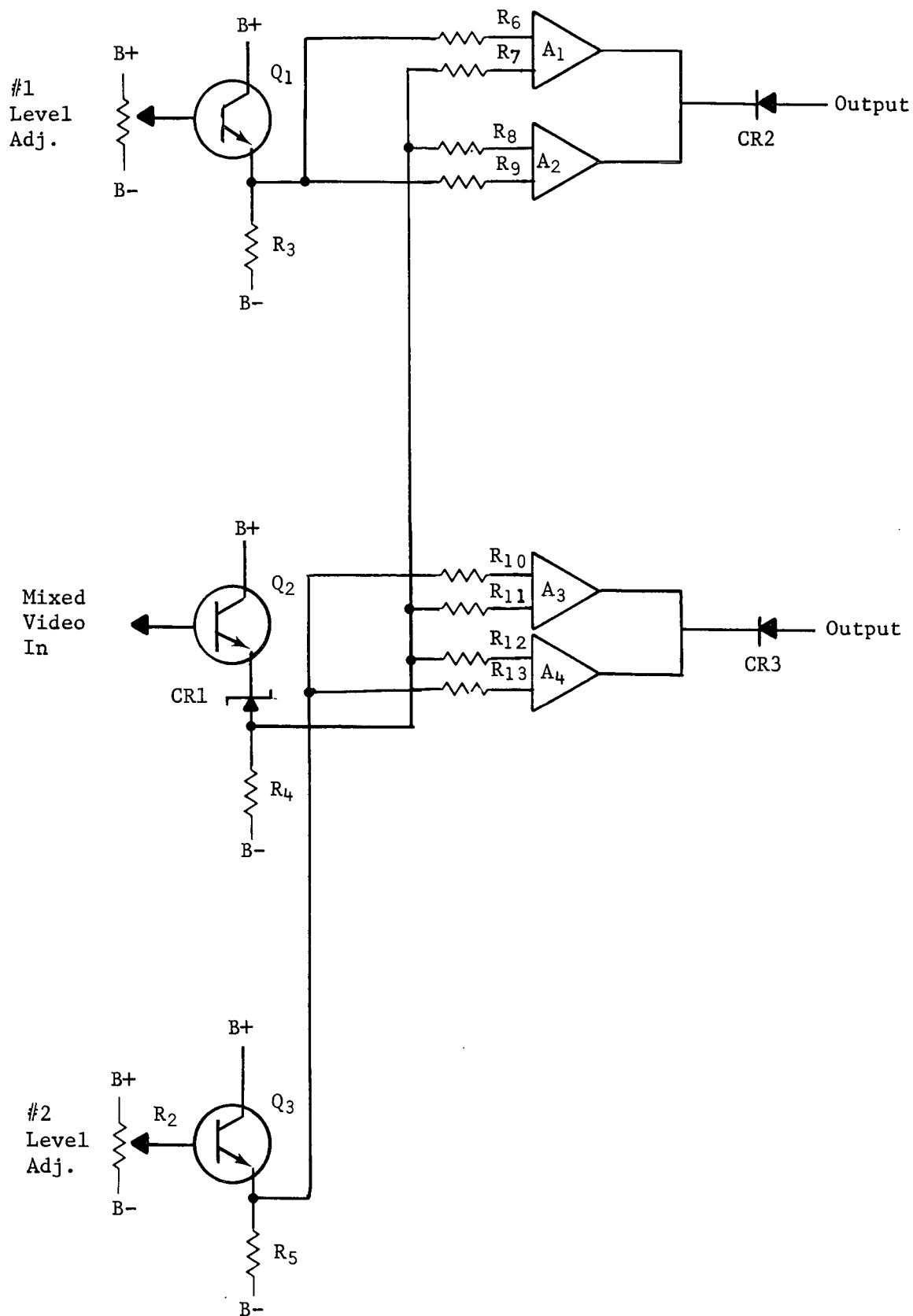


Figure 3-4 Iso-Density Contour Generators

The preceding discussion has been concerned mainly with qualitative enhancement of line-scan imagery. When one is dealing with infrared line-scanners, another quantity, quantitative processing, merits consideration. Thermal infrared radiation, because it is emitted from objects rather than reflected, yields information about the thermal character of an object. If it is assumed that the emissivity of the terrain being sensed is reasonably uniform, then the radiation is strictly a function of temperature. Using basically the same system as described above we have attempted to relate gray scale on an image to temperature in an absolute sense rather than as is usually the case, relating gray scale to relative temperature differences. This concept, although not yet totally successful, could be quite useful if proper ground calibration is obtained. First, we must assume that the detectors of an infrared line-scanner respond linearly to the incoming radiation, thereby allowing detector response (output signal in volts) to be related to temperature. This voltage, applied to the Z-axis of a CRT, can further relate beam brightness to temperature, and through a closed system, to a photographic image. Control must be exercised over the photographic process to assure that the density distribution is primarily on the linear portion of the log-E curve of the film. Ultimately then, film density, or gray scale, can be related to ground temperature.

Within the RS-14 sensor are two controlled-temperature calibration sources which are viewed by the scanning optics once each mirror rotation. Theoretically, one can use the information from these sources to make the correlation described above, but in the real world it is apparent that in order to correlate temperature of a ground target to an output signal, the reference must be viewed through the same atmospheric path as the ground target. It has been reported that the actual and apparent temperature of an object viewed from a remote platform varies as a function of path length (Garnier, 1971)<sup>1</sup>. It is for this reason that unless there are several well defined, locatable reference targets of known temperature, it is virtually impossible to present thermal imagery in a quantitative sense with an accuracy of better than  $\pm 8$  to  $10^{\circ}\text{C}$ .

The oscilloscope used in the processing described above requires a minus 5-volt to plus 5-volt-input on the cathode of the CRT to drive the spot intensity from zero to full brightness. By applying known steady-state voltages to the cathode input (i.e., 1.0-volt steps from -5 to +5 volts), a photographic step wedge can be generated that allows correlation of voltage and density. Proper density distribution requires some experimentation with f/stops

Garnier, B. J., 1971; "The Observation of Topographic Variations in Surface Radiative Temperature by Remote Sensing from a Small Aircraft". *Proceedings of the 7th Symposium on Remote Sensing of Environment*, Vol. 1, p. 495-500.

and the oscilloscope intensity control, but once optimized, the image produced permits correlation of density and temperature. It must be remembered that it is essential to obtain ground calibration data if absolute temperature measurement is desired.

### 3.3 Data Quality

One serious problem that arises with a system such as described above is data quality. Because of the non-availability of FM-reproduce electronics, it was necessary to request direct-record mode on magnetic tapes supplied by NASA. This recording mode will often introduce DC offset in the data. Also, it is not possible to reproduce frequencies below 100 Hz, although this is not critical for the vast majority of cases.

Another area of concern is that of wow and flutter. Unless the tape recorder is of very high quality, jitter is observed in the resulting image. Both analog and digital systems contain desirable and undesirable aspects, but a hybrid scheme might achieve an optimum configuration. In such a system, processing and experimentation would be performed with the data in analog form, and final hard copy produced from digital data using the logarithms developed in the analog processing. It should also be noted that in producing final hard copy, it would be highly desirable to utilize a flying-spot printer or a film recorder such as the Honeywell Model 1856. The 4x5-in. image obtained with the oscilloscope camera is not very satisfactory as a final product.

#### 4. INFRARED SPECTROMETER DATA REDUCTION

Little progress has been made during this report period. This is due primarily to degradation of existing data and the lack of new data. In order to test existing programs and continue development of software, it is imperative that additional data be obtained in which the sensor and its subsystems are functioning properly and the terrain overflown is a more simple case than in Mission 105. Ideally, the flight line should cover an area in which there are only a few rock types exhibiting distinct contacts. The Mission 105 data used in the work reported in the second annual report were collected over some of the most complex terrain in the Bonanza Test Site. Since no new data were available during the past year, existing programs could not be tested. However, the Mission 105 spectral data were used to examine techniques for removing what appears to be instrument noise from the data. The noise in question is unfortunately not periodic, nor does it contain any repeatable patterns or sequences. The frequency is very low, on the order of 200 to 500 Hz, and statistical techniques lose effectiveness at these frequencies.

It has become apparent that it is essential to perform a rigidly-controlled preflight calibration and to over-fly a water target at least once at the beginning of the mission and again at the end. Ideally, water calibration should be done at two altitudes in order to better characterize the atmosphere. The areal extent of the water target should be sufficiently large to allow the spectrometer to view the target for a minimum of 5 seconds. Water calibration spectra are critical to the successful reduction of spectrometer data.

Until some of the above-noted problems are corrected, it is not deemed advisable to expend more time and funds on the reduction of Mission 105 data.



## 5. INVESTIGATION OF THERMAL INFRARED ANOMALIES

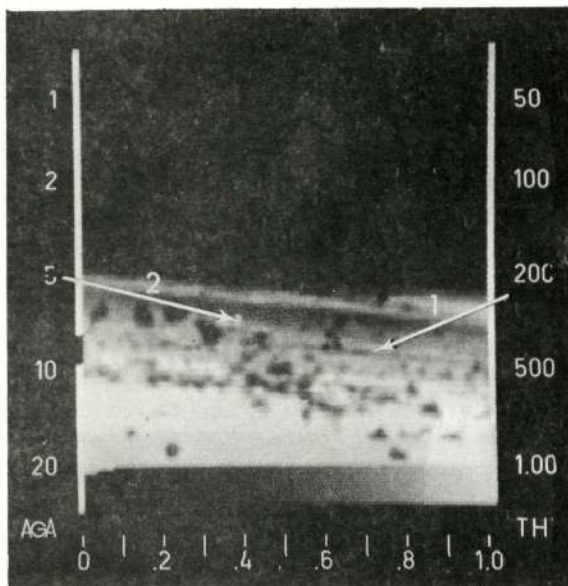
During the summer of 1971, while mapping his thesis area north-east of Canon City, Colorado, Mr. Gary Raines of Colorado School of Mines observed that thermal infrared imagery (8 - 14 $\mu$ ) obtained during Mission 153 showed a series of anomalous lineations in a broad alluvial valley south of Beaver Creek, northeast of Canon City. The IR imagery displayed a series of en-echelon linears that approximately paralleled the strike of the underlying Fountain Formation, buried here by as much as 50 feet of detrital material as judged by pits, apparently dug several years ago as water wells. The linears were cooler than the adjacent terrain and it was suggested that the cause was an upwelling of groundwater through the thick gravel deposits flooring the valley. The question arose as to whether the anomalies were transient or permanent, or even if they were real, representing warmer and cooler zones and not simply artifacts or extraneous markings on the film imagery.

To make this determination, it was decided in August, 1971, to transport the AGA Thermovision to the site and search for the anomalies. The AGA is a device for imaging in the 3 - 5 $\mu$  wavelength region, and is capable of detecting any thermal anomalies in question. The AGA was set up on a small hill overlooking the site (Figure 5-1) and Mr. Raines was given a butane torch (so he could be located on the AGA display) and a walkie-talkie. He was then "radio-controlled" to the edge of one of the dark zones which was clearly visible on the AGA display (Figure 5-2). Location "1" on this figure indicates an edge of the zone, location "2" is the butane torch held by Raines. Using a compass bearing obtained previously from the scanner imagery, Raines walked in a direction which should define a boundary of the anomalous area if it was, in fact, real. Flags were placed along the traverse and examination confirmed this to be true, indicating that the airborne scanner is capable of sensing variable moisture levels, apparently related to bedrock buried under several feet of gravel. There was no obvious excess of soil moisture near the surface, but the vegetation did appear to be somewhat thicker along the linears. Two explanations for the anomalies seem feasible. They could be effects of the paleo-erosional bedrock surface beneath the thick valley-fill, or they could indicate a series of strike faults providing a path for ground-water to rise to the surface.

On 21 December 1971, several seismic traverses were run perpendicular to the anomalous linear features (Figure 5-3). The seismograms recorded during this field trip (Figure 5-4) show good



Figure 5-1 AGA Thermovision Overlooking Valley



Reproduced from  
best available copy.

Figure 5-2 AGA Thermovision Image Showing  
Anomalous Linear Feature (1), and  
Ground Observer with Butane Torch (2)



Figure 5-3 Seismic Profiling Across Anomalous Area

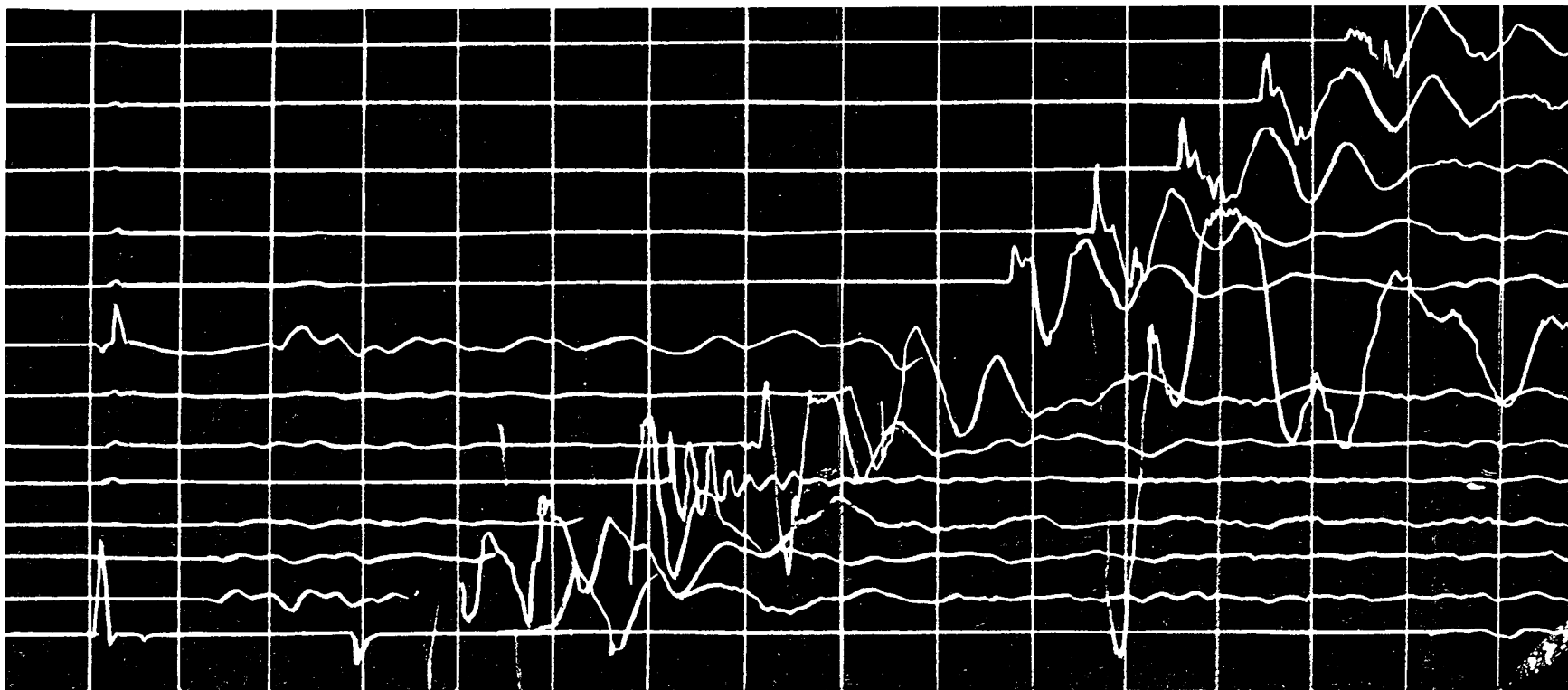


Figure 5-4 Typical Seismogram Showing First Arrivals

first-arrivals, and energy coupling into the ground is more than adequate. Plots of the time-distance curves showed there was not sufficient distance between the shot-point and the first geophone to yield information about the bedrock depth (Figure 5-5). The final shot was a reverse profile with the shot-point approximately 1000 meters from the alluvium-crystalline rock contact. The time-distance plot of this shot indicates the subsurface sediments are faulted as shown in Figure 5-6.

Because the seismic data collected was inconclusive, another trip is being planned in the near future during which extensive seismic, radiometric and soil surveys will be conducted to determine the source of the thermal anomalies observed.

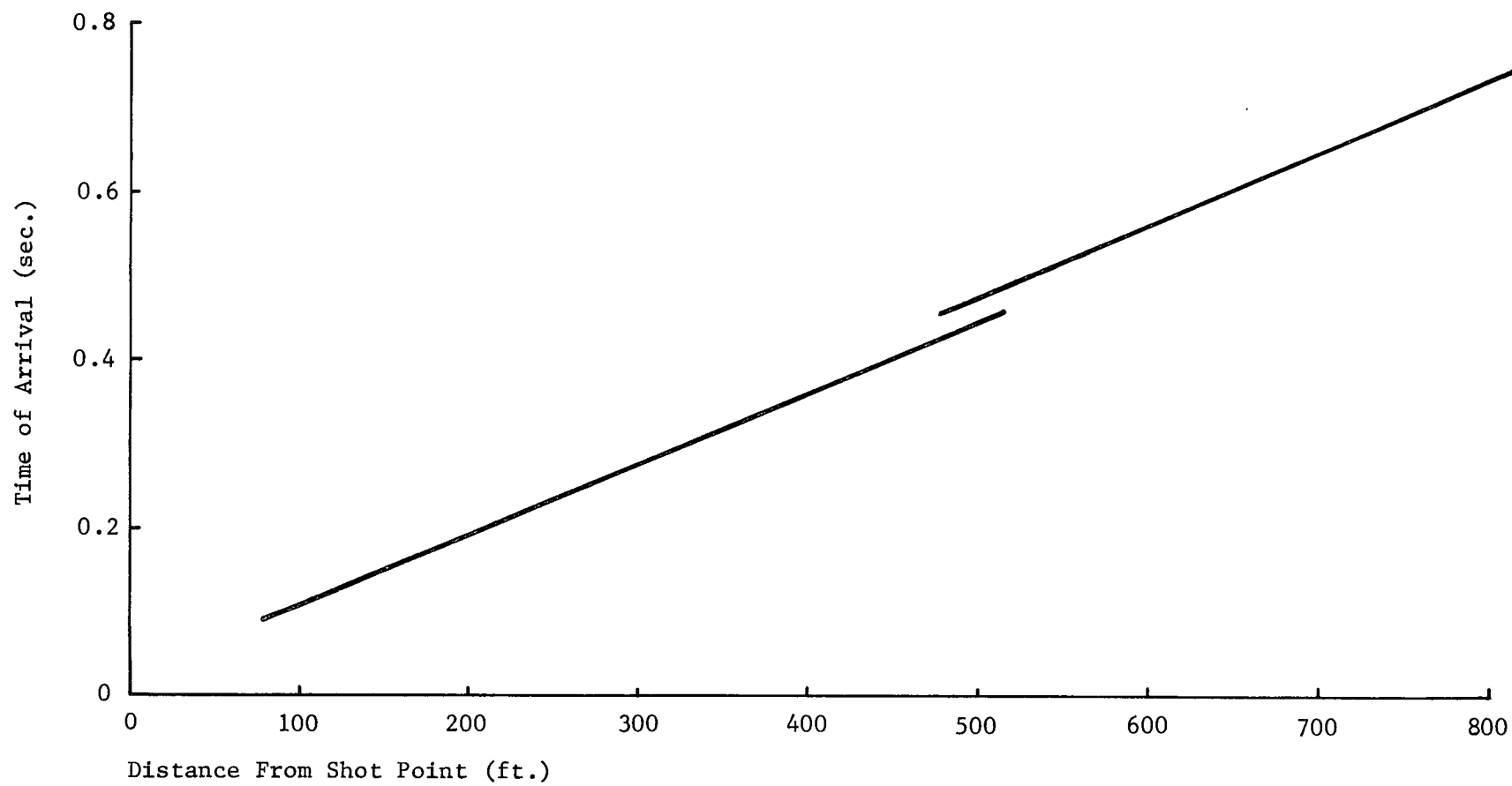


Figure 5-5 Time-Distance Plot, Reverse Profile

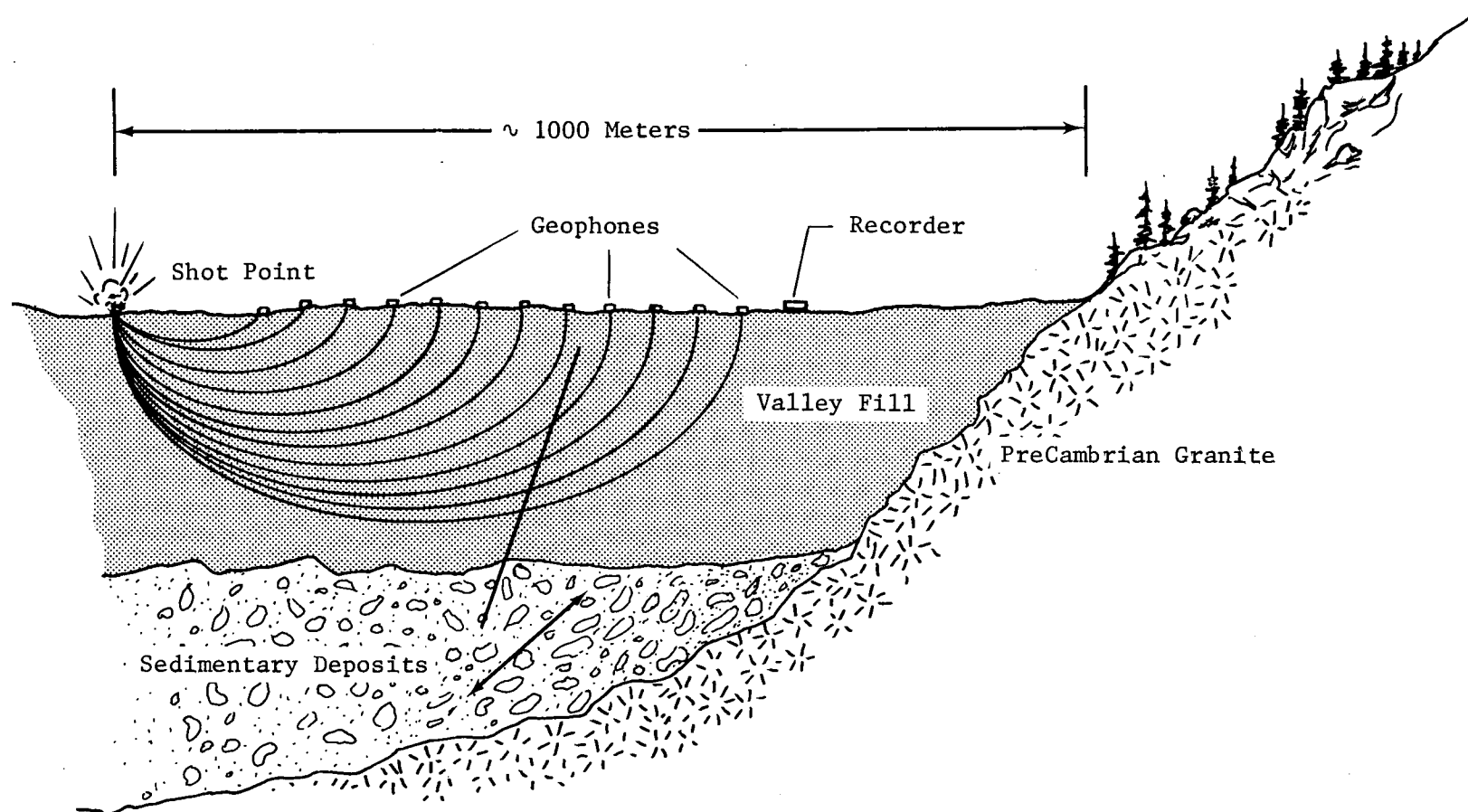


Figure 5-6 Section View Through Valley

5-7

## 6. IMAGE PROCESSING

The primary effort involving image processing during the third contract year emphasized use and application of the video image processing system. Several types of airborne imagery were evaluated.

### 6.1 Background and Theory

The video image processor enables real-time quantization of an image in terms of absolute and/or relative densities, and pseudo-color display of an image according to programmed density range values. The resulting processed image is enhanced due to the extended density viewing range, increased image contrast, and the ability to discard or suppress irrelevant information.

The primary purpose of this process is to perform exaggerative enhancement of an image, making the subtle more obvious or extracting information so that "buried" data in the background becomes more obvious. The video image processing technique expands the gray scale of the photographic H and D curve by substituting colors for the shades of gray, thereby more fully utilizing the response and sensitivity of the human eye. The process also does some pre-conditioning of the photographic image resulting in reduced eye fatigue, compresses the bandwidth, and exaggerates subtle variations in contrast ratios.

### 6.2 Equipment

The Video Image Processor equipment is divided into three general sections:

- 1) Input and controls;
- 2) Signal conditioning (processing);
- 3) Display and recording.

The overall system design is such that the qualitative and quantitative contribution of each element in the system can be determined.

The primary input source is a television camera with a plumbicon-type image tube. A video analyzer is connected to the camera output to monitor camera response and make appropriate adjustments.



By using the camera's black-and-white-level adjustments in conjunction with a calibrated step wedge, a video analyzer, and a digital voltmeter, the camera can be calibrated repeatedly to the same black and white range. The video analyzer functions as a select-line oscilloscope displaying an eight kHz wave form of the video information contained under a line superimposed on the video picture. The sweep voltage which falls under the intersection of two movable cross-hairs is displayed on a digital voltmeter with 0 volts as black and five volts as white on the gray scale.

The video quantizer slices the measured gray scale data of the camera into as many as 16 infinitely-variable increments which are connected to the abscissa of a matrix board, with the three primary color channels on the other coordinate. Connecting pins link the various levels of the slicer to the color channels. A second 16x16-in. matrix board is used to control the feedback, interaction and overlap of the sliced levels. Each color channel's intensity can be varied to provide desired visual effects. It is usually necessary to have one or more known reference points in the original image to successfully utilize this portion of the equipment.

The color monitor is a RGB (red-blue-green) type with three separate circuits for primary color inputs. Intermediate colors are produced by the interaction of the primary guns on the face of the video picture monitor. This permits pseudo-color pictures to be made from ordinary black and white video signals.

A video tape recorder and a disc recorder are available to record four channels of video signal. Selected bands of multispectral imagery of different wavelengths of the same scene can thereby be displayed simultaneously, superimposed on each other so either color additive or subtractive techniques can be used to minimize similar densities while enhancing dissimilar densities.

### 6.3 Data Collection

Data and imagery from two NASA Earth Resources Aircraft Program (ERAP) overflights flown during 1971 were used for video-image processing.

Mission 168 was flown over the Bonanza, Colorado, test site from June 14 through June 17. Five flights were made during which the following types of data were obtained:

- 1) Multispectral photography;
- 2) Early morning low-sun-angle black and white photography;
- 3) Predawn and daytime Infrared Scanner imagery;
- 4) Side-Looking Airborne Radar imagery.

Mission 184 was flown September 13 through 16. Four flights obtained color, color infrared, and multispectral photography, daytime and predawn Infrared Scanner imagery, and Side-Looking Airborne Radar.

Other data available from previous missions included imagery from Mission 101, a high altitude photographic mission, and Mission 105, a medium altitude mission. Processing of these data is reported in the first and second year summary reports.

Ground measurements were made during the overflights and appropriate data used to assist in interpreting the airborne imagery.

#### 6.4 Technical Procedures and Discussion

Previous work on Bonanza remote sensor data using the video-image processor had been limited to using multispectral photography and daylight thermal infrared scanner imagery data then available from Bonanza Missions 101 and 105. Partial success in delineating structural features such as fault line traces and fractures using both high and medium altitude photography and IR scanner were obtained, although in most cases these features were also visible using conventional stereo photogeological methods. Very little success in discrimination of lithology or soil types was obtained. See Bonanza first and second year summary reports for complete discussion of these analyses.

The availability of several different types of data from Missions 168 and 184 now permitted an attempt to evaluate the utility of all types of sensor imagery using the video-image processor.

Evaluation of each type of imagery is discussed independently. Specific comments applicable to each data type are included in each section, while recommendations pertaining to VIP in general and data collection and analysis are found in Sections 6.5 and 6.7.

Several specific areas to be investigated were selected by Colorado School of Mines (CSM) graduate students participating in the Bonanza program. During video processing, these students were asked to visit Martin Marietta and observe the approach being taken and comment on procedures. The problems presented were kept simple since it appeared that previous attempts at solving specific problems tended to be too complex for this stage of investigation.

6.4.1 Multispectral Photography - The theory and principles of multispectral (multiband) photography are discussed at length in the Bonanza second year summary report. In processing Missions 101 and 105 imagery during 1971, the technique used to discriminate lithology was to arbitrarily assign a color to the most obvious or known rock type, define its known or visible limits by trial and error methods, and then attempt to extrapolate this color to other areas. The major disadvantage with this method is that it required previous knowledge of what was being sought and had no set techniques for establishing new data points.

To overcome these deficiencies, a new approach was developed. After mounting the multiband frame and displaying it on the video monitor, two points representing lightest and darkest points on the imagery were selected. These correspond to the end-points of the gray scale being seen by the video camera. Using the video analyzer as a line-select oscilloscope, the two movable cross-hairs were centered on each end-point and sweep voltage for each point read on the digital voltmeter. The video quantizer is then set up to "slice" the total gray scale into equal increments and colors can then be assigned to the slices. The number of slices can range from two very broad bands to any number up to 16. The image is displayed on the RGB monitor with each color representing a select portion of the gray scale seen by the video camera, within the limits previously set up by the analyzer. This system allows the number of slices to be varied, the width of any or all segments changed and points selected within the frame of imagery to be used as calibration points for extrapolation to contiguous areas.

To test this procedure, a single frame of multispectral photography from Mission 184 [2424 film with a No. 92 filter (650-1000)] was selected by Mr. Gary Raines of CSM. The area was relatively clear of vegetation and the geology had been mapped by both ground and photogeologic methods. Figure 6-1 depicts the test area. Using points A and B as end-points, the analyzer was set up to slice the gray scale into eight equal segments, a color assigned to each slice, and the image displayed on the RGB monitor.

Reproduced from  
best available copy.



*Figure 6-1 Multispectral Photo (620-1000 nm)  
of Test Area Showing Control Points  
A and B*

The display was observed in two modes, sharply focused (Fig. 6-2) which presented a wealth of detail, and slightly out-of-focus (Figure 6-3) which eliminates much of the detail but gave a better display of gross features. Table 6-1 is a listing of the colors assigned. A geologic sketch map of the test area (Figure 6-4), prepared from field mapping by Mr. Raines, was compared to the display. Note the video processor appeared to display several of the geologic units with some degree of accuracy. The sketch map was not used during set-up, but only to check and verify the results. The procedure was repeated, but with different color assignments as shown in Table 6-2. Figure 6-5 is the new setup of the original frame with the geologic sketch-map superimposed.

It was decided to extend the area of study to include three additional frames to form a contiguous area covered by photography from the same mission. Figures 6-6, 6-7, and 6-8 are the contiguous frames, displayed with the same colors named in Table 6-2. Examination of the video-processed imagery shows a close correlation with the previously mapped lithology and indicates that it is possible to use this technique to extrapolate density information, e.g., lithology, from one frame to another.



*Figure 6-2 Video-Processed Photo of Test Area  
Using Eight-Slice Density Scale*

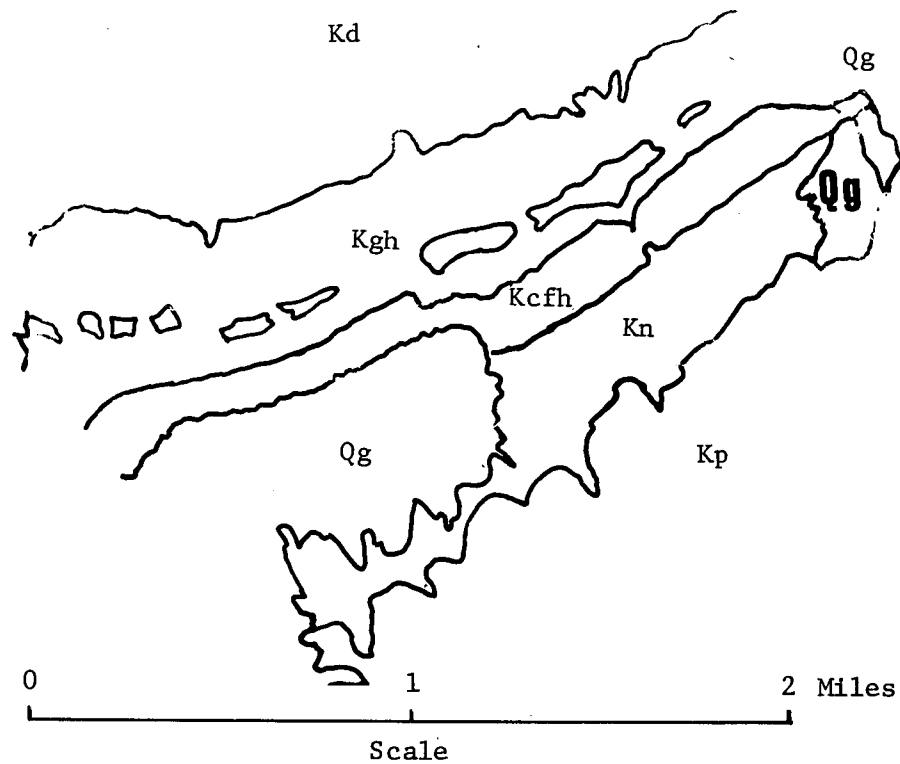
Reproduced from  
best available copy.



*Figure 6-3 Video-Processed Photo of Test Area  
Defocused Eight-Slice Density Scale*

Table 6-1 Colors Assigned to Densities for Figures 6-2 and 6-3

Density							
Light ←				→ Dark			
1	2	3	4	5	6	7	8
Red	Green	Brown	Light Green	Yellow	Light Blue	Violet	Dark Blue



Legend:

Qg	Quaternary Gravel	Kcfh	Codell - Ft. Hays Undifferentiated
Kp	Pierre Shale	Kgh	Greenhorn Limestone
Kn	Niobrara Formation	Kd	Dakota Sandstone

Figure 6-4 Geologic Sketch Map of Test Area

6-7

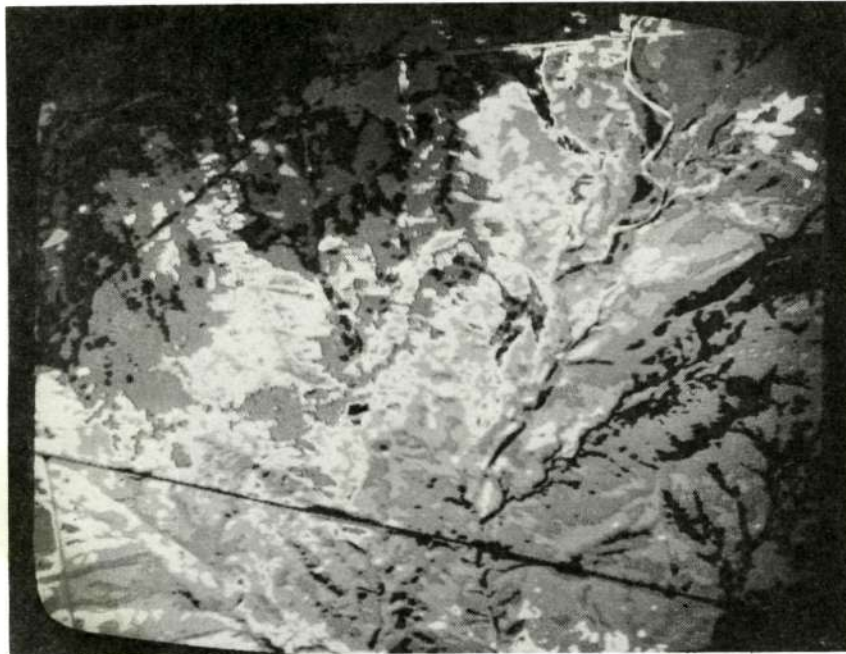
Table 6-2 Colors Assigned To Densities for Figures 6-5, 6-6, 6-7, and 6-8

Density							
Light ←							→ Dark
1	2	3	4	5	6	7	8
Red	Dark Blue	Light Blue	Gray	Pink	Brown	Light Green	Dark Green



Figure 6-5 Test Area in New Set-Up With Sketch-Map Superimposed



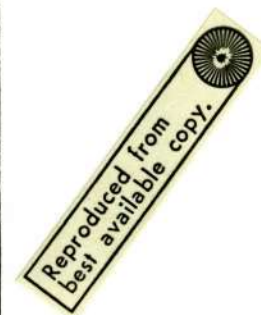
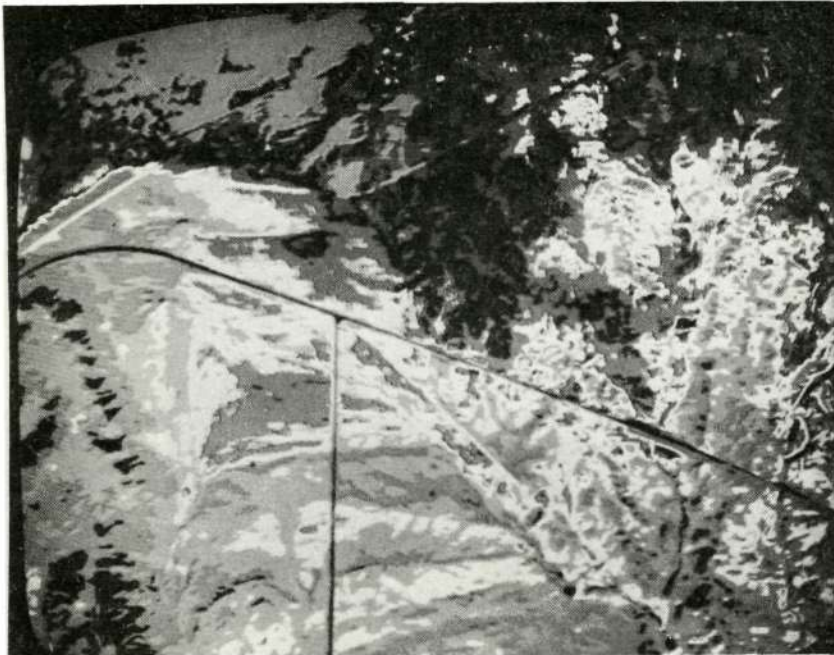


*Figure 6-6 Video-Processed Photo of Contiguous Area*



*Figure 6-7 Video-Processed Photo of Area Contiguous to Test Area*





*Figure 6-8 Video-Processed Photo of Area Contiguous to Test Area*

From the work done this reporting period, several observations can be made. A procedure has been developed to use multispectral photography to assist in discrimination of lithology and soil types. On the basis of experiments depicted in Figure 6-5, the procedure is repeatable, has definite objective value, and can be used to extend the area of interest over several frames of contiguous photography. Similar experimentation involving an area suggested by Mr. Daniel Knepper is now in progress.

A method of defining the width of density slices in the procedure has been suggested and will be further developed in the future. It appears that several different multispectral bands commonly used in NASA aircraft missions can be used for this procedure. A major limiting factor, however, seems to be the amount and type of vegetation found in an area since the vegetation, particularly evergreen types, seems to dominate a large center portion of the density range available in a photograph. Images that are sharply in focus are useful for defining large amounts of small detail which, in turn, will tend to mask what is being sought, while slightly defocused images eliminates much detail but enhances gross features.

6.4.2 Color Photography - A single frame of 9x9-in. aerial color film (S0397) from Mission 168 was subjected to video processing. Attempts to delineate lithology using the procedures described in Section 6.4.1 were not successful, probably due to the low contrast inherent in the color photography.

Previous work indicated that subtle linear features, including fault line traces and fractures, could be discriminated and mapped from color aerial photography. The procedure used differs from that used to discriminate lithology. The video quantizer was set up with very narrow slice of color assigned to a small range of the total gray scale. Then the bias-level control of the quantizer is used to reshade the background and shift the gray scale. By continually changing the bias levels, it is possible to emphasize and enhance linear features in the photograph. It should be noted that this procedure is, by nature, a "knob-twisting" technique and subjective as opposed to that used for discrimination of lithology described in 6.4.1. Further, the usual caution must be exercised to avoid attributing geologic significance to such straight-line cultural features as roads, power-lines, and fence lines.

6.4.3 Color Infrared Photography - Attempts to use color infrared photography from Mission 168 in the video processor to discriminate lithology with the procedures used in Section 6.4.1, were, generally, no more successful than the attempts with color aerial photography. Success with enhancing linear features was generally similar.

6.4.4 Low Sun Angle Photography - It was immediately evident that low-sun-angle photography, because of large areas of shadow and small density range in the sunlit areas, is not suitable for video enhancement.

6.4.5 Thermal Infrared Imagery (Predawn) - A positive transparency of predawn thermal infrared (8-14 micron) imagery from Mission 168 was subjected to video image processing.

Using the procedure outlined in Section 6.4.1, an attempt was made to discriminate lithologic units using this imagery. Although there was some indication of discrimination, no clear cut identification was obtained unless *a priori*: knowledge of the ground units was available.

Attempts to use the thermal imagery to construct a thermal contour map were hampered by lack of sufficient ground and aircraft calibration data. The two IR calibration sources in the scanner did not yield adequate information, either from the imagery or from the analog tape.

Previous work at Martin Marietta, unrelated to this contract, has demonstrated that video processing of thermal imagery can be quite successful, but is wholly dependent on adequate ground and aircraft calibration in order to arrive at absolute data points. See Section 3.0, Enhancement and Display of Infrared Line Scan Data, for further discussion.

6.4.6 Side-Looking Airborne Radar - Both real- and synthetic-aperture radar from Mission 168 was viewed on the video-image processor. Due to the nature of the imagery, no lithologic discrimination was attempted.

Since radar images are presently used to locate linear features, the scan was processed to enhance these features using procedures previously described. Although many linear features were observed during processing, all were visible on the unprocessed imagery. There appeared to be no difference in the quality of the real-versus synthetic-aperture imagery as viewed on the processor.

It is felt that video image processing of airborne radar does not enhance the ability of the interpreter to find and locate linear features.

## 6.5 Summary

Six types of imagery flown over the Bonanza Test Site on NASA Missions 168 and 184 were subjected to video image processing to ascertain the usefulness of the processor and the suitability of the imagery for geologic analysis. New techniques using the video-processor were developed for specific problems, including procedures for lithologic discrimination and linear feature enhancement.

Discrimination and identification of lithology was attempted using the six types of imagery available. A new procedure was developed which permits a more quantitative approach and gives repeatability. Low-sun-angle photography and side-looking airborne radar were not at all useful for this type of analysis. Color and IR color photography could be used to assist and corroborate lithologic mapping, but this type of imagery tends to emphasize

vegetation, masking the rocks and soils. Also, the density range of these films is quite narrow. Predawn thermal IR imagery results were marginal, with indications that some discrimination is possible, but more research is needed. Multispectral photography showed great promise, with results repeatable and quite accurate.

Prior work on discrimination and location of linear features had shown that color, IR color and multispectral photography were suitable for this type of problem. This year's work indicated that SLAR and thermal IR imagery could also be used, while low-sun-angle photography is generally unsuitable.

The ranking of the imagery for lithologic mapping would be as follows in descending order of usefulness:

- 1) Multispectral photography;
- 2) Thermal infrared imagery;
- 3) Color aerial photography;
- 4) Color infrared photography;
- 5) Low-sun-angle photography;
- 6) Side-looking airborne radar.

The ranking for linear feature mapping, in descending order of usefulness:

- 1) Side-looking airborne radar;
- 2) Color aerial photography;
- 3) Thermal infrared imagery;
- 4) Multispectral photography;
- 5) Color infrared photography;
- 6) Low-sun-angle photography.

## 6.6 Conclusions

Based on the work done this reporting period, the following conclusions can be stated: A technique has been developed to assist in the delineation and discrimination of lithologic units using multispectral photography. This procedure establishes parameters for set-up and analysis of imagery, permits extrapolation from one frame of imagery or area to another by use of selected control points, and is repeatable. It appears that imagery taken in the longer portion of the visible spectrum (600-700 nm) is best suited for this processing. It has been verified that video processing for discrimination and location of linear features is feasible for almost any type of imaging system now being used and that results are repeatable using a procedure described. If thermal imagery is to be of use for geologic problems, better ground truth and aircraft calibration data is required.

## 6.7 Recommendations

6.7.1 Data Collection - To fully use video processing of airborne imagery for specific geologic problems, it is necessary to first define the problem, then control the data acquisition parameters to yield the best data. For lithologic mapping, imagery should be obtained at a high sun-angle, particularly if timber is covering the area. This keeps shadowing effects to a minimum and also minimizes contrast differences over the target. For delineation of linear features, imagery should be collected with some shadowing, time of day being dependent on type of imagery. Color and IR color photography should be obtained with minimum solar-elevation angle of 45°. Multispectral photography should have a minimum solar-elevation angle of 35°.

To fully exploit predawn thermal infrared imagery, it is necessary to have accurate ground and aircraft calibration data available. Suggested ground locations would be water bodies at least 50 ft in diameter, roads and road intersections, large areas of similar composition such as fields or parking lots, and if feasible, the roofs of buildings. Small rock outcrops are difficult to identify using the video processor. It would also be desirable if ground points were selected to cover the entire range of temperatures expected.

6.7.2 Processing - Recommendations regarding processing can be divided into two categories; improvement in equipment and improvement in procedures and techniques. Equipment used for video processing is now being improved, modified and updated. The present

light source used to illuminate the transparencies is unsuitable for this type of processing. A new spherical integrating-cavity light source is now on order which will give a uniform light distribution and eliminate the hot spot presently being seen. This will allow the viewing of an entire frame of 9x9-in. photography with no associated loss of data as it now the case. Currently, only a 3x3-in. area can be viewed. Even with this small viewing area, it is estimated there is a 10% differential in intensity across the area. A rigid mount for the video camera is being planned to eliminate accidental movement and to establish consistent camera stations to eliminate viewing distortions. It is also planned to install dial knobs on the video quantizer so that exact settings of color levels can be recorded.

The procedures used for analysis should be formalized and adhered to in order to standardize data processing. It is recommended that future processing use a consistent assignment of colors. These colors would then be a basic part of the procedures; for example, red would always represent the light end of the density gray scale, and blue the dark end. A calibrated gray scale should be adopted so that the processor can be continually calibrated to a known source.

It is evident that much work remains to be done before video image-processing becomes a completely viable remote sensor data analysis tool. It is recommended that work be continued in testing techniques and procedures, and that investigators be encouraged to define and present geologic problems which may be solved by video image processing.

## 7. FIELD SUPPORT ACTIVITIES

7.1 Six persons from Martin Marietta were in the Canon City and Salida areas for four days in support of Mission 168.

7.2 Muhm and Worman took the AGA Thermovision to the Canon City area on 11 August 1961 to assist in interpreting some thermal anomalies appearing on Mission 153 infrared imagery. See Section 5 for a more complete discussion

7.3 Six persons from Martin Marietta were in the Canon City, Salida, and Great Sand Dunes areas for five days in support of Mission 184.

APPENDIX D

PAPERS PRESENTED/WRITTEN  
BY CSM AND MMC PERSONNEL

*B*

Hulstrom, R. L., 1972, The "cloud bright spot" effect on remote sensing: submitted for publication to Photogrammetric Engineering.

Reeves, R. G., 1972, Geologic Analyses of remote sensor data, the Bonanza Project Abs. : paper presented at the 1972 Annual Meeting of the American Association of Petroleum Geologists; manuscript in preparation for submission for publication.

Reeves, R. G., Biniki, R. M., Hulstrom, R. L., Muhm, J. R., and Worman, K. E. (translated by Remigio Martinez), 1972, Sitios de prueba y sus estudios (Test sites and their studies): Colorado School of Mines Bonanza Project Report (presented at the Inter-American Geodetic Survey Remote Sensing Course, Panama, May 1972).

Wychgram, D. C., 1972, Geologic remote sensing study of the Hayden Pass - Orient Mine area, northern Sangre de Cristo Mountains, Colorado: Colorado School of Mines Bonanza Remote Sensing Project Report 72-3.

Wychgram, D. C., 1972, Geology of the Hayden Pass - Orient Mine area, northern Sangre de Cristo Mountains, Colorado: a geologic remote sensing evaluation: Unpublished M.Sc. Thesis, Colorado School of Mines.



DISTRIBUTION LIST

NASA HEADQUARTERS

	Copies
Molloy, M. J.	1
Park, A. B.	1
Vitali, J. A.	1
Off. Sci. and Tech. Information	5

NASA - MSC

Amsbury, D.	1
McDonald, W.	1
Smistad, O.	1
Watkins, A.	1
Zeitler, E. O.	1
Data Center	5

EROS Program

Fischer, W. A.	1
Carter, W. D.	1
Hemphill, W. R.	1
Sioux Falls Data Center (Landis, G.)	5

MARTIN MARIETTA

Muhm, J.	5
----------	---

CSM

McBride, G. T., Jr.	1
Kuhn, T. H.	1
Jordan, A. R.	1
Gary, J. H.	1
Copeland, W. D.	1
Klodt, D. T.	1
Stermole, F. J.	1
Kent, H. C.	1
Weimer, R. J.	1
Grose, L. T.	1
Reeves, R. G.	1
Lee, K.	1
Jefferis, L. J.	1
Knepper, D. H.	1
Marrs, R. W.	1
Raines, G. L.	1
Bruns, D. L.	1
Bonanza Library	1